HYDRODYNAMIC AND HEAT TRANSFER CHARACTERISTICS OF A SOLAR HEATED AIR DUCT

Thesis for the Degree of Ph. D.

MICHIGAN STATE UNIVERSITY
MUHAMMAD ANWER MALIK

1967

THESIS

This is to certify that the

thesis entitled

HYDRODYNAMIC & HEAT TRANSFER CHARACTERISTICS OF A SOLAR HEATED AIR DUCT

presented by

MUHAMMAD ANWER MALIK

has been accepted towards fulfillment
of the requirements for

Ph. D degree in Ag. Engg

James B. Boyd
Major professor

Date 15 Nov 1967

O-169

ABSTRACT

HYDRODYNAMIC AND HEAT TRANSFER CHARACTERISTICS
OF A SOLAR HEATED AIR DUCT

by Muhammad Anwer Malik

Heated air has many applications in agriculture. The capturing of solar energy is done by means of a collector. Many types have been built and tested. For agricultural purposes, however, as low as 10 degrees rise of temperature in the outside air is sufficient to, say, speed up the drying of farm crops to moisture contents safe for storage.

For low temperature rise, a "no-glass" collector can be used. This consists primarily of a series of rectangular air ducts lying side by side with sheet metal covering on the top surface which is exposed to solar radiation. The "no-glass" collector is easily incorporated into the design of a building, as it essentially follows the pattern of a conventional roof. The only addition needed is some type of material to form the bottom of the duct.

Hydrodynamic and heat transfer characteristics of the air ducts mentioned above are studied in the present thesis.

The problem is essentially that of a fully developed turbulent flow in a rough rectangular duct heated uniformly on the top and having the other three sides essentially adiabatic. The analyses available for the unsymmetrically heated smooth ducts agree only qualitatively. Most of them

entail extensive numerical calculations and are of limited use. In the present thesis two analytical solutions are developed for fully-developed turbulent flow in a smooth unsymmetrically heated rectangular duct.

Two experimental ducts were built. The bottom for both of them was made of plywood and was insulated. The vertical walls were made of pieces of lumber. The top of one of the ducts was covered by a flat galvanized sheet. The other duct was covered by corrugated galvanized sheet. The second duct was used to estimate the increase in pressure drop and heat transfer when a flat top is substituted by a corrugated one.

The ducts were used to determine intake losses, intake length and friction coefficients. For both the ducts the friction coefficient was found to depend on Reynolds number and relative roughness. The corrugated roof resulted in an increase in friction coefficient of about 40 per cent.

The analytical results for the convective heat transfer coefficient for smooth duct successfully carried over to the rough duct when multiplied by a factor $\sqrt{f/f_0}$.

The increase in the heat transfer coefficient resulting from the use of corrugations was about 20 per cent.

Madsen's rule (54) was found to apply to the rough ducts.

James S. Boyd

Carl W. Hall

HYDRODYNAMIC AND HEAT TRANSFER CHARACTERISTICS OF A SOLAR HEATED AIR DUCT

By

Muhammad Anwer Malik

A THESIS

Submitted to
Michigan State University
in partial fulfillment of the requirements
for the degree of

DOCTOR OF PHILOSOPHY

Department of Agricultural Engineering

1967

ACKNOWLEDGMENTS

The author wishes to express his deepest gratitude to Dr. Frederick H. Buelow for his guidance, supervision and inspiration.

Thanks are due to my advisor Dr. James S. Boyd, for his supervision, inspiration and graciousness.

The author also wishes to thank the other members of the guidance committee: Dr. James V. Beck, Dr. Merle E. Esmay, and Dr. E. A. Nordhaus.

The author is grateful to Dr. Ronald C. Hamelink for his willingness to be on the Final Oral Exam Committee.

Dr. Carl W. Hall, Chairman of the Department, is thanked for giving financial grant for the project.

The assistance offered by Mr. Jim Cawood in the construction of test apparatus is gratefully acknowledged.

The author is indebted to the Campus Coordinator's Office at Washington State University for coordinating his overall program of study in this country.

TABLE OF CONTENTS

LIST OF TABLES

LIST OF FIGURES

NOMENCLATURE

a Shorter side of the rectangular duct.

$a^+ = \frac{a\sqrt{\tau_w/\rho}}{\nu}$

A Area of cross-section of the duct.

b Longer side of the rectangular duct.

C Perimeter of the duct.

C_p Specific heat at constant pressure.

d Diameter of circular tube.

d_h Hydraulic diameter of a duct = $\frac{4A}{C}$

d_* Diameter used in rough tubes = $\sqrt{\frac{4V}{\pi L}}$

f Coefficient of friction.

f_0 Coefficient of friction of hydraulically smooth duct.

g Acceleration due to gravity.

G Mass velocity.

h Convection heat transfer.

$h_{general}$ Generalized Madsen's heat transfer coefficient.

$h^*_{general}$ Generalized Madsen's heat transfer coefficient modified for rough ducts.

k Thermal conductivity of fluid.

K Absolute roughness.

K_1, K_2, K_3, K_4 Factors for computing entrance losses.

K^* Entrance loss factor defined on page 14.

K/d_h Relative roughness

L Length of duct.

Le Intake length.

Nu Nusselt Number = hd_h/k.

Nu_∞ Nusselt Number for fully developed flow.

$\overline{Nu}$ Average value of Nusselt Number over a distance.

P Pressure of air at distance x.

P_0 Pressure of stationary air ahead of the duct.

p_i Pressure at inlet of duct.

p_o Pressure at outlet of the duct.

Pr Prandtl Number = $C_p\mu/k$.

Pr_t Turbulent Prandtl Number = $\varepsilon_m/\varepsilon_q$.

q Heat flux at distance y.

q_i Intensity of incident solar energy.

q_w Heat flux at wall.

Q Volume of air flowing through the duct.

r Radial distance from the center of the tube.

r_o Radius of the tube.

$r_o^+ = \frac{r_o\sqrt{\tau_w/\rho}}{\nu}$.

R Radius of tube.

Re Reynolds Number = $u_m d_h/\nu$.

Re_{cr} Critical Reynolds Number.

Re_T = $U_* d_*/\nu$.

R_h Hydraulic radius = A/C.

t Temperature at distance y from the wall.

t^+ Dimensionless Temperature = $\dfrac{t_w - t}{q_w/\rho Cp\sqrt{\tau_w/\rho}}$.

t_b Temperature at the end of buffer layer.

t_B Bulk temperature of fluid.

t_c Temperature at central axis of the tube.

t_i Temperature of air entering the duct.

t_o Temperature of air leaving the duct.

t_w, t_{w_1} Temperature of the heated wall.

t_{w_2} Temperature of the wall opposite to the heated wall.

t_δ^+ Dimensionless temperature of fluid outside thermal boundary layer = $\dfrac{t_w - t_\delta}{q_w/\rho Cp\sqrt{\tau_w/\rho}}$.

u Velocity at distance y from the wall.

u^+ Dimensionless velocity = $u/\sqrt{\tau_w/\rho}$.

u_b Velocity at the outer edge of buffer layer.

u_b^+ = $u_b/\sqrt{\tau_w/\rho}$.

u_c Velocity at center.

u_c^+ = $u_c/\sqrt{\tau_w/\rho}$.

u_m Mean velocity.

u_m^+ = $u_m/\sqrt{\tau_w/\rho}$.

u_s Freestream velocity outside of the boundary layer either in a flat plate or intake region of a duct.

u_* Friction velocity = $u_m\sqrt{f/8}$.

v_λ Velocity in fluctuation of dimension = λ.

V Volume of the duct.

V_1 Volume of air entering the duct.

V_2 Volume of air as measured by the venturi.

x Axial distance measured along the duct.

x^+ $= x/d_h$.

y Distance from the heated wall of the duct.

y^+ $= y\sqrt{\tau_w/\rho}\ /\nu$.

y_1 Thickness of the laminar sublayer.

y_b Distance between the heated wall of the duct and outer edge of buffer layer.

y_o $= a/2$.

y_o^+ $\dfrac{y_o\sqrt{\tau_w/\rho}}{\nu}$

Greek Letters

α Thermal diffusivity.

δ Thickness of hydrodynamic boundary layer.

δ^+ $= \delta\sqrt{\tau\ /\rho}\ /\nu$.

δ_t Thickness of thermal boundary layer.

μ Dynamic viscosity.

ν Kinematic Viscosity.

κ Energy dissipated per unit mass and time.

λ_o Local degree of turbulence.

ρ Density of fluid.

τ Shear stress at distance y.

τ_w Shear stress at the wall.

ε_m Turbulent diffusivity for momentum.

ε_q Turbulent diffusivity for heat.

ε Used interchangeably for ε_m or ε_q when $\varepsilon_m = \varepsilon_q$.

CHAPTER I

INTRODUCTION

Although today's industrialized world acknowledges its dependence on earth for oil, coal and other energy sources, it remains oblivious to the fact that sun is actually the source of all energy. In burning wood, we release the solar energy that was stored in the living tree by chemical action. The fossil fuels--coal and oil, as well as natural gas--are in effect stored solar energy; they constitute the remains of plant material that flourished millions of years ago in sunlight.

The radiation emitted by the sun into the space amounts to 378×10^{18} kilowatts--an amazing figure indeed. Even the minute portion that is received by the earth-- 170 trillion kilowatts--is astronomically high.

Kingston Plant, in the Tennessee Valley Authority, is the largest steam power plant in the world with a capacity of 1.5 million kw. One hundred seventy million Kingston power plants would have to be built to match the amount of solar energy received by the earth. To get an idea of the enormity of solar energy, the following example is cited. If an area of approximately 6,500 square miles of desert land in New Mexico were covered with solar mirrors,

enough power could be obtained, assuming only 10 per cent efficiency of conversion, to meet the entire power requirement of the United States.

How long is the stored solar energy going to be available in the form of coal, oil and natural gas? This question has received some appalling answers. Dr. R. G. Jordan and Dr. James L. Threlkeld, both professors at the University of Minnesota, have thoroughly studied the United States fuel reserves and drawn the following conclusions:

More than 85 per cent of all fossil fuels ever mined has been consumed since 1900. By "fossil fuels" the authors mean deposits of coal and oil which required about 500 million years for their formation. This high consumption rate is rendered more alarming by the fact that coal and oil cannot be replenished in another 500 million years.

Coal supplies of the world are estimated to last not much beyond the twentieth century. So far as the situation of the oil-producing countries is concerned, an even darker picture is painted. The Middle East, the leading supplier of the commodity, is consuming its oil reserves at the rate of 6.6 billion barrels a year, a rate estimated to be tripled by 1975; the 174 billion barrels of oil covered by the soil of the Middle East will last only eight years. Other oil-producing countries have equally alarming figures to quote. Ironically enough as the fossil fuels are

rapidly diminishing, the demand for power is increasing in almost geometric proportions.

In the face of the present situation, nuclear energy is soon expected to have an impact on industry which will be in every sense as dramatic as those made by the steam engine or electric motor. Nevertheless, only the highly industrialized countries can meet the high cost of investment.

Although the underdeveloped and emergent nations are deprived of nuclear energy because of its deterring cost, they are very rich in solar energy. Exploitation of the solar energy, at an ever-increasing scale, has to be undertaken for a prosperous and happier world of the near future.

Solar energy costs nothing to generate, transmit or distribute. Inexpensive equipment has been used for several applications of solar power. The heating and distilling of water, desalting the saline and brackish water, operating air conditioning plants and heating homes are a few of the applications to name.

Flat Plate Solar Energy Collectors

Solar energy collectors, the apparatus used for connecting solar power, are broadly classified into two categories: the concentrating and the flat type. The concentrating collectors are used to increase the flux density of

incoming solar energy and are used where higher temperatures are desired, as in metallurgical industries. Reflectors and mirrors are frequently employed in this type of collectors to magnify the solar flux density. The flat type collectors are relatively inexpensive and used where moderate or low rise in temperature is needed. Flat type collectors may be subdivided into liquid and gas heaters.

The solar water heaters in general consist of copper tubing, with or without fins, laid on a bed of insulation and covered by one or more glass cover plates. The pipes and fins are painted black for maximum absorption of energy.

The air heaters are categorized as: the metal plate, the black gauze, and the glass shingle. The metal plate type air heaters, by far the most common, utilize flat metal plate blackened on the side exposed to the sun. If the air passes at the back of the metal plate, an insulation is generally used parallel to the metal plate. The air passes between the metal plate and the insulation.

Very little research has been done on the use of solar energy collectors on farms. With the availability of large space for placing collectors, a farm affords attractive possibilities for harnessing solar energy. Moreover the energy requirement for the farm as compared with the energy falling on the available space is low. The temperature rise required for drying products and heating farm buildings is low. As little as 10 degrees rise in the

temperature of the outside air is sufficient to accelerate drying of farm crops to moisture contents which are safe for storage (1). The solar collector that will heat air for drying crops in summer and fall can be used for heating farm buildings in winter and spring.

For small temperature rise, the collector can be of a simple design. The expenditure incurred would as a result be low. Research conducted at Michigan State University has shown that it is possible to heat air by passing it under the galvanized steel sheet roofing (1).

The solar energy collector consists primarily of a series of rectangular ducts laid side by side with the sheet metal covering on the top. The sheet metal is exposed to the sun. This collector can be easily incorporated into the construction of a building; as it is essentially the same as a conventional roof with rafters and metal roofing, or a trussed roof with metal roofing and nailing girts. The only additional feature needed is to use some material to constitute the bottom of the duct. Plywood coupled with insulation could be used effectively. The purpose of the present investigation is to study the heat transfer and hydrodynamic characteristics of the rectangular air duct formed by two rafters, constituting the vertical sides; plywood (plus insulation) forming the lower side and the galvanized steel sheet constituting the top. The two rafters constitute the shorter sides of the duct.

Nature of the Problem

It is a standard practice in the construction of roofs to place successive rafters two feet apart, measured from center to center. The longer side of the duct is, therefore fixed. The depth between the plywood and galvanized steel is the variable that can be employed to control heat transfer and pressure drop in the duct.

Lengths of 50 feet[1] or more for the ducts mentioned above will not be uncommon for use on the farm. The flow as a result will be fully developed (both hydrodynamically and thermally) for most part of the duct. Even an air flow as low as 150CFM (which, for a 50 foot long roof, means a flow of 1½CFM per square foot of roof area) will result in a Reynolds number of over 7500 in a 6-inch deep duct. A survey of literature on the critical Reynolds number is presented in Table 1.

A typical Reynolds number (Re) of 2300 is generally accepted for tubes and ducts (8). Between Reynolds numbers of 2300 to 7000 the flow is in the transition regime as found in several experimental studies.[2]

Since air flow in the present investigation is expected to be in excess of 1½CFM per square foot of roof area, it may be safely assumed that the flow in the ducts is turbulent. The hydrodynamic and thermal boundary

---

[1]For a 2" nominal depth it equals a length of 162.5 hyd. diameter.

[2]See, for instance, ref. 6.

TABLE 1.--Values of Re_{crit} for Noncircular Ducts as Reported by Various Investigators.

Investigator	Geometry	Re_{crit}
Nikuradse, J. (2)	Rectangle $\frac{b}{a}$ = 3.50	2800
	Equil. triangle	2800
	Right isoceles triangle	2800
	Acute triangle	2000-2360
	Trapezoid	2000-2360
Washington and Marks (3)	Rectangles, $\frac{b}{a}$ = 40 and 20	2400
Schiller, L. (4)	Rectangle $\frac{b}{a}$ = 3.52	1600
	Square	2100
Davis and White (5)	Rectangles, $\frac{b}{a}$ = 40	2800
Eckert and Irvine (6)	Rectangle $\frac{b}{a}$ = 3	5000 6000--Smooth entrance
	Isoceles triangle, 23°	1800--Abrupt entrance
Cornish, R. J. (7)	Rectangles $\frac{b}{a}$ = 2.92	2800

layers start simultaneously at the entrance of the duct. The duct has an abrupt entrance. The thermal boundary layer develops only on one side as the duct is heated only at the top.

The galvanized steel sheet is subjected to uniform heat flux. The bottom of the duct is adiabatic. This gives rise to axially uniform but unsymmetrical boundary conditions.

Since plywood, galvanized steel and lumber are used in the construction, the duct is expected to lie in the region of rough tubes.

The problem may be summarized as follows: to study fully developed turbulent flow in an unsymmetrically heated rough rectangular air duct, heated from above.

Another duct was also built where flat galvanized steel sheet was replaced by a corrugated sheet. The corrugations run normal to the direction of flow. This duct will serve to give an estimate of increase in heat transfer and pressure drop when corrugated top is used.

CHAPTER II

LITERATURE REVIEW

Hydrodynamic Characteristics of Circular and Noncircular Ducts with a Turbulent Flow

Critical Reynolds Number (Re_{cr})

A survey of literature on critical Reynolds number is summarized in Table 1.

With the conditions that are found in industrial applications flow is usually turbulent (9) when the Reynolds number exceeds the value 3000. By eliminating all disturbances, a critical Reynolds number of 500,000 was attained (9).

Intake Region

Near the entrance of a duct, the presence of the duct wall makes itself felt only a small distance into the fluid. The influence of the wall is confined to a thin viscous layer. This thin viscous layer, called boundary layer, grows in the downstream direction until it has finally penetrated through the whole flow. The cross section where this occurs marks the end of the "intake region" and the beginning of the "fully-developed flow region." Actually the flow approaches the developed velocity field asymptotically and there is always a certain arbitrariness in the definition of "intake length." In this thesis the intake

length will be defined as that length at which the pressure drop per unit length has reached a constant value within the accuracy of the measurements.

Deissler (10) analytically studied the intake region characteristics for smooth tubes and parallel plate channels. Integral heat transfer and momentum equations were used for calculating thermal and hydrodynamic boundary layers. The flow was assumed to be turbulent at all points along the passage.

Deissler has given the following equations relating hydrodynamic boundary layer thickness (δ) to distance along the passage.

1. For the tube.

$$\frac{x}{d} = \int_{\frac{Re}{2}}^{u_c^+ r_o^+} \left[\frac{1}{4}\left(\frac{\delta^+}{r_o^+}\right)\frac{1}{r_o^+}\left(2-\frac{\delta^+}{r_o^+}\right)u_c^+ - \frac{1}{2(r_o^+)^3} \int_0^{\delta^+} u^+(r_o^+ - y^+)dy^+ \right] d(u_c^+ r_o^+)$$

$$+ \int_0^{[\,]} \frac{1}{2(r_o^+)^2}\, d\left[\int_0^{\delta^+}(u_c^+ - u^+)\, u^+(r_o^+ - y^+)dy^+\right]$$

2. For parallel plate channel

$$\frac{x}{d_h} = \frac{1}{4}\int_{\frac{Re}{4}}^{u_c^+ \frac{a^+}{2}} \frac{\delta^+ u_c^+}{(r_o^+)^2} - \left(\frac{1}{(r_o^+)^2}\int_0^{\delta^+} u^+ dy^+\right) d(r_o^+ u_c^+) +$$

$$\frac{1}{4}\int_0^{[\,]} \frac{1}{(r_o^+)^2}\, d\left[\bar{r}_o^+ \int_0^{\delta^+} (u_c^+ - \bar{u}^+)\, \bar{u}^+\, d\bar{y}^+\right]$$

where [] indicates that the variable of integration should be used as the upper limit.

An intake length of less than 10 hyrdaulic diameters ($d_h = \frac{4 \text{ x cross sectional area}}{\text{perimeter}}$) was noted.

Deissler has followed Prandtl's assumption: in the presence of a laminar boundary layer near the entrance, the turbulent portion of the boundary layer behaves as though the boundary layer were turbulent all the way from the entrance (11). Deissler's calculations which assume the flow to be turbulent at all points may be applied to the turbulent portion of the boundary layer even when a laminar boundary layer exists near the entrance.

Deissler (12) has investigated the effect of various factors on friction in the entrance region of smooth passages. The influence of Reynolds number, Prandtl number, passage shape and variable fluid properties is predicted. The results based on integral momentum equations indicate that approximately fully developed flow is generally attained in an intake length of less than 10 hydraulic diameters.

Deissler's (12) analysis agrees with the analysis of Pascucci (13), who obtained for turbulent flow in a tube

$$\frac{L_e}{d} = 3.80 \log_{10} Re - 2.14$$

Both of these analyses are somewhat higher than the corrected predition of Latzko (14).

$$\frac{L_e}{d} = 0.623\ (Re)^{\frac{1}{4}}$$

It should be pointed out, however, that all these analyses are considerably lower than the experimental values obtained by Schiller and Kirsten (15) who found lengths of 50 diameters and greater to be necessary for the attainment of the fully developed flow. It should be mentioned that the long intake lengths found in these experiments refer to the length required for the velocity profile to develop rather than the pressure gradient or shear stress to reach their fully developed values. They apparently did not measure pressure drops.

The same result was obtained in Hartnett's (16) experiments where at the tube center the velocity profile was still developing slightly at values of x/d greater than 75 although pressure gradients had long before reached their fully developed values.

Hartnett et al. (17) found experimentally that rectangular ducts with abrupt entrance have an intake length of less than 20 hydraulic diameters ($d_h = \frac{2ab}{a+b}$ for a rectangular duct).

Friction Coefficient

Pressure drop for fully developed flow in tubes is given by Fanning's equation

$$\frac{dP}{dx} = \frac{f}{d_h} \rho \frac{u_m^2}{2}$$

For fully developed turbulent flow in tubes coefficient of friction f is given by Blasius law.

$$f = \frac{0.316}{(Re)^{\frac{1}{4}}}$$

Blasius law holds good for smooth ducts of noncircular cross section when Reynolds number is based on hydraulic diameter (18).

For isothermal flow in ducts, the integrated flow equation based on perfect gas laws is as follows (19).

$$P_i^2 - p_o^2 = \frac{f\ L\ G^2\ R\ T}{g\ d_h\ M} \left(1 + \frac{4.61 d_h}{f\ L} \log_{10} \frac{P_i}{P_o}\right)$$

where R is gas constant = 1546 ft lb_f per (lb. mole) (R°) and M is molecular weight lb_m per (lb. mole).

In ducts of appreciable length the last term in the parentheses can be neglected unless the pressure drop is significant. The resulting equation is

$$P_i - P_o = \frac{f\ L\ G^2}{2\ g\ \bar{\rho}\ d_h} = \frac{f\ L}{d_h}\ \bar{\rho}\ \frac{u_m^2}{2g}$$

where $\bar{\rho}$ is the density of fluid at the average pressure

$$\frac{p_i + p_o}{2}$$

In uniform horizontal ducts, an approximate result is as follows (19)

$$P_i - P_o = 2.30\ \frac{G^2}{g\ \bar{\rho}}\ \log_{10}\ \frac{v_o}{v_i} + \frac{f\ L\ G^2}{(d_h\ \bar{\rho})(2g)}$$

Intake Losses

For design purposes, it is essential to determine the overall pressure drop which fluid would experience in flowing through a duct length L. Entrance and intake losses constitute an important part of the total pressure drop. This loss is particularly important in short ducts. The following method has been adopted to determine the overall pressure drop. Frictional pressure is calculated as if established flow conditions would exist over the full length L and a second term is added which accounts for the increase in pressure drop due to inlet and intake conditions.

$$P_o - P = f\ \frac{L}{d_h}\ \rho\ \frac{u_m^2}{2} + \overset{*}{K}\ \rho\ \frac{u_m^2}{2}$$

where P_o is the pressure of stationary fluid ahead of the duct and P is the pressure at distance L from the inlet.

The four components of constant $\overset{*}{K}$ in the above equation account for the following losses:

1. K_1: Loss due to acceleration of fluid from rest to the constant velocity u_m just before it reaches the inlet.
2. K_2: Loss due to abrupt contraction at inlet.
3. K_3: Loss due to the momentum flux increase in the intake region which is connected with the transformation of the velocity fluid.
4. K_4: Loss due to an increase in friction in the inlet region.

For laminar flow through a circular tube $K_1 + K_2 = 2$. Calculations by Schiller (20) show that

$$K_1 + K_2 + K_3 = 2.16.$$

Goldstein (21) calculated the parameter $(K_1 + K_2 + K_3)$ to be 2.41.

For turbulent flow in a round tube the value of $\overset{*}{K}$ is found to be 1.058.

Rough Pipes and Ducts

Most pipes used in engineering practice cannot be regarded as being hydraulically smooth. The resistance to flow offered by rough walls is larger than that given by equations for smooth pipes.

Two types of roughness in relation to the resistance formula for rough pipes have been noted. The first kind of roughness causes a resistance which is proportional to the square of the velocity, meaning therby that the coefficient of friction is independent of the Reynolds number. This type of roughness corresponds to relatively coarse and tightly spaced roughness elements, e.g., rough cast iron or cement. In such cases the nature of the roughness can be expressed with the aid of a single roughness parameter K/R_h, the so-called relative roughness, where K is the height of a protrusion and R_h denotes the radius or the hydraulic radius of the cross section. The resistance coefficient is, therefore, a function of relative roughness in the first type of roughness. For geometrically similar roughness Fromm (22) and W. Fritsch (23) found that coefficient of friction is proportional to $(K/R_h)^{0.314}$.

The second type of roughness occurs where the protrusions are more gentle or when a small number of them is distributed over a relatively large area, such as those in wooden ducts and commercial steel pipes. In such cases the

coefficient of friction depends both on the Reynolds number and the relative roughness.

Extensive and systematic measurements have been carried out on rough pipes by Nikuradse (24) who used circular pipes covered on the inside very tightly with sand of a definite grain size glued on to the wall. By varying the size of the pipes and the grain size, he was able to vary the relative roughness from about 1/1500 to 1/15.

Based on Nikuradse's findings, three different regions are to be considered in the case of rough pipes.

1. hydraulically smooth regime

$$0 \leq \frac{K\sqrt{\tau_w/\rho}}{\nu} \leq 5 \qquad f = f(\frac{K}{R_h}, Re)$$

The size of the roughness is so small that all protrusions are contained within the laminar sublayer.

2. transition regime

$$5 \leq \frac{K\sqrt{\tau_w/\rho}}{\nu} \leq 70 \qquad f = f(\frac{K}{R_h}), Re)$$

Protrusions extend partly outside of the laminar sublayer and an additional resistance as compared with the smooth pipe, is mainly due to the form drag experienced by the protrusions in the boundary layer.

3. Completely rough regime

$$\frac{K\sqrt{\tau_w/\rho}}{\nu} > 70 \qquad\qquad f = f(\frac{K}{R_h})$$

Here all protrusions reach outside the laminar sublayer and the largest part of the resistance to flow is due to the form drag which acts on them.

Von Kármán derived the following formula for completely rough pipes from the similarity laws.

$$f = \left[2 \log (\frac{R_h}{K}) + 1.68 \right]^{-2}$$

Closer agreement is obtained with experiments when the constant 1.68 is replaced with 1.74. The resistance formula for the rough pipes becomes

$$f = \left[2 \log \frac{R_h}{K} + 1.74 \right]^{-2}$$

An equation which correlates the whole transition regime:

$$5 \leq \frac{K\sqrt{\tau_w/\rho}}{\nu} \leq 70$$

was introduced by Colebrook (25).

$$\frac{1}{\sqrt{f}} = 1.74 - 2 \log \left[\frac{K}{R_h} + \frac{18.7}{R_h\sqrt{f}} \right]$$

Moody (26) has reported an extensive experimental work on commercially rough pipes. His graphs of f against Re for different values of relative roughness is in essence identical with Nikuradse's results.

Colebrook's function, when solved for relative roughness, gives

$$\frac{K}{d_h} = \log^{-1}\left(0.57 - \frac{1}{2\sqrt{f}}\right) - \frac{9.3}{Re\sqrt{f}}$$

Moody's and Nikuradse's graphs are applicable to ducts of noncircular cross sections. Pipe diameter of the duct should be replaced by the hydraulic diameter of the duct.

Several analytical and presumptive theories have been advanced about the nature of turbulent flow in rough pipes and the effect of roughness on friction factor. Piggott (27) has suggested that the presence of roughness protrusions on the pipe wall cause the formation of a stagnant fluid film at the boundary region of the fluid stream. Since the thickness of this stagnant film is proportional to the mean length of the roughness protrusions, it tends to decrease the effective diameter of the fluid stream in the same proportion. The resulting reduction in effective diameter causes a significant increase in the resistance to flow.

Heat Transfer Characteristics of Circular and Noncircular Ducts with a Turbulent Flow

Fully Developed Turbulent Heat Transfer in Smooth Ducts

Reynolds' analogy is expressed as

$$q = - \tau \, c_p \frac{dt}{du}$$

For fully developed flow in a tube, integrating this equation and assuming that $\frac{q}{\tau} = \frac{q_w}{\tau_w} = \text{const.}$ we obtain

$$t_c - t_w = \frac{q_w}{\tau_w} \frac{u_c}{c_p} \qquad (Pr = 1)$$

Replacing u_c by u_m and t_c by t_B (though not quite correct) and multiplying both sides by the tube wall surface area, there is obtained, for the total heat flow to the fluid

$$Q_w = R \frac{c_p}{u_m} (t_B - t_w)$$

where R is the resistance ($R = \tau_w \, \pi d \, L = \Delta P \, \pi \frac{d^2}{4}$). This simple relation between the heat flow Q_w and the resistance R holds true only for a medium with Pr = 1. Since all gases have Prandtl numbers which deviate only slightly from unity, the expression for Q_w is useful in obtaining a first approximation for the heat transfer when the resistance is known.

Prandtl (28) and Taylor (29) independently arrived at the following expression for turbulent heat transfer coefficient for a flat plate

$$h = \frac{\tau_w \, c_p / u_s}{1 = \frac{u_b}{u_s} (Pr - 1)}$$

This relation has been modified to apply to fully developed heat transfer in tubes. The resulting expression is

$$St = \frac{0.0384 \, (Re)^{-1/4}}{1 + 1.5 \, Pr^{-1/6} (Re)^{-1/8} (Pr - 1)}$$

This relation is superseded by the following expression which assumes the presence of buffer layer in conjunction with distinct laminar and turbulent layers.

$$St = \frac{Nu}{RePr} = \frac{(\phi_m / \theta'_B) \frac{f}{8}}{1 + \phi_m \sqrt{\frac{f}{8}} \left\{ 5 \, (Pr-1) + 5 \ln \left[(5Pr + 1)/6 \right] \right\}}$$

where

$$\theta'_B = \frac{t_B - t_w}{t_c - t_w}$$

and

$$\phi_m = \frac{u_m}{u_c}$$

and for the turbulent velocity profile $\phi_m = 0.82$. In reality it changes somewhat with Reynolds number. The friction coefficient f is given for smooth tubes as

$$f = \frac{0.316}{(Re)^{1/4}} \qquad Re < 10^5$$

For Reynolds number greater than 10^5, the general resistance law developed by L. Prandtl, T. Von Kármán and coworkers (30) is

$$\frac{1}{\sqrt{f}} = 2.0 \log_{10} \left[(Re) \sqrt{f} \right] - 0.8$$

The problem of forced heat convection in turbulent flow through a tube at uniform surface temperature was first analyzed by Latzko in 1921. He gave the following equaiton for temperature distribution in a circular tube when flow is fully developed.

$$\frac{\partial}{\partial r} \left[r\left(\frac{\frac{d^2}{4} - r^2}{d}\right) \frac{\partial t^*}{\partial r} \right] = Hr \left[1 - \left(\frac{2r}{d}\right)^2 \right]^{1/7} \frac{\partial t^*}{\partial x}$$

where t^* = temperature difference between the wall and the given point, and

$$H = \frac{8}{7} \frac{u_m^{1/4} (d)^{3/28}}{0.199\nu^{1/4}}$$

Other symbols have the same meanings as given under NOMENCLATURE.

Latzko arrived at the following solution for the temperature distribution:

$$\frac{t^*}{t_w - t_B} = 1.29e^{-P_1 x} (0.9544n - 0.0212n^3 + 0.0668n^5)$$

$$- 0.180e^{-P_2 x} (-0.7472n - 4.275n^3 + 6.022n^5)$$

$$+ 0.048e^{-P_3 x} (20.34n - 54.80n^3 + 35.47n^5)$$

where

$$n = [1 - (\frac{2r}{d})^2]^{1/7}$$

$$P_n = \zeta_n \frac{1}{d} \sqrt[4]{\frac{\nu}{u_m d}}$$

$$\zeta_1 = 0.1510, \quad \zeta_2 = 2.844, \quad \zeta_3 = 29.42$$

Latzko further derived the following equation for a local heat transfer coefficient

$$h = \left[0.0345 u_m \rho\, c_p \left(\frac{\nu}{u_m d}\right) \right] \left[\frac{1.078 e^{-P_1 x} + 0.134 e^{-P_2 x} + 0.980 e^{-P_3 x}}{0.970 e^{-P_1 x} + 0.024 e^{-P_2 x} + 0.006 e^{-P_3 x}} \right]$$

Sparrow and Siegel (31) have examined the effect of wall boundary conditions on Nusselt number for turbulent heat transfer in both the fully developed and thermal entrance region of a circular tube. The comparisons are made for:

1. Uniform wall temperature
2. Uniform wall heat flux.

Computations were carried out for the uniform wall temperature case, [reference (32)] using the same eddy diffusivity and velocity distribution as for uniform wall heat flux in references (33) and (34). The calculations were carried out under the assumption of equal diffusivity of heat and momentum.

The results for Pr = 0.7 are presented for four values of Reynolds number (10^4, 5×10^4, 10^5, 5×10^5). The per cent difference was defined as

$$Y = \frac{(Nu)_{\text{uniform flux}} - (Nu)_{\text{uniform wall temperature}}}{(Nu)_{\text{wall temperature}}}$$

The largest values of Y were recorded at low Reynolds numbers, and for each case the values drop at larger distances from

the tube entrance. For the ranges of variables considered, the effect of the two different wall boundary conditions was found to be always less than 10 per cent.

At higher values of Prandtl number (Pr = 10 and Pr = 100) there was essentially no influence of the two boundary conditions in the range of Reynolds numbers considered. It may be concluded that for turbulent flow the heat transfer mechanism in the thermal entrance and fully developed regions is quite insensitive to the two wall boundary conditions. This conclusion is supported by the findings of Deissler (12) who carried out calculations for the thermal entrance region of a circular tube (using a boundary layer model) for Pr = 0.73. Further support is given by Seban and Shimazaki (35) who considered fully developed flow in a circular tube for Pr = 1.

Sparrow, Siegel and Hallman (33) have given the analytical results for the fluid temperature distribution and Nusselt number for tube with a uniform wall heat flux. The fluid temperature distribution is given by

$$\frac{t - t_i}{q_w \frac{d}{2K}} = \frac{2}{RePr} \frac{x}{d} + G(r) + \sum_{n=1}^{\infty} C_n \phi_n(r) e^{-4\beta_n^2 x/d \, Re}$$

where $G(r)$ is the fully developed temperature distribution, β_n and ϕ_n are the eigenvalues and eigenfunctions, r is the distance from tube axis measured in the radial direction.

The Nusselt number given by the authors is

$$Nu = G(d/2) \frac{1}{1 + \sum_{n=1}^{\infty} A_n \exp(-4\beta_n^2 x/dRe)}$$

where

$$A_n = C_n \phi_n(\tfrac{d}{2})/G(\tfrac{d}{2})$$

Sparrow and Siegel (32) have considered turbulent heat transfer in tubes with uniform wall temperature. The analytical results are given for fluid temperature distribution and heat transfer coefficients. The fluid temperature distribution is given by

$$\frac{t - t_w}{t_i - t_w} = \sum_{n=1}^{\infty} C_n \phi_n(r) \exp(-4\beta_n^2 x/d\ Re)$$

where β_n and ϕ_n are the eigenvalues and eigenfunctions, r is the distance from the tube axis measured in a radial direction, and C_n are constants.

The Nusselt number is given by

$$Nu = Pr \frac{\sum_{n=1}^{\infty} C_n (\frac{d\phi_n}{dr})_{d/2} \exp(-4\beta_n^2 x/d\ Re)}{\sum_{n=1}^{\infty} \frac{C_n}{\beta_n^2} (\frac{d\phi}{dr})_{d/2} \exp(-4\beta_n^2 x/d\ Re)}$$

Deissler (12) has given analytical solution for fully developed turbulent flow in a tube having uniform heat flux. According to him

$$Nu = \frac{d^+ Pr}{t_B^+}$$

and $Re = u_b^+ d^+$

where

$$t_B^+ = \frac{\int_0^{\frac{d^+}{2}} \frac{t^+ u^+ (\frac{d^+}{2} - y^+)}{1 - \beta t^+} dy^+}{\int_0^{\frac{d^+}{2}} \frac{u^+ (\frac{d^+}{2} - y^+)}{1 - \beta t^+} dy^+}$$

and

$$u_b^+ = \frac{8}{(d^+)^2} \int_0^{\frac{d^+}{2}} u^+ (\frac{d^+}{2} - y^+) dy^+$$

and β is a heat transfer parameter given by

$$\beta = \frac{q_w \sqrt{\tau_w}/\rho}{c_p \tau_w g t_w}$$

The physical properties in Deissler's equations are evaluated at wall temperature. Dittus and Boelter (35) recommend the following empirical equations for tubes

$$Nu = 0.0243\ (Re)^{0.8}\ (Pr)^{0.4}$$

for heat flow from the wall to the fluid and

$$Nu = 0.0265\ (Re)^{0.8}\ (Pr)^{0.3}$$

for heat flow from the fluid to the wall.

From a review of the work of various experimenters, McAdams (36) has concluded that a fair correlation of their results for the heating and cooling of various fluids in turbulent flow in horizontal tubes is shown by the equation

$$Nu = 0.023\ Re^{0.8}\ Pr^{0.4}$$

This equation applies when the Reynolds number is within the range of 10,000 to 12,000, the Prandtl number is between 0.7 and 120. and the physical properties of the fluid are evaluated at the bulk temperature.

Martinelli (37) derived an equation based on the following assumptions:

1. Heat and momentum are transferred by molecular action alone in the laminar sublayer.
2. Heat and momentum are transferred by molecular action and by eddy diffusion in the buffer layer.

3. Heat is transferred by thermal conduction and eddy diffusion in the turbulent core, and momentum is transferred by eddy diffusion alone.

With these assumptions Martinelli's equation for fully developed turbulent flow in an isothermal tube is

$$Nu = \frac{0.04\ PrRe^{7/8}}{Pr + \ln(1 + 5Pr) + \frac{1}{2(1+\beta)} \ln \frac{Re^{7/8}}{300}}$$

In this equation β is a factor which depends on the ratio of molecular conduction to the eddy diffusion heat transfer in the turbulent core.

Lyon (38) developed an approximation of the Martinelli equation for values of $Pr < 0.1$. This equation which gives values within 10 per cent of the Martinelli's values.

$$Nu = 7 + 0.025\ (Re)^{0.8}\ (Pr)^{0.8}$$

In Martinelli's and Lyon's equations the physical properties are evaluated at the bulk temperature if the difference between the bulk temperature and that of the surface the fluid is in contact with, is not large. At higher rates of heat transfer, the temperature which is selected is usually the bulk temperature or the mean of bulk and surface temperatures.

On the basis of foregoing observation and as a result of tests with viscous oils, Sieder and Tate (39) concluded

the surface conductance for both the heating and the cooling of viscous liquids in turbulent flow is well expressed by

$$Nu = 0.027(Re)^{0.8}(Pr)^{1/3}\left(\frac{\mu_B}{\mu_w}\right)^{0.14}$$

Colburn (40) has given the following relation for turbulent flow

$$\frac{h}{G\ c_p}\ (Pr)^{2/3} = 0.023(Re)^{-0.2}$$

McAdams, Nicolai and Keenan (41) give the following expression for the fully developed turbulent flow

$$\left(\frac{h}{G\ c_p}\right)\ (Pr)^{2/3} = 0.027(Re)^{-0.23}$$

Use of Hydraulic Diameter for Noncircular Ducts

The predictions of fully developed turbulent pressure drops and heat transfer in noncircular ducts is presently based on the hydraulic diameter concept. It is seen that for a wide variety of duct shapes, the pressure drop and heat transfer correlations which are valid for circular tubes may be applied to noncircular ducts if the hydraulic diameter $\frac{4 \times \text{cross sectional area}}{\text{perimeter}}$ is substituted for the characteristic dimension in the friction factor and the Reynolds number.

A large number of investigations which correlate pressure drop data based on hydraulic diameter concept have been summarized by Claireborn (18) and Eckert and Irvine (6). It should be noted, however, that the hydraulic diameter concept does not hold for all geometries; for example, experimental studies (42, 43) have shown that the hydraulic diameter rule can be in error by as much as 20 per cent in small opening angle triangular ducts. For laminar flow the pressure drop is even more sensitive to the shape of duct cross section, and the hydraulic diameter does not satisfactorily correlate the result of circular and noncircular shapes.

The hydraulic diameter rule, although it has enjoyed considerable success, has little rational justification for its use and it throws no light on the basic mechanisms involved in noncircular duct flow. Deissler and Taylor (44) have attempted to construct a model of turbulent and noncircular duct flow from which calculations of the velocity field and pressure drop may be made. Essentially their procedure consists of the specification that on lines normal to the duct walls the velocity distribution may be characterized by the universal velocity profile which has been established for circular tubes. The analysis neglects the secondary flows.

The heat transfer characteristics of noncircular geometries have been investigated to a lesser extent than the

flow. An experimental investigation (42) of turbulent heat transfer in an electrically heated triangular duct with an opening angle of 11.46° has shown that the use of hydraulic diameter overestimates the average heat transfer coefficient by as much as 100 per cent. Another serious limitation of the hydraulic diameter concept is that the local heat transfer conditions cannot be determined. This applies in particular to the circumferential variations of wall temperature or specific heat flow at the wall. This is reckoned as a serious limitation, since in certain geometries the local temperatures can be considerably higher than those predicted by the average results. This can result in serious design and metallurgical setbacks.

Deissler (12) has given the following equations for a parallel plate channel

$$Nu = \frac{2a^+ Pr}{t_B^+}$$

and

$$Re = 2\, u_p^+\, a^+$$

where

$$t_B^+ = \frac{\int_0^{a^+/2} \frac{t^+ u^+}{1 - \beta t^+}\, dy^+}{\int_0^{a^+/2} \frac{u^+\, dy^+}{1 - \beta t^+}}$$

and

$$u_p^+ = \frac{2}{a^+} (1 - \beta t_B^+) \left[\int_0^{a^+/2} \frac{u^+}{1 - \beta t^+} \, dy^+ \right]$$

$$\beta = q_w \sqrt{\tau_w / \rho} / g \, c_p \, \tau_w \, t_w$$

The physical properties in Deissler's equations noted above should be evaluated at wall temperature.

Sparrow and Lin (45) have presented analytical results for the fully developed heat transfer characteristics of turbulent flow in a parallel plate channel with symmetric uniform wall heat flux. The results were obtained by integrating the energy equation utilizing a suitably chosen eddy diffusivity for heat. The fully developed Nusselt numbers were presented as a function of Prandtl number for the range Pr = 0.7 to 100. The Reynolds number, which appeared as parameter, ranged from 10,000 to 500,000. The results were compared with McAdam's (36) empirical correlation of circular tube data,

$$Nu = 0.023 \, Re^{0.8} \, Pr^{0.4}$$

This correlation is usually regarded as the first approximation to noncircular geometries provided that hydraulic diameter is used. The comparison indicated that the use of the hydraulic diameter is reasonably successful in

bringing together the results for the two geometries. The analytical results for both geometries suggested that the dependence of the Nusselt number on Prandtl number is more complex than the simple power law appearing in the empirical correlation. The largest deviation between the theory and empirical correlation appeared in the mid-range of Prandtl numbers (10).

Barrow (46) has given the following analytical expression for fully developed turbulent flow in a smooth parallel plate channel, both walls of which are subjected to constant and equal heat flux.

$$Nu = \frac{0.1986\ Re^{7/8}\ Pr}{9.74\ Pr + 5.03\ Re^{1.8} - 9.74}$$

Barrow used the following expressions for velocity distribution

$$u^+ = 6.2 \log_{10} y^+ + 3.6 \qquad \text{in turbulent region}$$

$$u^+ = y^+ \qquad \text{for laminar sublayer}$$

The presence of buffer layer was neglected in Barrow's analysis.

Barrow (47) conducted a theoretical and experimental study of heat transfer in fully developed turbulent flow in a smooth parallel plate channel. In theoretical analysis,

surface heat flux at the walls was assumed to be uniform in flow direction. In the experiments, the flow conditions were simulated by ducts of large aspect ratio. The theory is more rigorous than the one given in earlier paper (46) and is adequately supported by the experimental data. The theoretical expression for Nusselt number is:

$$Nu = \frac{0.139\ Re^{7/8}}{5.03\ Re^{-1/8} - 3.06} \qquad (Pr = 0.7)$$

This equation follows more closely the line representing McAdams' well-established expression

$$Nu = 0.023\ Re^{0.8}\ Pr^{0.4}$$

particularly in the higher range of Reynolds number.

In his analysis Barrow assumed a turbulent and a laminar sublayer. Velocity distribution in the channel was taken from Corcoran et al. (48).

$$u^+ = \frac{1}{0.0695} \tan h\ (0.0695\ y^+) \qquad 0 \leq y^+ \leq 27$$

$$u^+ = 5.5 + 2.5\ \ln\ y^+ \qquad y^+ > 27$$

The following expressions were used for ε_q.

1. $0 \leq y^+ \leq 27$, $\varepsilon_q = \left[1 - \frac{2y^+}{a^+} \right]$

$$\left[\nu \cosh^2 (0.0695\ y^+)\right] - \nu$$

2. $27 \leq y^+ \leq \frac{a^+}{3}$,

$$\varepsilon_q = \left[1 - \frac{2y^+}{a^+}\right]\left(\frac{y^+\nu}{2.5}\right) - \nu$$

3. $\frac{a^+}{3} \leq y^+ \leq \frac{a^+}{2}$, $\qquad \varepsilon_q = \frac{a^+\nu}{22.5} - \nu$

Pr_t was assumed to be unity.

Fully Developed Turbulent Flow in Unsymmetrically Heated Ducts

Unsymmetrically heated ducts have received attention rather lately.

As a first approximation the results given under symmetrically heated tubes can be used by substituting hydraulic diameter of the duct for the tube diameter. It is to be emphasized that full perimeter is used in computing hydraulic diameter, even when only a part is heated or cooled (49). Only in calculating the heat flow from basic heat transfer equations is the heated area alone to be used.

Henry Barrow (46) has given a semi-theoretical analysis of unsymmetric heat transfer in fully developed two-dimensional heat transfer between parallel plates. The boundary conditions consisted of a heat flux q_w through one

wall and a heat flux of $-\gamma q_w$ through the other; where γ is a factor ranging between -1 and 1.

The velocity distribution in the channel as used by Barrow is

$$u^+ = 6.2 \log_{10} y^+ + 3.6$$

for the turbulent layer and

$$u^+ = y^+$$

for the laminar sublayer.

The laminar sublayer with this velocity distribution extends to $y^+ = 9.74$ Barrow gives the following expression for the Nusselt number.

$$Nu = \frac{0.1986\ Re^{7/8}\ Pr}{5.03\ (2 - \gamma)\ Re^{1/8} + 9.74\ [Pr - (2 - \gamma)]}$$

Barrow (47) presented another theoretical and experimental study of unsymmetric heat transfer in fully developed turbulent flow in a parallel plate channel. The heat fluxes at the plate surface were of different magnitudes and in the theoretical treatment each surface heat flux was assumed to be axially uniform. Ducts with large aspect ratios were used to simulate two-dimensional flow. Heat transfer measurements were made firstly with one wall insulated and then with heat transfer at both walls. The

heat transfer coefficients found experimentally for the wall through which heat flowed to the fluid, were seen to be less than the accepted value for the case of symmetrical heat transfer. The heat transfer coefficient was seen to decrease with an increase in the degree of asymmetry. The theory based on an analogy of heat and momentum transfer is more rigorous than the one reported in reference (46) by the same author.

According to new analysis, the expressions for Nusselt number are:

Case 1.--Wall heat fluxes of equal magnitude but of opposite sign.

$$Nu = \frac{Re\ Pr\ q_w}{c_p\ \rho\ u_n(t_w - t_B)}$$

where

$$t_w - t_B = \frac{q_w\ Pr}{c_p \rho \sqrt{\tau_w/\rho}} \left[I_1 + I_2 + I_3 \right]$$

The integrals I_1, I_2, I_3 are given by the following expressions:

$$I_1 = \int_0^{27} \frac{dy^+}{\left[Pr\left(1 - \frac{2y^+}{a^+}\right) \cosh^2 (0.0695y^+) - (Pr-1) \right]}$$

$$I_2 = \int_{27}^{a^+/3} \frac{dy^+}{(1 - \frac{2y^+}{a^+})(\frac{y^+}{2.5})\,Pr - (Pr - 1)}$$

and

$$I_3 = \frac{a^+}{6\left[(Pr\,\frac{a^+}{2.5}) - (Pr - 1)\right]}$$

Case 2.--One wall of the channel insulated.

The following expression is given for the Nusselt number.

$$Nu = \frac{0.1986\ Re^{7/8}}{I_1 + I_2 + I_3 + I_4}\ (\frac{t_{w_1} - t_{w_2}}{t_{w_1} - t_B})$$

where

$$I_1 = \int_0^{27} \frac{(1 - \frac{y^+}{a^+})\,dy^+}{Pr\,\cosh^2(0.0695y^+)(1 - \frac{2y^+}{a^+}) - (Pr - 1)}$$

$$I_2 = \int_{27}^{a^+/3} \frac{(1 - \frac{y^+}{a^+})\,dy^+}{(1 - \frac{2y^+}{a^+})(y^+\,\frac{Pr}{2.5}) - (Pr - 1)}$$

$$I_3 = \frac{a^+}{6\left[\,Pr\,\frac{a^+}{22.5} - (Pr - 1)\,\right]}$$

$$I_4 = \int_{27}^{a^+/3} \frac{(\frac{y^+}{a^+})\,dy^+}{(1 - \frac{2y^+}{a^+})(\frac{y^+}{2.5})\,Pr - (Pr - 1)}$$

These formulas although more accurate need extensive numerical computation and have obvious limitations for practical use.

Hatton (50) has considered fully developed turbulent flow in a parallel plate channel with one wall insulated and the other one having a constant axially uniform heat flux. He has solved the energy equation:

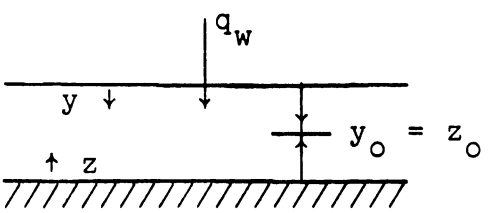

$$u^+ \frac{\partial t}{\partial x^+} = 4\,Z^+ \frac{\partial}{\partial Z^+}\left[\frac{\alpha + \varepsilon_q}{\nu}\,\frac{\partial t}{\partial Z^+}\right]$$

$$X^+ = \frac{x}{d_h}\;;\quad Z^+ = y_o^+ - y^+$$

The solution results in

$$Nu = \frac{4Z_o^+}{\theta_{q_w}^+ - \theta_{q_b}^+} \left(\frac{d\theta_q^+}{dZ^+}\right)_{Z_o^+}$$

where

$$\theta_q^+ = \frac{t - t_i}{\frac{q(y-y_o)}{2K}}$$

(t_i: the temperature at entrance to heated duct)

$$\theta_{q_b}^+ = \frac{\int_{-Z_o^+}^{Z_o^+} u^+ \theta_q^+ \, d Z^+}{\int_{-Z_o^+}^{Z_o^+} u^+ \, d Z^+}$$

Hatton and Quarmby (51) have presented a solution to the problem of fully developed turbulent flow in a parallel plate channel heated on one side only. A constant eddy diffusivity is assumed for the central region of the channel. In the solution of the energy equation Pr_t was assumed to be unity.

By the principle of superposition, the result is obtained for unequal uniform heat fluxes on each side of the passage. The results of Hatton and Quarmby entail extensive

numerical computations and their applicability is limited.

Hatton, Quarmby and Grundy in a later paper (52) made a few modifications in the analysis. ε_m is assumed to be constant over the middle third. $\varepsilon_m/\varepsilon_q$ is not taken to be unity. A semi-empirical relation is used for the value $\varepsilon_m/\varepsilon_q$.

Sparrow, Lloyd and Hixon (53) have conducted experiments on rectangular ducts with unsymmetrical thermal boundary conditions. Results are found to be in qualitative agreement with analytical predicitons for parallel plate channel.

Madsen (54) has suggested a characteristic heat transfer coefficient for parallel plates with axially uniform but unsymmetrical heat fluxes. This heat transfer coefficient is independent of heat flux symmetry and is defined as follows:

$$h_{general} = \frac{q_{w_1} + q_{w_2}}{(\overline{t_{w_1}} - t_B) + (\overline{t_{w_2}} - t_B)}$$

where suffixes 1, 2 refer to the two walls in the parallel plate.

Novotny, McComas, Eckert and Sparrow (55) studied fully developed turbulent flow in ducts. The aspect ratios ranged between 1:1 to 1:10. The heating conditions were such that the two longer walls were uniformly heated and the

two shorter walls were essentially adiabatic. The results for Nusselt Number (Nu) as a function of Reynolds Number (Re) were compared with the circular tube empirical correlation of Colburn (40) as well as with the analytical results of Siegel and Sparrow (34), for the circular tube and Sparrow and Lin (45) for the parallel plate channel. Both analytical studies (45, 34) were carried out for the case of uniform wall heat flux. The analysis for the parallel plate channel yielded Nusselt numbers which were approximately 5 per cent larger than the results of the circular tube analysis at a Reynolds number of 10^5 and approximately 10 per cent higher at a Reynolds number of 10^4. The experimentally-determined Nusselt numbers were, apart from some scatter, bracketed by the results of the two analyses. Additionally it was found that the empirically-based Colburn (40) correlation of circular tube data, which is frequently used for engineering calculations, lay somewhat higher than the experimental data, especially at the highest Reynolds numbers. The hydraulic diameter used in the analysis was based on total perimeter.

Entrance Region Studies for Symmetrically and Unsymmetrically Heated Circular and Noncircular Smooth Ducts with Turbulent Flow

Symmetrically Heated Ducts.--The thin boundary layers and consequently severe temperature gradients at the wall near the entrance produce high heat transfer coefficients in the entrance region.

As far back as 1913, Nusselt (56) drew attention to the effect of the length of tube on heat transfer and suggested the following equation

$$Nu = a' \, Re^{n} \, Pr^{m} \, (\frac{d}{L})^{c}$$

with c = 0.055. This equation gives zero heat transfer as $\frac{L}{d} \to \infty$.

In 1943, H. Hausen (57) gave the following expression for the average Nusselt number in entrance region over length x of a smooth tube

$$\overline{Nu} = 0.116 \left[(Re)^{2/3} - 125 \right] (Pr)^{1/3} \left[1 + (\frac{d}{x})^{2/3} \right] (\frac{\mu_B}{\mu_w})^{0.14}$$

where μ_B is the viscosity at bulk temperature and μ_w is the viscosity at wall temperature.

Local Nusselt number at a distance from the entrance is obtained by differentiation of equation given above.

$$Nu = 0.116\left[(Re)^{2/3} - 125\right](Pr)^{1/3}\left[1 + \frac{1}{3}\left(\frac{d}{x}\right)^{2/3}\right]\left(\frac{\mu_B}{\mu_w}\right)^{0.14}$$

Hausen's expressions are particularly useful in the case of fluids where the variation of viscosity is the dominant factor.

Latzko (58) in 1951 investigated theoretically the effect of what he called "the starting section." He assumed a unit Prandtl number and found that the local heat transfer starts with infinity at the commencement of heating and decreases rapidly along the lengths of the tube until a limit given by

$$h_\infty = 0.0384 \frac{\rho\, u_m\, c_p}{Re^{1/4}}$$

is reached. Heat transfer coefficient in the entrance region as determined by Latzko is given by

$$h = \acute{P}\, u_m\, \rho\, c_p\, (Re)^{-1/4}$$

where $\acute{P}$ = a function of ω and

$$\omega = 1.41\, X - 0.048\, X^2 + 0.168\, X^3$$

and

$$X = \left(\frac{x}{d}\right)^{0.8} (Re)^{-1/5}$$

In 1930, Eagle and Ferguson (59) heated water in condenser tubes. In one of the experiments, the local heat transfer coefficients at x/d = 2 and x/d = 94 were measured. The former was found to be 50 per cent greater. This was probably the first experimental detection of entrance region thermal effects.

In 1952, Davies and Al-Arabi (60) heated water using an electrically-heated pipe and measured the local and average heat transfer coefficients. The following equation was suggested to represent average heat transfer coefficient for x/d > 5

$$\overline{Nu} = Nu_{\infty} \left[1 + 2.8 \left(\frac{d}{x}\right)\right]$$

Hartness (61) heated water and oil in an electrically-heated pipe. The local heat transfer coefficients were measured. A length of 15 diameters brings the local coefficients within approximately 1 per cent of the value that is reached asymptotically in a long tube.

Deissler (12) made a theoretical study of turbulent heat transfer in the entrance region of smooth passages. He considered tubes and parallel plate channels. The results were given in a graphical form for local heat transfer coefficients against length. The results indicate that approximately fully developed heat transfer and friction are attained in an entrance length of less than 10 diameters.

Deissler has given the following expressions for entrance region of smooth tubes with turbulent flow

$$Nu = \frac{d^+ Pr}{t_B^+}$$

$$Re = d^+ u_p^+$$

where

$$t_B^+ = \frac{\int_0^{d^+/2} \frac{t^+ u^+ (\frac{d^+}{2} - y^+)}{1 - \beta t^+} dy^+}{\int_0^{d^+/2} \frac{u^+ (\frac{d^+}{2} - y^+)}{1 - \beta t^+} dy^+}$$

$$= \frac{\int_0^{\delta_t^+} \frac{t^+ u^+ (\frac{d^+}{2} - y^+)}{1 - \beta t^+} dy^+ + \frac{t_c^+}{1 - \beta t_c^+} \int_{\delta_t^+}^{d^+/2} u^+(\frac{d^+}{2} - y^+) dy^+}{\int_0^{\delta_t^+} \frac{u^+ (\frac{d^+}{2} - y^+)}{1 - \beta t^+} dy^+ + \frac{1}{1 - \beta t_c^+} \int_{\delta_t^+}^{d^+/2} u^+(\frac{d^+}{2} - y^+) dy^+}$$

and

$$u_p^+ = \frac{8}{(d^+)^2} (1 - \beta t_B^+) \left[\int_0^{\delta_t^+} \frac{u^+(\frac{d^+}{2} - y^+)}{1 - \beta t^+} dy^+ + \frac{1}{1 - \beta t_c^+} \int_{\delta_t^+}^{d^+/2} u^+(\frac{d^+}{2} - y^+) dy^+ \right]$$

where β = heat transfer parameter

$$= \frac{q_w \sqrt{\frac{\tau_w}{\rho}}}{c_p \rho \tau_w t_w}$$

The corresponding equations for flow between flat plates are

$$Nu = \frac{2 a^+ Pr}{t_B^+}$$

and $Re = 2 u_p^+ a^+$

where

$$t_B^+ = \frac{\int_0^{\delta_t^+} \frac{t^+ u^+}{1 - \beta t^+} dy^+ + \frac{t_c^+}{1 - \beta t_c^+} \int_{\delta_t^+}^{a^+/2} u^+ dy^+}{\int_0^{\delta_t^+} \frac{u^+}{1 - \beta t^+} dy^+ + \frac{1}{1 - \beta t_c^+} \int_{\delta_t^+}^{a^+/2} u^+ dy^+}$$

and

$$u_p^+ = \frac{2}{a^+} (1-\beta t_B^+) \left[\int_0^{\delta_t^+} \frac{u^+}{1-\beta t^+} dy^+ + \frac{1}{1-\beta t_c^+} \int_{\delta_t^+}^{a^+/2} u^+ dy^+ \right]$$

Physical properties in the above equations are to be evaluated at the wall temperature.

Al-Arabi (62) gives the expression for average Nusselt number for length L of the tube.

$$\overline{Nu} = Nu_{\infty} \left(1 + \frac{S\ d}{L}\right)$$

where

$$S = \left[\frac{6000}{Re} + 0.55\right] \left(\frac{L}{d}\right)^{0.3}$$

Romanenko and Krylova (64) have suggested the following empirical relation for entrance length in smooth ducts.

$$\frac{x}{d_h} = 0.592\ (Re)^{0.48}$$

In the discussion on entrance region so far, the flow was hydrodynamically developed before it entered the heating section.

Limited information is available for the case where hydrodynamic and thermal boundary layers develop simultaneously.

W. Linke and H. Kunze (65) have given experimental results for local heat transfer coefficients in the entrance region of tubes. Entrance length was found to exceed 60 diameters. It appears that, except at the highest Reynolds number (101,600) the flow was laminar throughout the entrance region, for nearly all the friction factors were below the fully developed values. The unusually long length

through which a laminar flow was sustained is attributed to a bellmouth entrance.

Deissler in his studies (10, 12) on channels and tubes found that fully developed (hydrodynamically and thermally) flow resulted in less than 10 hydraulic diameters for simultaneously developing thermal and hydrodynamic boundary layers. The results of heat transfer coefficients are graphically presented against length. The results for tubes in this section are applicable to ducts when hydraulic diameter of the duct is substituted for tube diameter.

Unsymmetrically Heated Ducts.--As a first approximation the results of symmetrically heated ducts can be applied. For noncircular cross sections, the tube diameter should be replaced by the hydraulic diameter of the duct. The whole perimeter should be used in calculating the hydraulic diameter even when only a part of the duct is heated or cooled.

Hatton (50) has analytically determined the entrance length when two parallel plates are maintained at different temperatures. An entrance length of 20 hydraulic diameters is calculated for Reynolds number = 7096 and Pr = 1. At Re = 73612 and Pr = 1 this length increases to 30 hydraulic diameters.

Barrow and Lee (66) considered entrance length for the uniform heat flux on one wall (the other wall being adiabatic). In their analysis they assumed linear heat flux

across the thermal boundary layer and an eddy diffusivity distribution as given by Deissler (10). Local Nusselt number in the entrance region is given as:

$$Nu = \frac{-2a \left[\frac{d}{dy^+} (t_c^+ - t^+)\right] y^+ = 0}{\frac{\int_0^{a^+} u^+ t^+ dy^+}{\int_0^{a^+} u^+ dy^+}}$$

Barrow and Lee in another analysis (67) have assumed a linear variation of ε for y^+ ($y^+ > 26$). Smaller heat transfer coefficients and entrance lengths are predicted than would be obtained from Hatton and Quarmby's analysis (51). The difference as noted will result from different expressions for ε being used. According to Barrow and Lee (67) about 20 hydraulic diameters are required for the flow to develop thermally for Reynolds number up to 70,000. Hatton and Quarmby (51) predict a much larger entrance length equaling 130 hydraulic diameters. Since thermal boundary layer develops on only one side, unsymmetric boundary conditions will result in longer entrance lengths than would be required by symmetrically heated ducts.

Novotny et al. (55) conducted experiments with rectangular ducts having two heated and two unheated walls. Aspect ratios of the ducts ranged between 1:1 to 1:10. The thermal entrance length was noted to be less than 30 hydraulic

diameters. It was further noted that there was no clear influence of the side walls on the thermal development.

Fully Developed Turbulent Heat Transfer in Rough Tubes

The data available on rough tubes are mainly experimental.

A. Soennecken (68) noted in 1911 that the value of the coefficient of heat transfer is lower in rough tubes than that in smooth tubes. Stanton (69) obtained a contrary result. This was followed by experimentation by Pohl (70). He concluded that in all the rough tubes the heat transfer coefficient was lower than that in the smooth tube. Pohl did not give a direct measure of roughness.

Cope (71) used special knurling procedure to develop roughness in tubes. He found that in turbulent region surface roughness has very little effect on the heat transfer coefficient. Cope further concluded that for a given amount of heat being transferred, the smooth tube gives the lowest pressure drop.

Nunner (72) used spring rings which were placed in the tubes to create roughness. The disadvantage as noted by the cited author is that the rings do not form a single body with the tube. This may introduce an error of up to 13 per cent in determining value of h. Nunner noted considerable increase in heat transfer and pressure drop. Nunner gave the following empirical expression

$$Nu = 0.383\ Re^{0.68}\ (f)^{(\frac{Re}{100})^{-1/8}}$$

Brouillette (73) used triangular grooves to create roughness and found increased heat transfer and pressure drop. The measured values of the heat transfer coefficients for the rough tubes were from 10 to 100 per cent greater than those measured on a plain tube. The results indicated that the height of grooves is the deciding factor in raising the heat transfer. The number of grooves per unit of tube length had relatively little effect.

Hobler and Koziol (74) carried out experiments to investigate the influence of alternate and bilateral contractions of tubes during the forced flow of air in the range of Reynolds number of 200 to 60,000. Marked increase in heat transfer was noted above Re = 1,000.

Theoretical Analysis for Heat Transfer in Rough Tubes

For rough tubes the hydrodynamic conditions are expressed by means of λ_o, the local degree of turbulence. λ_o is given by

$$\lambda_o = (\frac{\nu^3}{\kappa})^{1/4}$$

Assuming homogeneous and isotropic turbulence in a tube of diameter d, the following expression is obtained

$$\frac{h\ d_*}{k} = \frac{2}{\sqrt{\pi}} \left(\frac{d_*}{\lambda_o}\right) (Pr)^{0.5}$$

and based on experimental results the following expression is obtained:

$$\lambda_o = 28\ \frac{\nu}{u_*}$$

The preceding two equations result in

$$Nu = \frac{h\ d_*}{k} = 0.04\ \left(\frac{u_*\ d_*}{\nu}\right)(Pr)^{0.5}$$

or

$$\frac{Nu}{Pr^{0.5}} = 0.04\ Re_T$$

This equation was developed for <u>smooth</u> tubes. As the relation for λ_o contains only ν and u_*, it may be expected to hold also for tubes with rough walls. This was proved experimentally by V. Kolár (75). The value of d_* to be used in equations for rough ducts is suggested by most authors to be

$$d_* = \sqrt{\frac{4\ V}{\pi\ L}}$$

where V is the volume of the duct.

It was shown by Kolár (76) that Nunner's expression for rough tubes (72)

$$Nu = 0.383\ Re^{0.68}\ (f)\left(\frac{100}{Re}\right)^{1/8}$$

is equivalent to

$$\frac{Nu}{Pr^{0.5}} \simeq 0.05\ Re_T \qquad (Pr = 0.72)$$

which is similar to equation cited above as

$$\frac{Nu}{Pr^{0.5}} = 0.04\ Re_T\ .$$

CHAPTER III

THEORETICAL ANALYSIS

Unsymmetrically Heated Parallel Plate Channel

Fully developed turbulent flow in a smooth parallel plate channel will be considered. One of the plates is adiabatic whereas the other one transfers heat at a constant rate to the air flowing in the channel. In actual practice a parallel plate channel will be simulated by a duct of large aspect ratio. The problem is schematically presented in Figure 1.

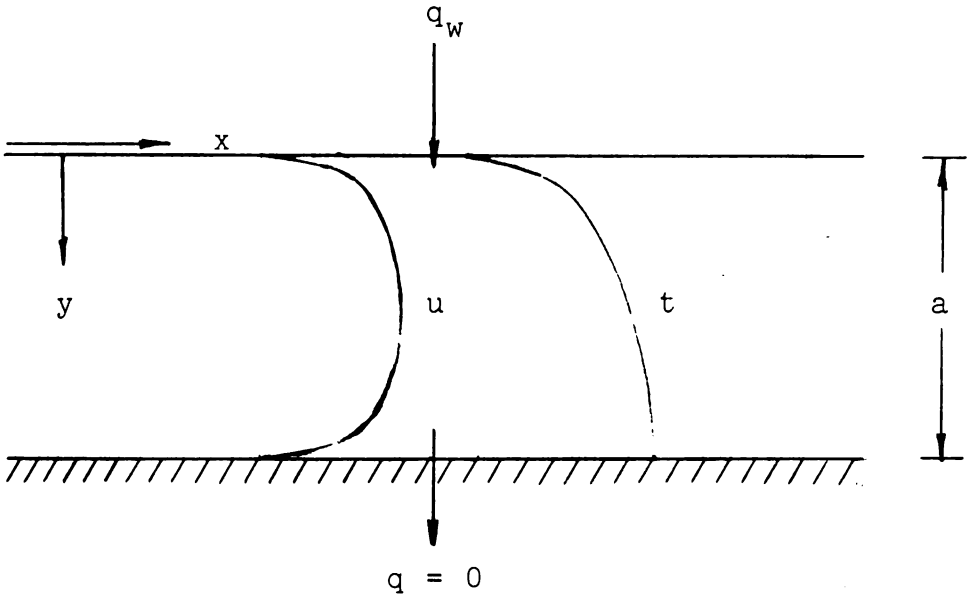

Figure 1.--Fully developed turbulent flow in an unsymmetrically heated parallel plate channel.

The plates are spaced distance "a" apart as shown in Figure 1. Hydraulic diameter (d_h) for this parallel plate channel will equal 2a.

Assumptions

1. The velocity distribution in the channel is given by the following:

a. $u^+ = y^+ \qquad y^+ \leq 5$

b. $u^+ = 5[1 + \ln\frac{y^+}{5}]$ for buffer layer, $5 \leq y^+ \leq 30.$

c. $u^+ = 5.5 + 2.5 \ln y^+ \qquad y^+ > 30.$

2. The flow in the laminar sublayer is completely laminar.

3. In the buffer layer the flow changes gradually from laminar to turbulent

4. In the turbulent core, the turbulent diffusivity is much larger than the laminar viscosity or heat conductivity. The laminar terms in shear stress and specific heat flow will be neglected.

5. $\varepsilon_m = \varepsilon_q \qquad$ i.e., $Pr_t = 1$

Nusselt number is defined as

$$Nu = \frac{q_w}{(t_w - t_B)} \frac{d_h}{k} \tag{1}$$

In order to find temperature drop ($t_w - t_B$), the laminar sublayer, the buffer layer and the turbulent core will be considered separately.

Temperature Drop in Laminar Sublayer

The linear temperature drop in the laminar sublayer is given by

$$\Delta t_{\ell} = \frac{q_w}{k} y_1 = \frac{q_w}{\rho c_p} \frac{Pr}{\nu} y_1$$

Introducing the dimensionless value $y^+ (y_1^+ = 5)$ one gets

$$\Delta t_{\ell} = \frac{q_w}{\rho c_p} \sqrt{\frac{\rho}{\tau_w}} Pr \; y_1^+ = \frac{q_w}{\rho c_p} \sqrt{\frac{\rho}{\tau_w}} 5 \; Pr \qquad (2)$$

Temperature Drop in the Buffer Layer

Shear stress and the specific heat flow for the buffer layer are given by:

$$\tau_b = (\nu + \varepsilon)\rho \frac{du}{dy}$$

$$q_b = - (\frac{\nu}{Pr} + \varepsilon)\rho \; c_p \frac{dt}{dy}$$

(Subscript b refers to the buffer layer.)

The second equation above gives temperature drop in the buffer layer as:

$$\Delta t_b = \frac{q_b}{\rho c_p} \int_{y_1}^{y_b} \frac{dy}{(\frac{\nu}{Pr} + \varepsilon)}$$

The first equation above gives eddy diffusivity as:

$$\varepsilon = \frac{\tau_b}{\rho} \frac{dy}{du} - \nu$$

Shear stress and specific heat flow are assumed to be constant in the laminar and buffer layer. Accordingly we can replace q_b and τ_b by q_w and τ_w respectively.

Using dimensionless u^+ and y^+ one gets

$$\frac{\rho}{\tau_w} \frac{du}{dy} = \frac{1}{\nu} \frac{du^+}{dy^+}$$

Using von Kármán's equation for the velocity in the buffer layer:

$$u^+ = 5 \left[1 + \ln \frac{y^+}{5} \right]$$

one obtains

$$\frac{du^+}{dy^+} = \frac{5}{y^+}$$

Therefore

$$\varepsilon = \nu \frac{y^+}{5} - \nu$$

and

$$\Delta t_b = \frac{q_w}{\rho c_p \nu} \int_{y_1}^{y_b} \frac{dy^+}{(\frac{1}{Pr} + \frac{y^+}{5} - 1)}$$

$$= \frac{q_w}{\rho c_p} \sqrt{\frac{\rho}{\tau_w}} \int_5^{30} \frac{dy^+}{\frac{1}{Pr} + \frac{y^+}{5} - 1}$$

which on integration yields:

$$\Delta t_b = \frac{5q_w}{\rho c_p} \sqrt{\frac{\rho}{\tau_w}} \ln (5 \, Pr + 1) \qquad (3)$$

Temperature Drop in the Turbulent Core

In an unsymmetrically heated parallel plate channel, the temperature profile and the velocity profile are dissimilar as shown in Figure 1. As a result of this the Reynolds analogy is not valid for the turbulent core. For this case a modified Reynolds analogy has been suggested by Mizushina (77). His method will be used as follows: It is assumed that:

1. Velocity is uniform in the turbulent region and equals u_m.
2. Eddy diffusivity (ε) is constant along the turbulent region.

Consider the energy balance at distance y from the heated wall for a strip of width Δx, located at distance x from the entrance; consider a unit depth of the strip. The energy balance results in:

$$- \rho c_p \varepsilon_q \frac{\partial t}{\partial y} \Delta x = u_m \rho c_p \frac{\partial t}{\partial x} (a - y) \Delta x \qquad (4)$$

Similarly at distance y_b the energy balance yields:

$$q_w \Delta x = u_m \rho c_p \frac{\partial t}{\partial x} (a - y_b) \Delta x \qquad (5)$$

Since the flow is fully developed $\partial t/\partial x$ = constant.

Equations (4) and (5), on division and integration, give:

$$t - t_b = \frac{-q_w}{\rho c_p \varepsilon (a-y_b)} \{a(y-y_b) + (\frac{y_b^2}{2} - \frac{y^2}{2})\} \qquad (6)$$

where t_b is the temperature at distance y_b from the wall.

Since the velocity is assumed to be uniform in the turbulent case, the bulk temperature (t_B) for fully developed flow in a channel can be approximated by:

$$t_B = \frac{1}{a - y_b} \int_{y_b}^{a} t \, dy \qquad (7)$$

Substituting for t from equation (6), in equation (7) one gets:

$$t_b - t_B = \frac{q_w}{\rho c_p \varepsilon_q (a-y_b)^2} \left[\left(\frac{a^3}{3} - \frac{y_b^3}{3}\right) + (a\, y_b^2 - a^2 y_b) \right] \quad (8)$$

Since y_b is small compared to the plate spacing a, the equation (8) approximates to:

$$t_b - t_B = \frac{q_w}{\rho c_p \varepsilon_p} \left[\frac{a}{3} - y_b \right] \quad (9)$$

which is the temperature drop in the turbulent core.

Temperature drop $(t_w - t_B)$

Since

$$t_w - t_B = \Delta t_\ell + \Delta t_b + (t_b - t_B) \quad (10)$$

After substituting for component temperature drops from equations (2), (3) and (9) the equation (10) changes to

$$t_w - t_B = \frac{q_w}{\rho c_p} \sqrt{\frac{\rho}{\tau_w}}\, 5\, Pr +$$

$$\frac{q_w}{\rho c_p} \sqrt{\frac{\rho}{\tau_w}}\, 5\, \ln(Pr+1) + \frac{q_w}{\rho c_p} \frac{1}{\varepsilon_q} \left[\frac{a}{3} - y_b \right] \quad (11)$$

Since

$$Nu = \frac{q_w}{(t_w - t_B)} \frac{d_h}{k}$$

and

$$St = \frac{h}{\rho\ c_p\ u_m} = \frac{q_w}{\rho\ c_p\ u_m\ (t_w - t_B)} \qquad (12)$$

Substitution for $(t_w - t_B)$ from equation (11) in euqation (12) results in the following expression for Stanton number.

$$St = \left[u_m \sqrt{\frac{\rho}{\tau_w}} \{5Pr + 5\ln(5Pr+1) + \frac{1}{\varepsilon_q} \sqrt{\frac{\tau_w}{\rho}} (\frac{a}{3} - y_b)\} \right]^{-1} \qquad (13)$$

For turbulent flow in parallel plate channels, the Blasius law satisfactorily correlates the data, when hydraulic diameter $d_h = 2a$ is substituted for tube diameter. For a channel, it is, therefore, obtained

$$\frac{\tau_w}{\rho} = 0.0384\ u_m^2\ (Re)^{-1/4} \qquad (14)$$

where

$$Re = \frac{u_m\ (2a)}{\nu}$$

Substituting the value of $\frac{\tau_w}{\rho}$ from equation (14), equation (13) results in:

$$St = \frac{0.1958\ Re^{-1/8}}{5Pr + 5\ln(5Pr+1) + 0.0326\ \frac{\nu}{\varepsilon_q}\ Re^{7/8} - 30.59\ \frac{\nu}{\varepsilon_q}} \qquad (15)$$

A constant value of ε_q across the turbulent core is given by Hatton (78) as:

$$\frac{\nu}{\varepsilon_q} = \left[0.36m^+ \left(1 - \frac{m^+}{y_o^+}\right) - 1\right]^{-1}$$

where

$$y_o = \frac{a}{2} \quad \text{and} \quad m^+ = \frac{1}{2}\left(y_o^+ + 26\right).$$

In the ducts that are experimentally studied in the present thesis,

$$a = \frac{1}{12}\text{ft} \text{ hence } y_o = \frac{1}{24}\text{ft} \text{ and } d_h = 2a = \frac{1}{6}\text{ft}.$$

Since

$$\frac{\tau_w}{\rho} = 0.0384\ u_m^2\ (Re)^{-1/4}$$

the following expressions result:

$$m^+ = \left[0.02442\ Re^{7/8} + 13\right]$$

$$y_o^+ = 0.0488\ Re^{7/8}$$

and

$$\frac{\nu}{\varepsilon_q} = \frac{1}{[0.00435\ Re^{7/8} - 1246.65\ Re^{-7/8} + 1]}$$

Substituting for $\frac{\nu}{\varepsilon_q}$ in equation (15), the following expression results for Stanton number (St).

$$St = \frac{0.1958\ Re^{-1/8}}{5Pr + 5\ln(5Pr+1) + \frac{0.0326Re^{7/8} - 30.59}{0.00435Re^{7/8} - 1246.65Re^{-7/8} - 1}} \qquad (16)$$

It is to be noted that equation (16) will apply to a special case where plate spacing equals one inch. For different plate spacings appropriate values of y_o^+ and m^+ should be substituted in equation (15).

Symmetrically Heated Parallel Plate Channel

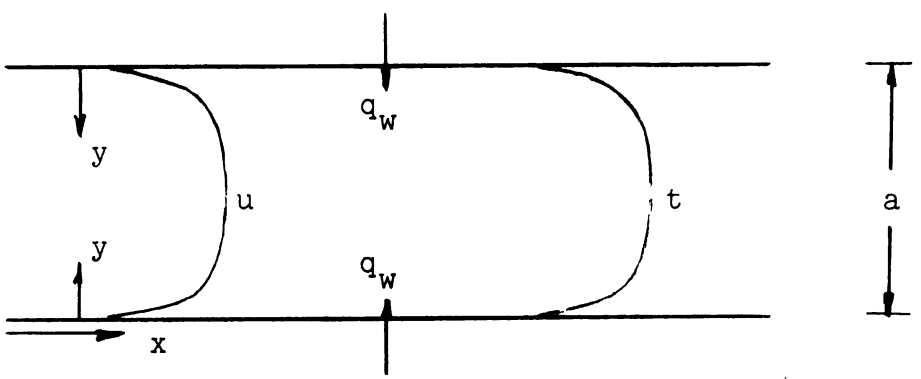

Figure 2.--Fully developed turbulent flow in symmetrically heated parallel plate channel.

The problem is schematically representd in Figure 2. Here the specific heat flow through the two plates is constant and equal. Other conditions remain the same as in the last section.

As before temperature drop through laminar sublayer, buffer layer and turbulent core will be determined separately.

Temperature Drop Through Laminar Sublayer

$$\Delta t_{\ell} = \frac{q_w}{\rho c_p} \sqrt{\frac{\rho}{\tau_w}}\, 5Pr \tag{17}$$

Temperature Drop Through the Buffer Layer

$$\Delta t_b = \frac{q_w}{\rho c_p} \sqrt{\frac{\rho}{\tau_w}}\, 5\ln (5Pr + 1) \tag{18}$$

Temperature Drop Through the Turbulent Core

Since the temperature and velocity profiles are similar, Reynolds analogy is valid for the turbulent core. Hence

$$t_b - t_B = \frac{q_w}{c_p \tau_w} (u_m - u_b) = \frac{q_w}{\rho c_p} \sqrt{\frac{\rho}{\tau_w}} \left[u_m^+ - u_b^+ \right] \tag{19}$$

Substituting $y_b^+ = 30$ in the von Kármán's equation for the buffer zone, namely:

$$u^+ = 5\left[1 + \ln \frac{y^+}{5}\right]$$

the following expression results:

$$u_b^+ = 5\left[1 + \ln 6\right]$$

Substitution for u_b^+ in equation (19) gives

$$t_b - t_B = \frac{q_w}{\rho c_p}\sqrt{\frac{\rho}{\tau_w}}\left[u_m^+ - 5(1+\ln 6)\right] \qquad (20)$$

Temperature Drop $(t_w - t_B)$

Since

$$t_w - t_B = \Delta t_\ell + \Delta t_b + (t_b - t_B)$$

Substituting for component temperature drops from equations (17), (18) and (20), the following equation is obtained for $(t_w - t_B)$:

$$t_w - t_B = \frac{q_w}{\rho c_p}\sqrt{\frac{\rho}{\tau_w}}\left[5Pr + 5\ln(5Pr+1) + u_m^+ - 5(1+\ln 6)\right]$$

Using

$$\frac{\tau_w}{\rho} = 0.0384\, u_m^2\, (Re)^{-1/4}$$

the following expression is obtained for Stanton number:

$$St = \frac{0.1958\ Re^{-1/8}}{5(Pr-1) + 5\ \ln\left(\frac{5Pr+1}{6}\right) + 5.10\ Re^{1/8}} \qquad (21)$$

Simplified Analysis for the Unsymmetrical Case

In this analysis no account will be taken of the buffer or transition zone. The turbulent layer is divided into a laminar sublayer and the turbulent core. Figure 3 is a schematic representation of the problem.

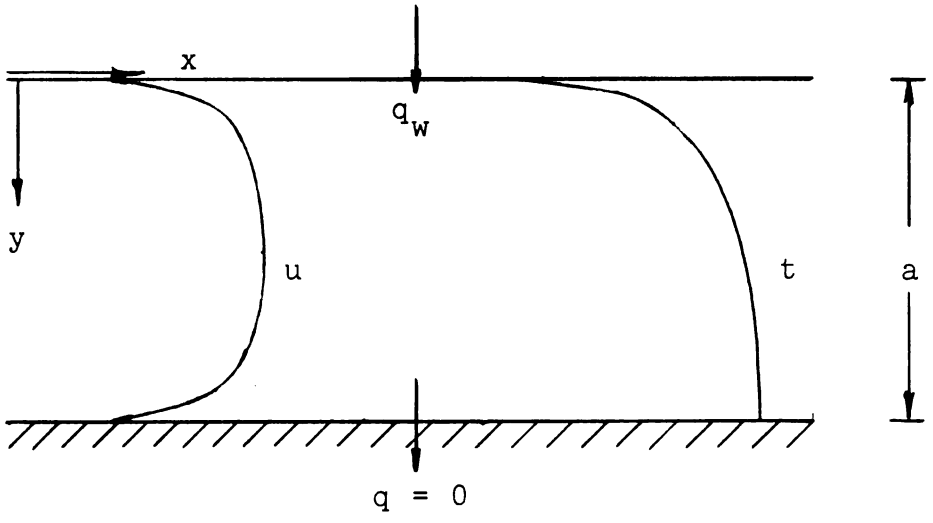

Figure 3.--Fully developed turbulent flow in an unsymmetrically heated parallel plate channel.

Laminar Sublayer

Here Reynolds analogy applies. Conduction is the dominant mode of heat transfer. Therefore for the laminar sublayer one gets:

$$\frac{q}{\tau} = - \frac{k}{\mu} \frac{dt}{du}$$

Assuming that

$$\frac{q}{\tau} = \text{constant} = \frac{q_w}{\tau_w}$$

one gets

$$q_w = \tau_w \frac{k}{\mu} \frac{1}{u_1} (t_w - t_1) \qquad (22)$$

where u_1 is the velocity at the border of laminar sublayer and the turbulent core. t_1 is the temperature at the border between the two layers.

Turbulent Core

Modified Reynolds analogy as suggested by Mizushina (77) will be used here as well. The assumptions are the same as before, namely:

1. Velocity is uniform in the turbulent core
2. ε_q is constant across the turbulent region.

For a strip of width Δ_x located at distance x from the entrance and having a unit depth normal to the plane of

paper, an energy balance at distance y from the heated wall results in:

$$- \rho c_p \varepsilon_q \frac{\partial t}{\partial y} \Delta x = u_m \rho c_p \frac{\partial t}{\partial x} (a-y)\Delta x \qquad (23)$$

Similarly energy balance at distance y_1 results in:

$$q_w \Delta x = \rho c_p u_m (a-y_1) \frac{\partial t}{\partial x} \Delta x \qquad (24)$$

Equations (23) and (24) on division and integration result in:

$$t = t_1 - \frac{q_w}{\rho c_p \varepsilon_q (a-y_1)} \left[a(y-y_1) + \left(\frac{y_1^2}{2} - \frac{y^2}{2}\right) \right] \qquad (25)$$

Since u_m is assumed to be uniform in the turbulent core, the bulk temperature t_B is approximated by

$$t_B = \frac{1}{a - y_1} \int_{y_1}^{a} t \, dy \qquad (26)$$

Substituting for t from equation (25), equation (26) gives

$$\frac{t_1 - t_B}{q_w} = \frac{1}{\rho c_p \varepsilon_q (a-y_1)^2} \left[\frac{a^3}{3} - \frac{y_1^3}{3} + a y_1^2 - a^2 y_1 \right] \qquad (27)$$

For a symmetrically heated parallel plate channel, it is known from Reynolds analogy that :

$$\frac{(t_1 - t_B)_{symmetrical}}{(u_m - u_1)_{symmetrical}} = \left(\frac{q_w}{c_p \tau_w}\right)_{symmetrical} \tag{28}$$

Furthermore for the case of symmetrical heating it is seen that

1. $- \rho c_p \varepsilon_q \frac{\partial t}{\partial y} = u_m \rho c_p \frac{\partial t}{\partial x} \left(\frac{a}{2} - y\right)$

2. $q_w = u_m \rho c_p \frac{\partial t}{\partial x} \left(\frac{a}{2} - y_1\right)$

and

3. $(t_B)_{symmetrical} = \frac{1}{\left(\frac{a}{2} - y_1\right)} \int_{y_1}^{a/2} t \, dy$

These three equations can be developed into an expression analogous to equation (27). The resulting expression is:

$$\left(\frac{t_1 - t_B}{q_w}\right)_{symmetrical} = \frac{2}{\rho c_p \varepsilon_q (a-2y_1)^2} \left[\frac{a^3}{12} - \frac{a^2 y_1}{2} + a y_1^2 - \frac{2}{3} y_1^3\right] \tag{29}$$

Combining equations (27), (28) and (29) the temperature drop for the turbulent core for unsymmetrically heated parallel plate channel is found to be:

$$t_1 - t_B = q_w \frac{\frac{1}{(a-y_1)^2}\left[\frac{a^3}{3} - a^2 y_1 + a y_1^2 - \frac{y_1^3}{3}\right]}{\frac{2}{(a-2y_1)^2}\left[\frac{a^3}{12} - \frac{a^2 y_1}{2} + a y_1^2 - \frac{2}{3} y_1^3\right]} \cdot \frac{u_m - u_1}{c_p \tau_w}$$

Since y_1 is small compared with the plate spacing "a" one gets:

$$t_1 - t_B = 2 q_w \left\{\frac{u_m - u_1}{c_p \tau_w}\right\}$$

approximately

or

$$q_w = \frac{(t_1 - t_B)\, c_p \tau_w}{2(u_m - u_1)} \tag{30}$$

Since the film heat transfer coefficient is defined by

$$h = \frac{q_w}{(t_w - t_B)}$$

Equations (22) and (30) can be used to derive the following expression:

$$\frac{1}{h} = \frac{\mu u_1}{\tau_w k} + \frac{2(u_m - u_1)}{c_p \tau_w}$$

or

$$\frac{1}{h} = \frac{u_m}{\tau_w c_p}\left[\mathrm{Pr}\,\frac{u_1}{u_m} + 2\left(1 - \frac{u_1}{u_m}\right)\right] \tag{31}$$

For fully developed turbulent flow in a smooth tube we have

$$\frac{u_l}{u_m} = 2.44\ (Re)^{-1/8}$$

This expression describes the flow in a channel with sufficient accuracy if hydraulic diameter ($d_h = 2a$) is used instead of tube diameter.

Substituting for $\frac{u_l}{u_m}$ in (31) and rearranging gives the following expression for Stanton number:

$$St = \frac{h}{\rho c_p u_m} = \frac{0.0192\ Re^{-1/4}}{1 + 1.22\ Re^{-1/8}\ (Pr-2)} \qquad (32)$$

Simplified Analysis for Symmetrically Heated Parallel Plate Channel

Here again the buffer layer will be neglected.

Laminar Sublayer

As for the case of unsymmetric heating in the last section, it is seen that

$$q_w = \tau_w \frac{k}{\mu} \frac{l}{u_l} (t_w - t_l) \qquad (33)$$

Turbulent Layer

As explained before, Reynolds analogy applies for the turbulent boundary layer which gives:

$$\frac{t_1 - t_B}{q_w} = \frac{u_m - u_1}{c_p \tau_w} \tag{34}$$

Equations (33) and (34) result in the following expression:

$$\frac{1}{h} = \frac{t_w - t_B}{q_w} = \frac{\mu u_1}{\tau_w k} + \frac{u_m - u_1}{c_p \tau_w} \tag{35}$$

Using

$$\frac{u_1}{u_m} = 2.44 \ (Re)^{-1/8}$$

and rearranging, the following result is obtained.

$$St = \frac{0.0384 \ Re^{-1/4}}{1 + 2.44 \ Re^{-1/8} \ (Pr - 1)} \tag{36}$$

CHAPTER IV

EXPERIMENTAL INVESTIGATION

Construction of Equipment

Two rectangular ducts (each having a cross-sectional area 1" x 4" and a length of 10') were constructed on a 1/4" thick (Grade A) sheet of plywood. The other two dimensions of the sheet measured 1½' x 10'. The details of the construction are as follows:

Three pieces of lumber (1" x 1½" x 10') were fastened on the plywood sheet so that they measured 5½" from center to center leaving a gap of 4" between successive pieces. The pieces of lumber were placed parallel to the longer side of the plywood sheet, with the one-inch sides being normal to the sheet. A flat galvanized steel sheet (27 guage galvanized 0.02" thick) was used to cover the entire length of the pieces of lumber (i) and (ii) (Figure 4). The sheet measured 5" in width and was symmetrically placed on the pieces of lumber (i) and (ii). The sheet was nailed to the pieces of lumber. This completed the construction of the duct with the flat covering which will hereafter be referred to as Duct A.

A corrugated sheet of galvanized steel was used to cover the space over the pieces of lumber (ii) and (iii)

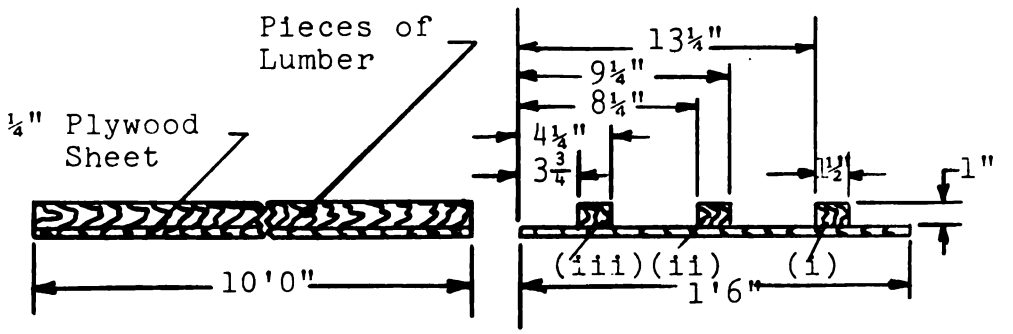

Fig. 4.--First Stage in the construction of the apparatus.

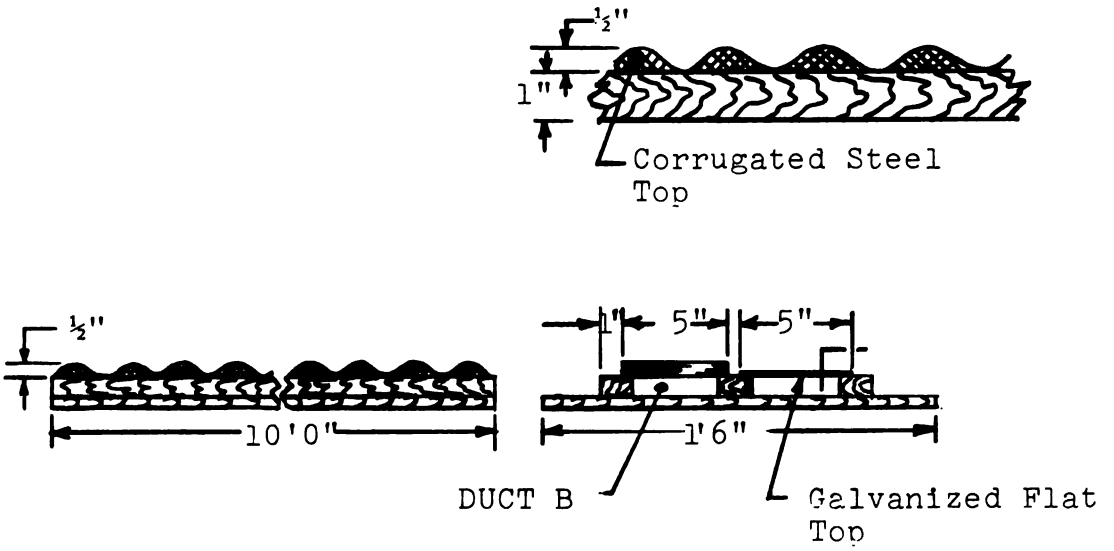

Fig. 5.--Second Stage in the construction of the apparatus.

(Figure 4). The corrugations were placed normal to the direction of the flow of air. The corrugated sheet (27 guage galvanized 0.02" thick) measured 5" in width and was symmetrically placed on the pieces of lumber (ii) and (iii). A cushioning material was placed between the corrugations and the pieces of lumber after which the corrugated sheet was nailed to the latter. This acted as a seal. The troughs of the corrugations touched the pieces of lumber. The corrugations measured approximately 1½" between successive crests, with a vertical distance of 1/2" between crests and troughs. This duct with the corrugated top will hereafter be referred to as Duct B (Figure 5). Both of the ducts were painted with black asphalt paint (two coats each) on the side exposed to the sun.

The plywood sheet was put on three triangular stands which oriented the ducts at an angle of 45° to the horizontal. The 45° angle was chosen because in the period from September 23 through October 24 the rays of the sun are inclined at nearly 45° between 10:00 a.m. and 3:00 p.m.* As a result, the rays of the sun will impinge nearly perpendicular to the ducts. Maximum radiation will, therefore, be intercepted.

---

*For details on how to calculate the inclination of solar rays refer to: Art. 14.6-14.8, pp. 315-323 of Thermal Environmental Engineering by James L. Threlkeld, Prentice Hall, Inc.

An extension was built on one side of the plywood sheet so that the ducts A and B enlarged into two insulated chambers where baffles were used to mix up the air before its exit temperature was measured. These exit chambers led into a plenum chamber, the other side of which was connected to a venturi (Figure 6). The venturi had a throat diameter of 2" and a pipe diameter of 4". The dimensions of the pipe preceding and succeeding the venturi are shown in Figure 7. The pipe succeeding the venturi was bent at a right angle before it entered the plenum chamber No. 2. Fans were connected at the other end of the plenum chamber (Figure 7). The whole apparatus was put on a trailer.

Instrumentation

Measurement of Incident Solar Energy

The solar energy incident on the duct roof was measured by Eppley pyrheliometer (Eppley Laboratory, Inc., No. 1551). The calibration for the pyrheliometer was 1 μV = 0.117 BTU/hr. sq. ft.

The output of the pyrheliometer was recorded by Eppley Potentiometer (No. 328) which could be read accurately to the nearest one micro volt. With another possible adjustment error of one micro volt, the possible error in calculating incident solar energy (for 300 BTU/hr. $ft.^2$) will be 0.078 per cent.

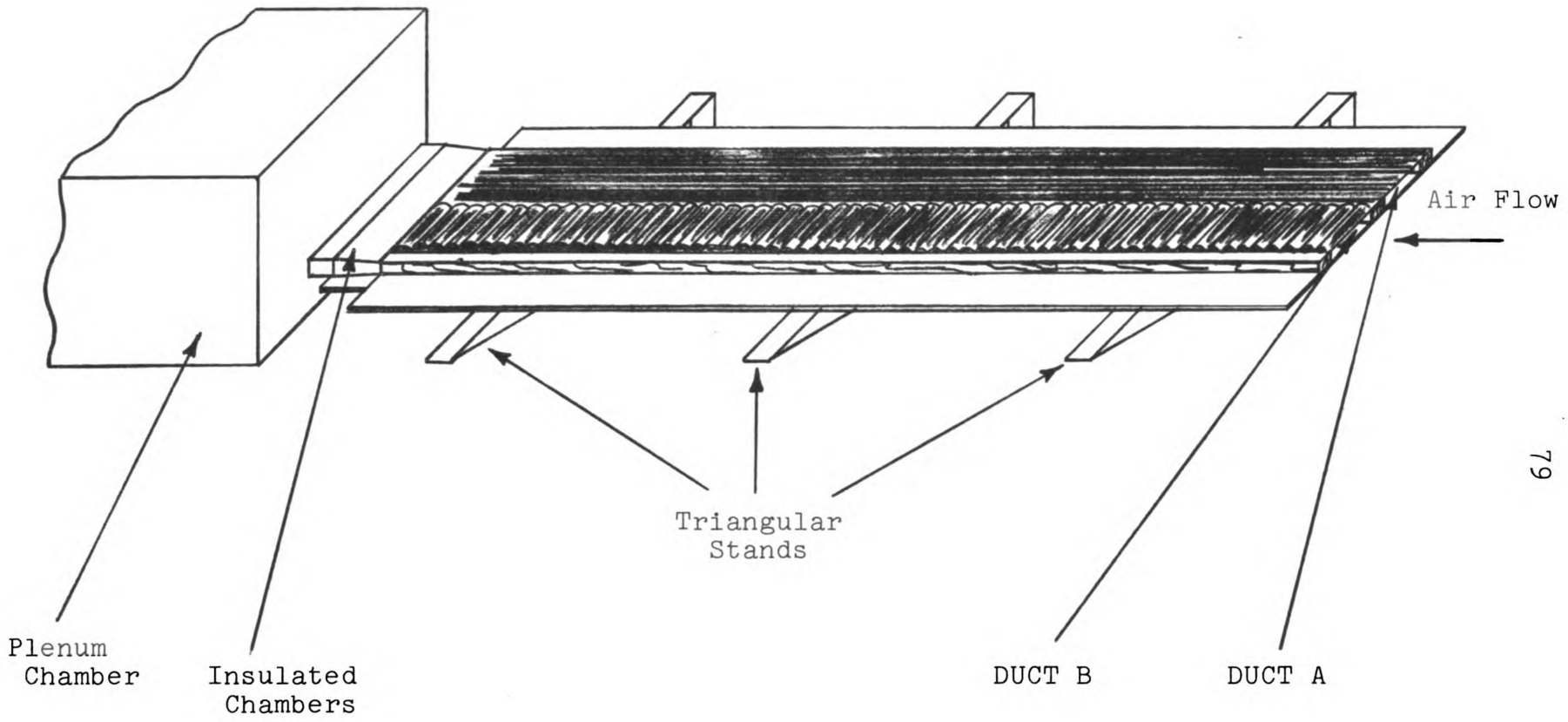

Fig. 6.--The apparatus as it looked after the completion of the 3rd Stage of construction.

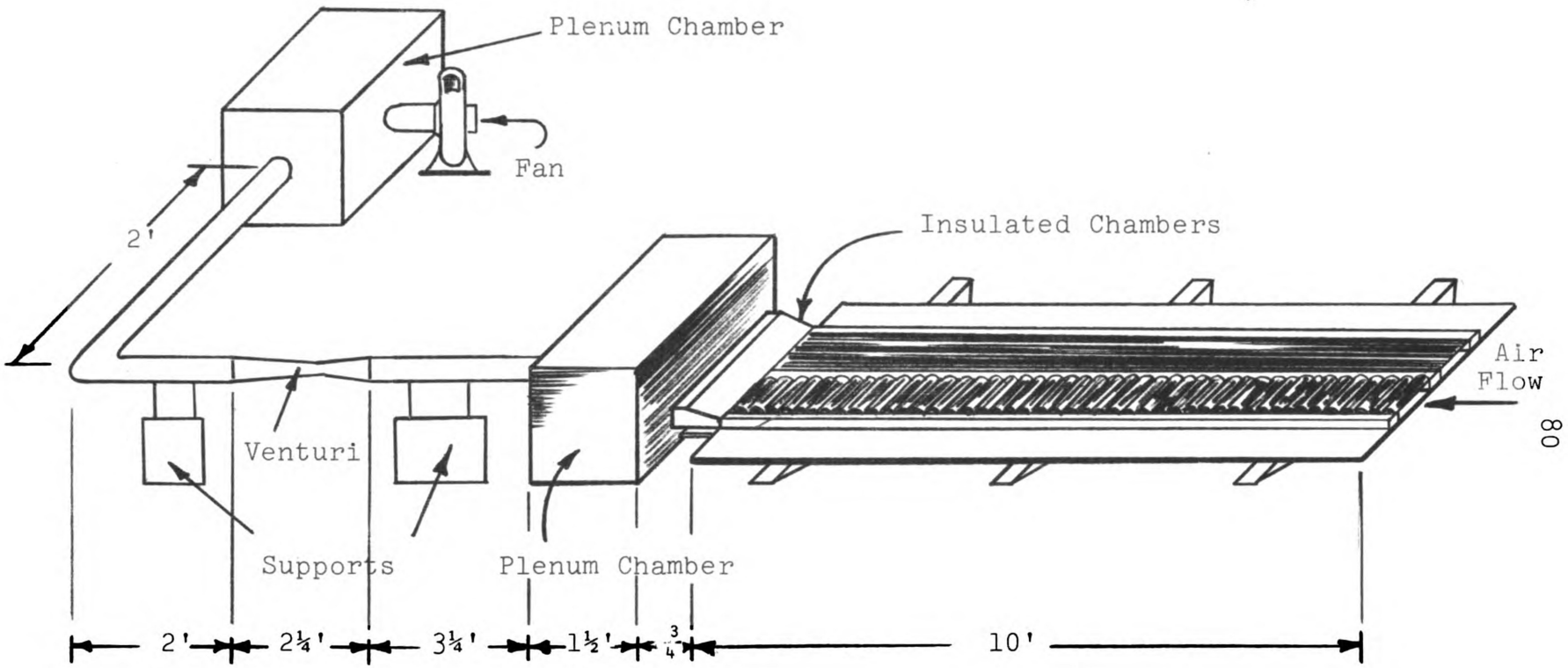

Fig. 7.--Apparatus for conducting experiments (trailer is not shown in the Figure).

Measurement of Temperature of Upper and Lower Sides of the Ducts

Copper-constantan thermocouples made of 24 calibration copper and constantan wires were used. Thermocouples were soldered to the underside of the flat and corrugated galvanized steel sheets. On the corrugated sheet the thermocouples were soldered to the underside of the crests (Figure 8). Thermocouples were also embedded in the lower plywood sheet to measure the temperature of the lower sides of the ducts. The plan for the thermocouples for the top and bottom sides of th two ducts is shown in Figure 8.

As may be noted in Figure 8, the successive thermocouples along the top and bottom of Duct A are placed six hydraulic diameters apart. In Duct B, the corresponding distance is approximately 9". An exact distance of 9" could not be maintained for the following reason: the thermocouples were soldered to the underside of the crests of the corrugated sheet; the distance between successive crests was 1½". Slight deviations in the distance of successive crests were, however, noticeable along the length of the sheet. This distance was also affected when the sheet was being nailed to the pieces of lumber during the construction of Duct B.

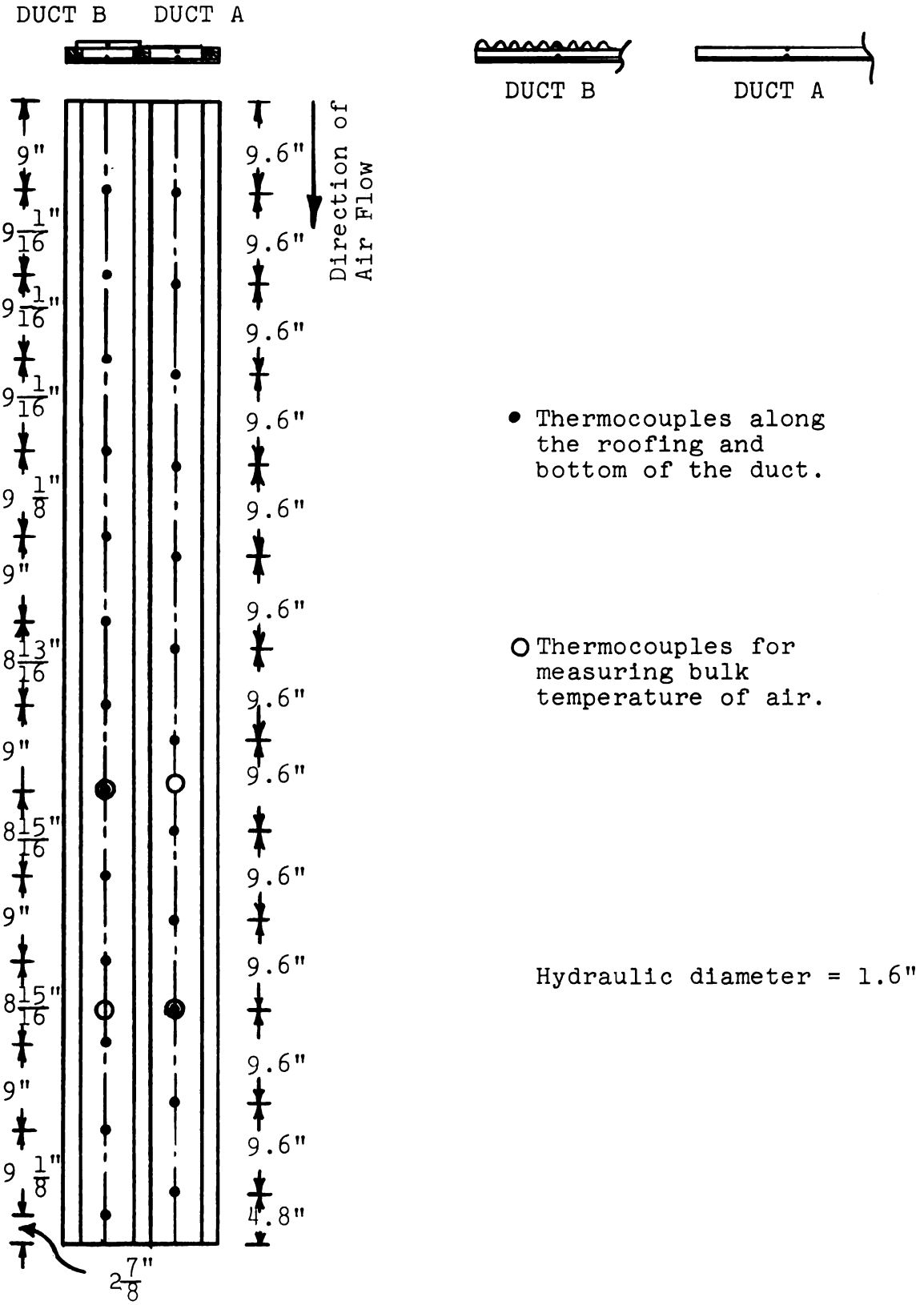

Fig. 8.--Location of thermocouples.

Location of Thermocouples along the Roofing and Bottom of the Ducts A and B.

	Duct A		Duct B		
$\frac{x}{d_h}$	Thermo-couples along the roofing	Thermo-couples along the bottom	Thermo-couples along the roofing	Thermo-couples along the bottom	Distance from the leading edge (inches)
6	A_1	A_{13}	B_1	B_{14}	9
12	A_2	A_{14}	B_2	B_{15}	$18\frac{1}{16}$
18	A_3	A_{15}	B_3	B_{16}	$27\frac{1}{8}$
24	A_4	A_{16}	B_4	B_{17}	$36\frac{3}{16}$
30	A_5	A_{17}	B_5	B_{18}	$45\frac{5}{16}$
36	A_6	A_{18}	B_6	B_{19}	$54\frac{5}{16}$
42	A_7	A_{19}	B_7	B_{20}	$63\frac{1}{8}$
48	A_8	A_{20}	B_8	B_{21}	$72\frac{1}{8}$
54	A_9	A_{21}	B_9	B_{22}	$81\frac{1}{16}$
60	A_{10}	A_{22}	B_{10}	B_{23}	$90\frac{1}{16}$
66	A_{11}	A_{23}	B_{11}	B_{24}	99
72	A_{12}	A_{24}	B_{12}	B_{25}	108
			B_{13}	B_{26}	$117\frac{1}{8}$

Location of Thermocouples Used for Measuring Bulk Temperature of Air.

Duct A		Duct B	
Thermocouples	Distance from the leading edge	Thermocouples	Distance from the leading edge
A_{25} A_{26} A_{27}	72"	B_{27} B_{28} B_{29}	$72\frac{1}{8}$"
A_{28} A_{29} A_{30}	96"	B_{30} B_{31} B_{32}	$96\frac{1}{16}$"

Bulk Temperature of Air

The bulk temperature of the air flowing in the ducts was measured at two points inside the ducts. For Duct A, the distances of 6' and 8' from the entrance were chosen. Equivalently these distances were 45 and 60 hydraulic diameters, and the flow here was expected to be fully developed. The corresponding distances for Duct B were 72-1/8" and 96-1/16", which are very nearly the same as in Duct A. The reason for the distances not being exactly 6' and 8' (as is the case of Duct A) is that the bulk temperatures were measured where the crest of the nearest corrugation occurred.

For the measurement of bulk temperature at a given point inside the duct, three thermocouples were placed parallel to the flow of air. The thermocouples were mounted on a taut wire and successive thermocouples placed 1/4" apart. Aluminum foil sheets were used to shield the thermocouples from the effects of radiation. The thermocouples and the aluminum foils alternated. The set-up is shown in Figure 9. The average of the readings of three thermocouples was recorded as the bulk temperature at the given point. The thermocouples were located in the middle of the longer side of the duct.

All the thermocouples were connected to a Brown Electronik potentiometer (Model No. 153 x 65 P 12-x-2F)

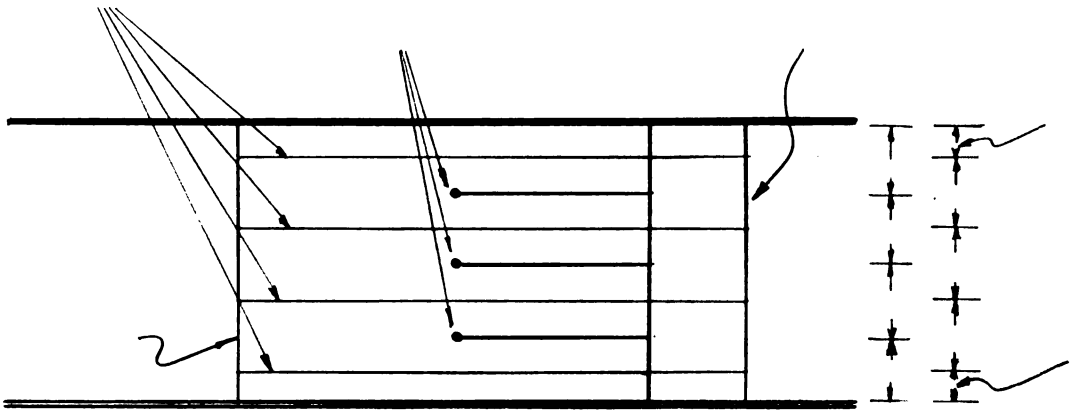

FIGURE 9.--Location of Thermcouples for measuring bulk temperature of air.

which recorded the temperature automatically. Temperature could be read accurately to 0.5°F.

Measurement of Air Leaving the Ducts

Mercury-in-glass thermometers were used for measuring the temperature of the air leaving the ducts. The thermometers were inserted in the insulated exit chambers (Figure 7).

Measurement of Humidity Ratio of Air Entering the Duct

A sling psychrometer was used for measuring the dry bulb and the wet bulb temperature of air. Both thermometers were mercury-in-glass type with a bare bulb diameter of 0.25". Both thermometers were unshielded.

The temperature of the air entering the duct was measured by a mercury-in-glass thermometer. It was assumed that the entering air temperature is the same as that of the outside air.

Measurement of Flow

The venturi shown in Figure 7 was used to measure air flow. The venturi had a throat diameter of 2" and a pipe diameter of 4". Calibration for the venturi was taken from a thesis.* An inclined tube manometer was used to measure the drop of pressure in the converging section of the venturi. The manometer could accurately record pressure drops of up to 0.005 inches of water.

An adjustable opening was used at the fan outlet to vary the flow. The following fans were used.

1. Aerovent Fan no. 124 Type DF Ser. 58351 Model SKC BB-41 D HP 1/2 RPM 3450.
2. Frame E.85 No. 1715000 A PH 1 ILG Electric Ventilating Co.

The first fan (Aerovent No. 124) was used alone until the flow requirement exceeded its capacity. The second fan was then turned on so that the two together would supply the required volume of air.

---

*Stephen Weller, "Air flow characteristics of a scale model chamber," Michigan State University, Dept. of Ag. Eng., M.S., 1966.

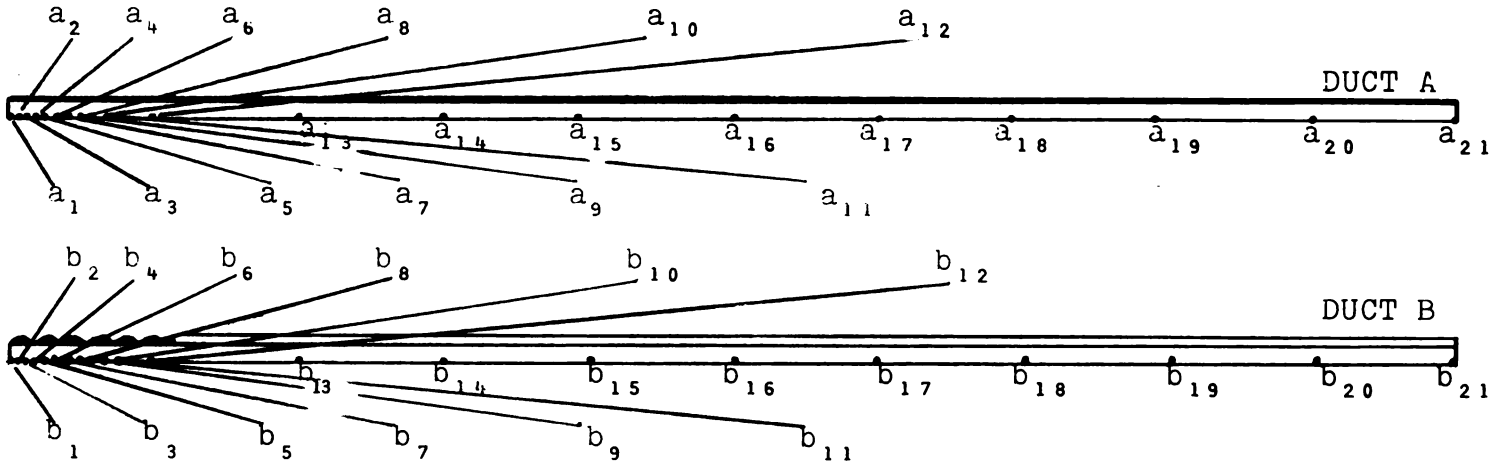

Tube	a_1	a_2	a_3	a_4	a_5	a_6	a_7	a_8	a_9	a_{10}	a_{11}	a_{12}	a_{13}	a_{14}	a_{15}	a_{16}
Distance from entrance	$\frac{1}{16}$"	$\frac{3}{4}$"	$1\frac{1}{2}$"	$2\frac{1}{4}$"	3"	4"	5"	6"	7"	8"	9"	12"	24"	36"	47"	60"

Tube	a_{17}	a_{18}	a_{19}	a_{20}	a_{21}
Distance from entrance	72"	84"	95"	108"	$119\frac{15}{16}$"

Tube	b_1	b_2	b_3	b_4	b_5	b_6	b_7	b_8	b_9	b_{10}	b_{11}	b_{12}	b_{13}	b_{14}	b_{15}	b_{16}
Distance from entrance	$\frac{1}{16}$"	$\frac{3}{4}$"	$1\frac{1}{2}$"	$2\frac{1}{4}$"	3"	4"	5"	6"	7"	8"	10"	12"	24"	36"	48"	60"

Tube	b_{17}	b_{18}	b_{19}	b_{20}	b_{21}
Distance from entrance	$7\frac{1}{2}$"	84"	96"	$107\frac{1}{2}$"	$119\frac{15}{16}$"

Fig. 10.--Location of pressure tubes.

Measurement of Pressure Drop of Air along the Duct

Eighth-inch copper tubes were made flush with the plywood. The pressure tubes were located along the center lines of ducts A and B. The plan for the tubing is given in Figure 10. Rubber hoses connected the copper tubes to a pressure manifold (Figure 11), which in turn was connected to an inclined tube manometer. Pressure of air passing a given tube in the duct could be measured by releasing the pinch clip on the corresponding hose.

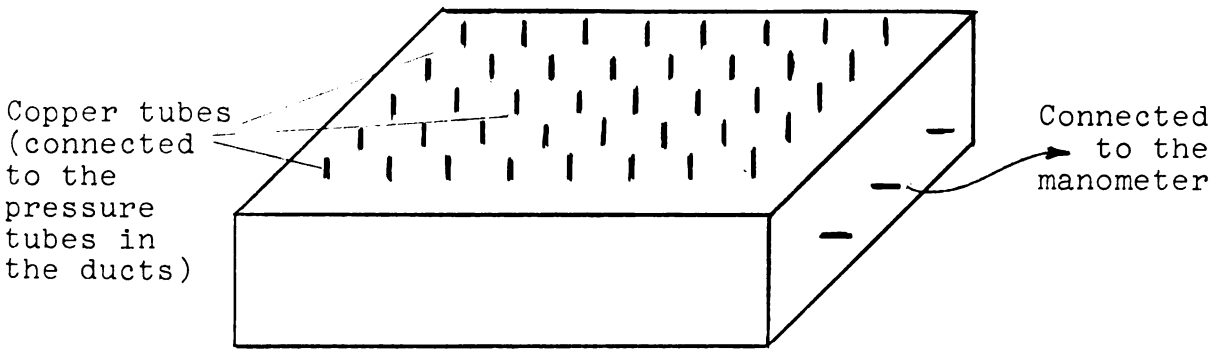

Figure 11.--Pressure manifold.

The inclined tube manometer could record pressure correctly to 0.005 inches of water. In the vertical position the manometer could read correctly to 0.025 inches of water. The manometer could be used in an inclined position for measuring pressure up to 1.2 inches of water. With the vertical position, the range increased to six inches of water.

Experimental Procedure

Data for Hydrodynamic Characteristics

The data for hydrodynamic characteristics of the ducts were collected indoors.

When Duct A was being tested the entrance to Duct B was closed. Later on Duct A would be closed to study Duct B.

The tests were run under essentially isothermal conditions. The range of the Reynolds number studied was between 10,000 and 50,000. For each rate of flow (which was controlled by the adjustable opening at the fan outlet) pressure was recorded for the pressure tubes by the manometer.

The following procedure was followed for both ducts.

1. Starting with Re = 10,000, the pressure drop was recorded as a function of the length of duct. Pressure recorded at a given point along the length was the weighted average of three readings. This was affected to minimize the error, particularly at low pressure drops.

2. The procedure was repeated for the next Reynolds number under investigation (which was 15,000). The entire range of Reynolds numbers (10,000 to 15,000) was thus covered. This constitutes a set of readings, which hereafter will be referred to as Set I. This was followed by seven sets of readings, giving a total of eight sets. These sets of readings will hereafter be referred to as the Sets 1 through 8.

Data for Heat Transfer Characteristics of the Ducts

The data for heat transfer characteristics of the ducts were collected on days when the sky was almost clear. This ensured a steady incoming solar radiation which was necessary for valid test data. The trailer carrying the apparatus was rotated about every twenty minutes so that the ducts faced the sun at all times.

Before any tests were conducted, the ducts were allowed to warm up for at least half an hour. No data were taken until all temperatures remained stabilized for at least 10 minutes. While the temperatures were approaching constant values, the air flow, incident solar energy, the dry and wet bulb temperatures, and the temperatures of air entering and leaving the duct were noted. The barometric pressure was noted once a day at noon; a mercury-in-glass barometer was used.

For a particular Reynolds number the Ducts A and B would be opened one at a time, keeping the entry to the other one closed.

After all temperatures had remained constant for ten minutes the thermocouple temperatures were recorded. Air flow was changed and the procedure repeated.

CHAPTER V

ANALYSIS, RESULTS AND DISCUSSION

Analysis of Data

Hydrodynamic Characteristics

The pressure readings from the tubes are plotted against the duct length for each Reynolds number. This is done for both the ducts A and B. Figures 12 and 13 represent typical graphs showing pressure drop versus duct length for the ducts A and B.

These graphs are used to determine intake length, intake losses and coefficients of friction, as will be explained under the section "Results and Discussion."

Heat Transfer Characteristics

The following procedure is used for both the ducts A and B for each Reynolds number under investigation.

1. The bulk temperature of air is plotted against the duct length. Three points are plotted on the graph:
   a. Temperature of air leaving the duct
   b. Temperature of air at 6 feet from the entrance for duct A and 72-1/2 inches for duct B. This

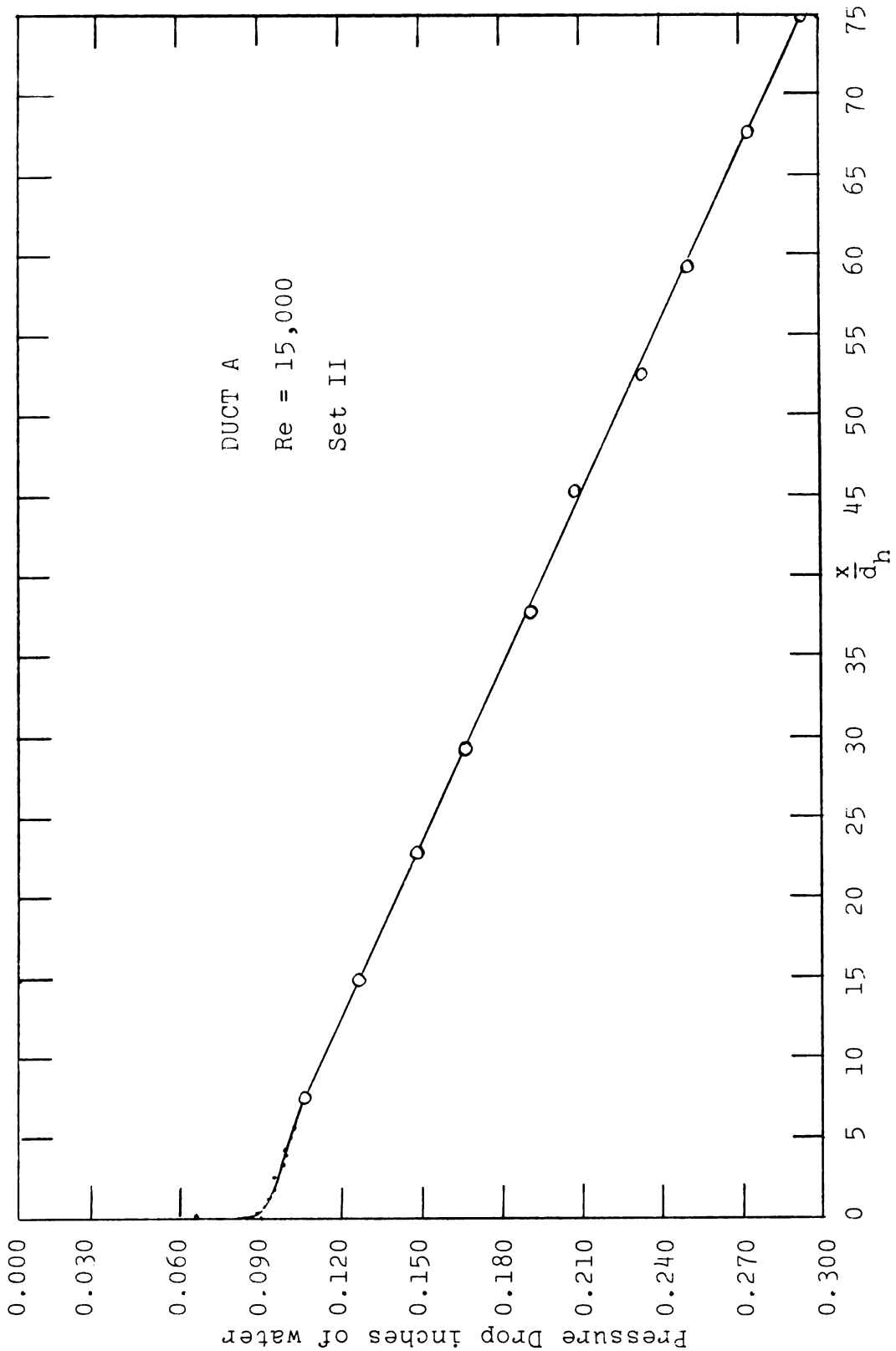

Fig. 12.--Pressure drop vs. length of Duct A.

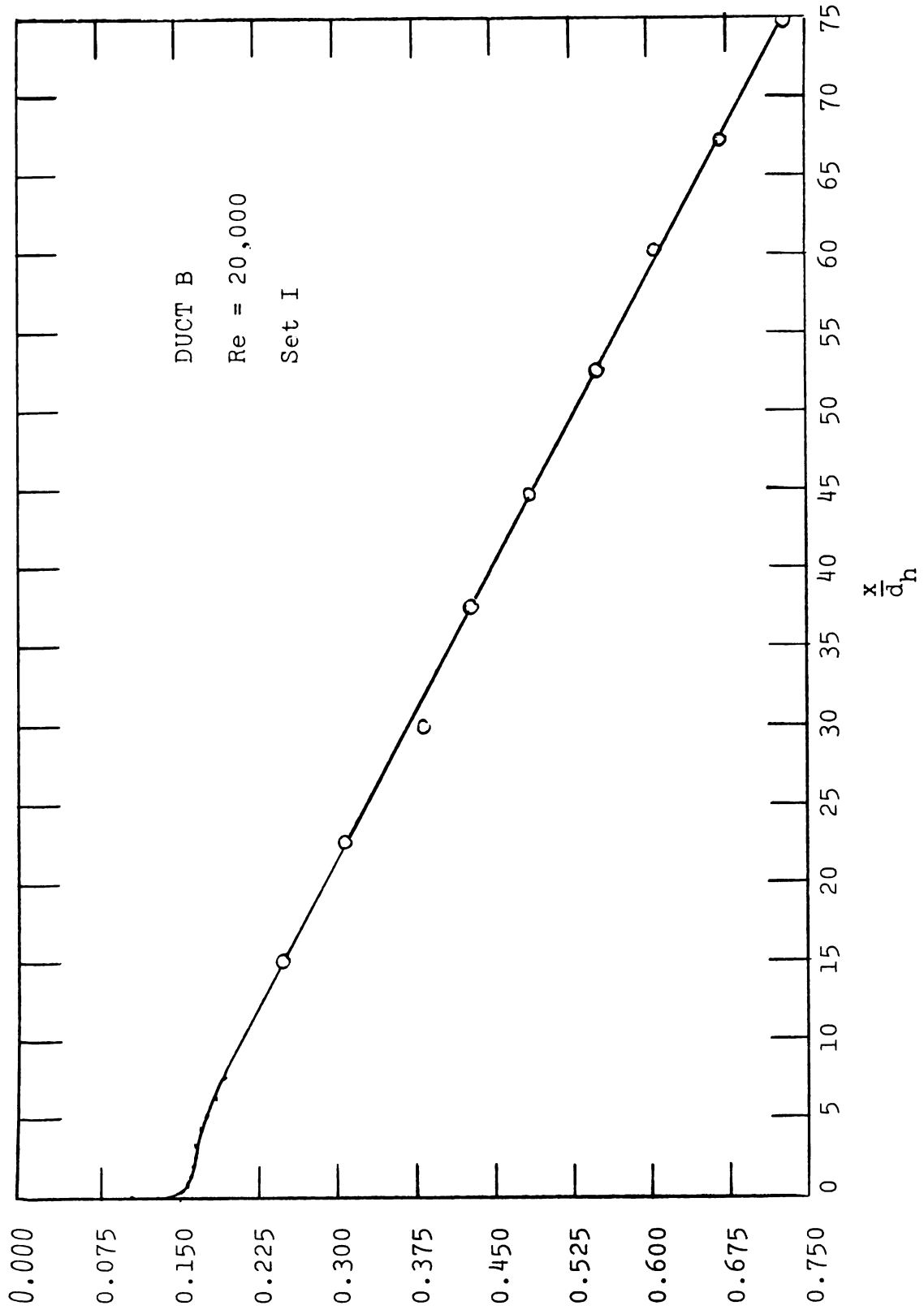

Fig. 13.--Pressure drop vs. length of Duct B.

temperature is mean of three thermocouple readings. The thermocouples were placed parallel to the direction of flow.

c. Temperature of air at 8 feet for duct A and 96-1/16 inches for duct B from the entrance. This temperature is the mean of three thermocouple readings just as above.

2. The temperatures of the top and bottom horizontal walls are plotted against the duct length.

Figures 14 and 15 represent typical temperature versus length graphs for the two ducts.

Analysis of Sling Psychrometer Data

The following symbols will be used in this part of the analysis:

W Humidity ratio of moist air. Lbs. water per lb. dry air.

$C_{p,a}$ Specific heat of moist air = 0.24 + 0.45W BTU per (lbs. dry air) (F).

W_s Humidity ratio at saturation. Lbs. water per lb. dry air.

$W_{s,wb}$ Humidity ratio at saturation. Calculated at wet bulb temperature. Lbs. water per lb. dry air.

$t_{db}=t$ Dry bulb temperature--F^{o}.

t_{wb} Wet bulb temperature--F^{o}.

t_s Temperature of surfaces surrounding psychrometer--F^{o}.

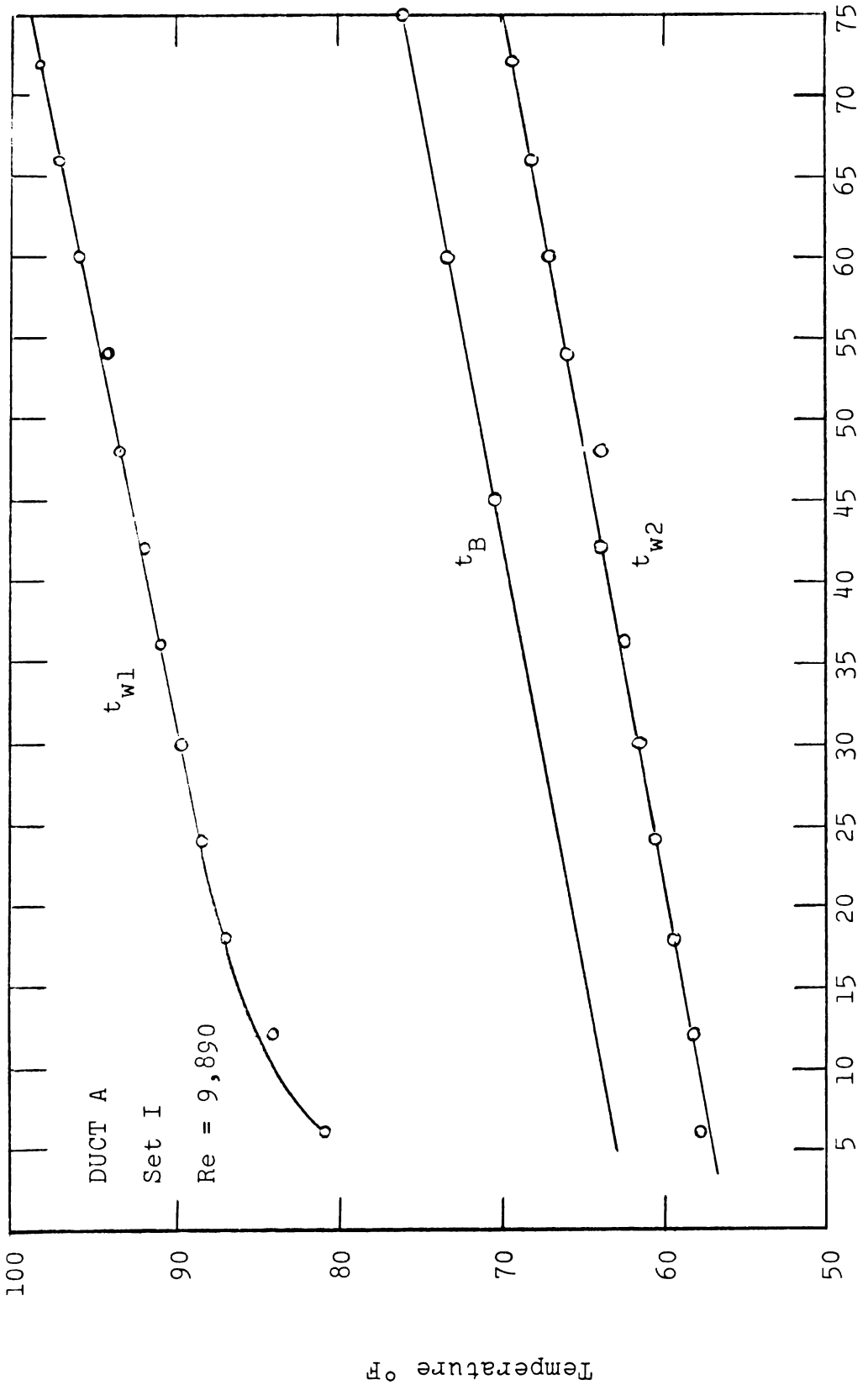

Fig. 14.--Temperatures t_{w1}, t_{w2}, and t_B vs. length of Duct A.

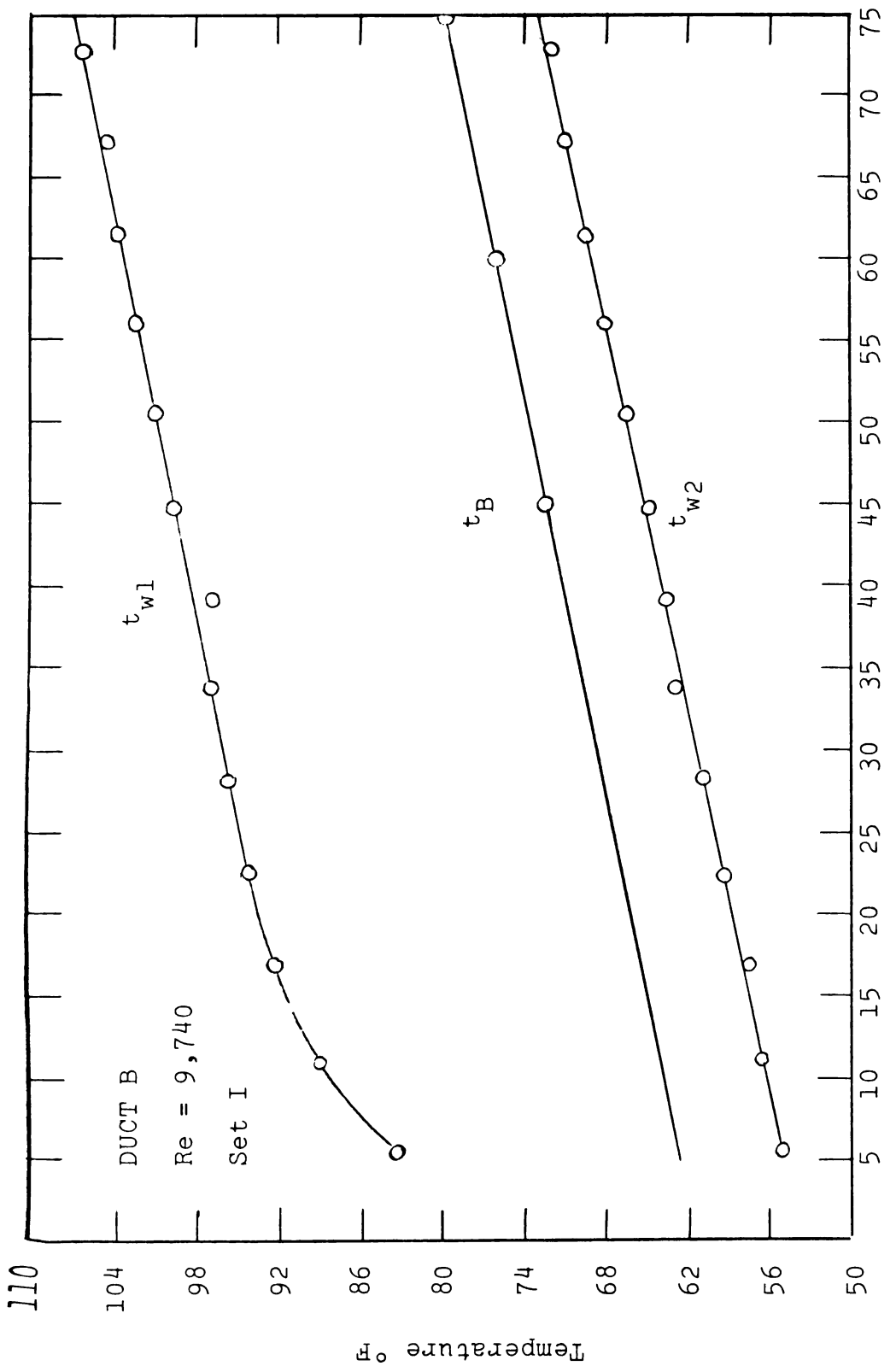

Fig. 15.--Temperatures t_{w1}, t_{w2}, and t_B vs. length of Duct B.

h Enthalpy of moist air = 0.24t+W(1061+0.45t). BTU per lb. dry air.

V_1 Volume of moist air entering the duct. Cu. ft. per minute.

P Barometric pressure--Psia or inches Hg.

P_w Partial pressure of water vapor; Psia or inches Hg. $P_{w,s}$ for saturated water vapor at t; $P_{ws,wb}$ for saturated water vapor at t_{wb}.

h_f Enthalpy of saturated liquid water. BTU per lb.

h_g Enthalpy of saturated water vapor. BTU per lb.

h_{fg} Latent heat of vaporization of water = h_g-h_f. BTU per lb; $h_{fg,wb}$ evaluated at wet bulb temperature.

h Convection heat transfer coefficient. BTU per (hr.) (sq. ft.) (F).

h_D Convection mass transfer coefficient. Lbs. water per (hr.) (Sq. ft.) (lb. water per lb. dry air).

Le Lewis number--$h/h_D C_{P,a}$ --dimensionless.

h_R Radiation heat transfer coefficient. BTU per (hr.) (sq. ft.) (F).

f_s Coefficient used in Equation (37)--dimensionless.

m Mass of moist air. lb./hr.

m_a Mass of dry air. lb./hr.

k Thermal conductivity of air. BTU per (hr.) (F) (ft.).

Δt Change in temperature of moist air--F°.

Δh Change in enthalpy of moist air=$\Delta t(0.240+0.45W)$. BTU per lb. dry air.

The dry and wet bulb temperatures recorded by the sling psychrometer are analyzed as follows:

1. Calculate $W_{s,wb}$ from the following equation:

$$W_{s,wb} = 0.622 \frac{f_s P_{ws,wb}}{P - f_s P_{ws,wb}} \tag{37}$$

where the magnitudes of f_s have been given by Goff (81). Its values are listed in Table 2.

TABLE 2.--Values of the Coefficient f_s.

Temp.--F°	f_s
40	1.0044
50	1.0044
60	1.0044
70	1.0045
80	1.0047
90	1.0048
100	1.0050

The values of $P_{ws,wb}$ to be used in equation (37) are taken from reference (82).

2. W was calculated from the following equation:

$$W = W_{s,wb} - \acute{K} (t_{db} - t_{wb}) \tag{38}$$

where

$$\acute{K} = \frac{LeC_{p,a}}{h_{fg,wb}} \left[1 + \frac{h_R}{h} \right] \tag{39}$$

assuming that $t_s = t$

$$h_R = 0.173\varepsilon_{wb} \frac{\left(\frac{T}{100}\right)^4 - \left(\frac{T_{wb}}{100}\right)^4}{(t-t_{wb})} \tag{40}$$

where ε_{wb} is the emissivity of wet bulb.

For the flow of air normal to single wires or cylinders, McAdams (83) has suggested the following relations:

$$\frac{hd}{k} = 0.615 \left(\frac{\rho Vd}{\mu}\right)^{0.466} \quad \text{for } 40 < Re < 4.000 \tag{41}$$

$$\frac{hd}{k} = 0.174 \left(\frac{\rho Vd}{\mu}\right)^{0.618} \quad 4000 < Re < 40,000 \tag{42}$$

where d is the bulb diameter and V the velocity of air. Threlkeld (84) has presented the ratio $\frac{h_R}{h}$ in the forms of graphs. The graphs are based on equations (40), (41), and (42). A value of $\varepsilon_{wb} = 0.9$ was used in equation (40).

Figures (10.5), (10.6) and (10.8) of reference (84) were used to determine Le and $\frac{h_R}{h}$. An air velocity of 800 ft. per min. was used.

Values of $h_{fg,wb}$ were taken from reference (82).

3. Mass of dry air flowing through the duct was calculated as follows:

The volume of air flowing through the venturi was corrected for pressure drop and temeprature rise using perfect gas relations. This gave the volume of air corresponding to the temperature and pressure at entrance to the duct. Let this volume be indicated by V_1 . Mass of

dry air = $m_a = \frac{V_1}{v}$

where

$$= 53.35\ (460 + t)/(P - P_w)$$

the mass of dry air flowing through the duct being known, Reynolds number is given by:

$$Re = \frac{m_a.(1+w)}{A} \cdot \frac{d_h}{\mu}$$

where A = 1/36 sq. ft. for either duct A or B, d_h = 1.6 in.

The property values are inserted at mean bulk temperature and then multiplied by $(\frac{\mu B}{\mu_w})^{0.14}$ where μ_B and μ_w are evaluated at mean bulk and mean wall temperature respectively.

4. In fully developed flow $\frac{\partial t}{\partial x}$ = constant and on the graphs of temperature against duct length, this condition is indicated by the wall and bulk temperatures increasing linearly along the duct length.

The experiments showed that fully developed flow was attained in less than 3 feet from the duct entrance.

The enthalpy increase for air in passing through a length 3 feet (between 5 feet and 8 feet from the entrance) for either duct was calculated as:

$$m_a \Delta h' = m_a \, (t'-t'') \, (0.24 + 0.45w)$$

where t' and t" are the bulk air temperatures at two points located at distances 8 feet and 5 feet from the entrance. Since the width of the duct is 4 inches, a length of 3 feet along the duct will give an area of heated wall equal to 1 sq. ft.

5. The Nusselt number for heat transfer between the heated wall and air is then defined as:

$$Nu = \frac{m_a \Delta h'}{\overline{t_{w_1} - t_B}} \cdot \frac{d_h}{k}$$

where $\overline{t_{w_1} - t_B}$ is the mean of the temperature difference:

$t_{w_1} - t_B$, in fully developed region.

Property values are inserted at mean bulk temperature and then corrected for variation in physical properties by using a multiplication factor $(\frac{\mu_B}{\mu_w})^{0.14}$. As before μ_B and μ_w are evaluated at mean bulk and mean wall temperature respectively.

Results and Discussion

Hydrodynamic Characteristics of the Ducts

Air velocity, air flow and corresponding Reynolds numbers studied for each duct are given in Table 3.

TABLE 3.--Air Flow (CFM) and Corresponding Reynolds Numbers.

U_m--ft./sec.	Q--CFM	Re
12.084	20.14	10,000
18.126	30.21	15,000
24.168	40.28	20,000
30.210	50.35	25,000
36.252	60.42	30,000
48.336	80.56	40,000
60.420	100.70	50,000

Under each section, the results for duct A will be presented first. This will be followed by the results for duct B.

Intake Length.--As explained earlier, the flow in a duct attains the fully developed velocity profile asymptotically. In the present thesis the intake length will be defined as that length where pressure gradient attains a constant value, commensurate with the accuracy of the measuring instruments.

The graphs showing pressure against duct length for each Reynold number are used to locate the duct cross section where the pressure gradient assumes a constant value. The

distance of this cross section from the entrance of the duct is, by definition, the intake length. The results for the intake length are presented in Table 4. Results for Latzko (14) are also tabulated for comparison.

$\frac{Le}{d_h}$ is plotted against Reynolds number in Figure 16. The present analysis approximates the intake length by the formula:

$$\frac{Le}{d_h} = 1.022\ Re^{0.166} \qquad (43)$$

The present results deviate from Latzko's results by as low as 2.3 per cent and as high as 11.7 per cent in the range of Reynolds numbers studied. This deviation as noticed in Figure 16 increases with a rise in the magnitude of Reynolds number.

Latzko (14) assumed that the boundary layer is turbulent starting at the entrance. The tube was further assumed to be smooth.

In the present analysis, the presence of laminar boundary layer was observed for a very short distance of about two hydraulic diameters at lower Reynolds numbers. This distance became exceedingly small reducing to less than one hydraulic diameter at higher Reynolds numbers. It may safely be assumed that at higher Reynolds numbers the boundary layer is turbulent right at the entrance. In other words, at higher Reynolds numbers the duct A fulfills the

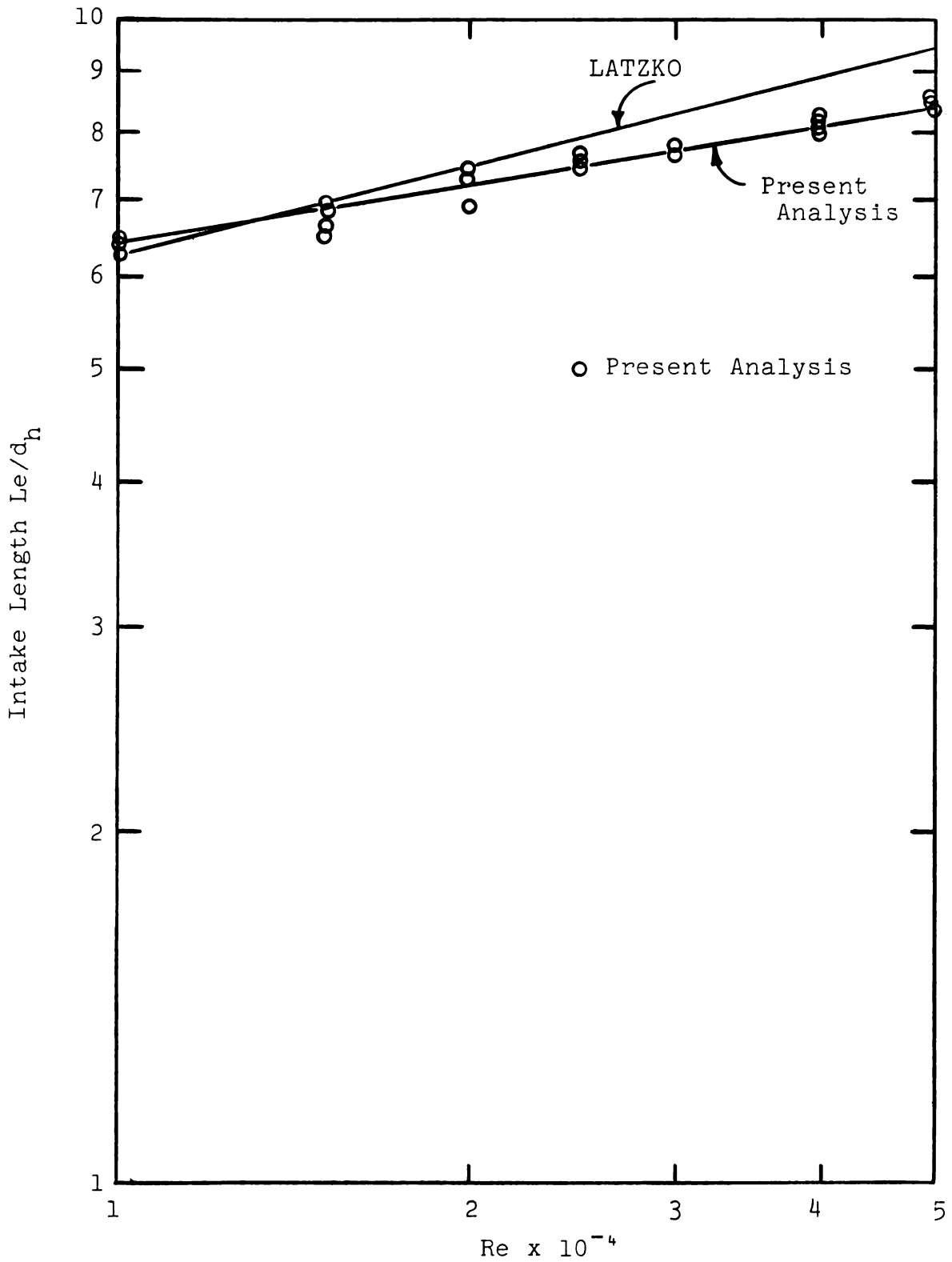

Fig. 16.--The intake length of Duct A.

TABLE 4.--Intake Length for Duct A.

Re	Le/d_h								Latzko*
	Set I	Set II	Set III	Set IV	Set V	Set VI	Set VII	Set VIII	
10,000	6.45	6.40	6.50	6.45	6.40	6.50	6.45	6.40	6.23
15,000	6.55	6.90	6.95	6.95	6.90	7.00	6.90	6.60	6.92
20,000	7.25	7.25	7.50	7.20	7.25	7.25	6.90	6.95	7.48
25,000	7.50	7.45	7.55	7.45	7.45	7.50	7.70	7.50	7.92
30,000	7.75	7.70	7.75	7.70	7.75	7.75	7.70	7.70	8.28
40,000	8.20	8.25	8.30	8.30	8.25	8.25	8.00	8.30	8.92
50,000	8.40	8.40	8.35	8.35	8.40	8.40	8.60	8.35	9.40

*Latzko (14)-- $\frac{Le}{d_h} = 0.623^{0.25}$.

TABLE 5.--Intake Length for Duct B.

Re	Le/d_h							
	Set I	Set II	Set III	Set IV	Set V	Set VI	Set VII	Set VIII
10,000	9.05	9.30	9.25	9.30	10.05	9.30	9.30	9.25
15,000	10.05	10.00	10.05	9.60	10.25	10.50	10.00	10.05
20,000	11.00	11.10	11.05	11.15	11.00	10.25	11.00	10.75
25,000	11.50	11.55	11.55	11.50	11.45	12.50	11.45	11.55
30,000	12.10	12.05	12.05	12.20	12.25	12.20	12.05	12.10
40,000	12.80	13.35	12.00	12.75	12.70	12.65	13.00	13.00
50,000	13.75	13.55	13.70	13.75	13.50	13.45	13.75	13.50

assumptions made by Latzko (14) except that it is rough and not hydraulically smooth. The additional roughness causes the turbulent boundary layer to develop faster, thereby resulting in a shorter intake length than what will be predicted by Latzko (14).

At lower Reynolds number, on the other hand, the presence of laminar boundary layer results in a longer intake length than in the case of Latzko's analysis (14). It is because turbulent layer develops faster than the laminar one. The increase in the intake length due to the presence of laminar layer, it seems, is not offset by the roughness of the tube which causes the turbulent layer to develop faster.

The corresponding values of intake length (Le/d_h) for duct B are given in Table 5. The results are graphically presented in Figure 17. The intake length (Le/d_h) is approximated by the relation:

$$\frac{Le}{d_h} = 0.918\ Re^{0.24} \tag{44}$$

Friction Coefficient for Fully Developed Flow

For a noncircular cross section, the fully developed friction coefficient is given by:

$$f = \frac{-d_h \left(\frac{dP}{dx}\right)}{\rho\, u_m^2/2} \tag{45}$$

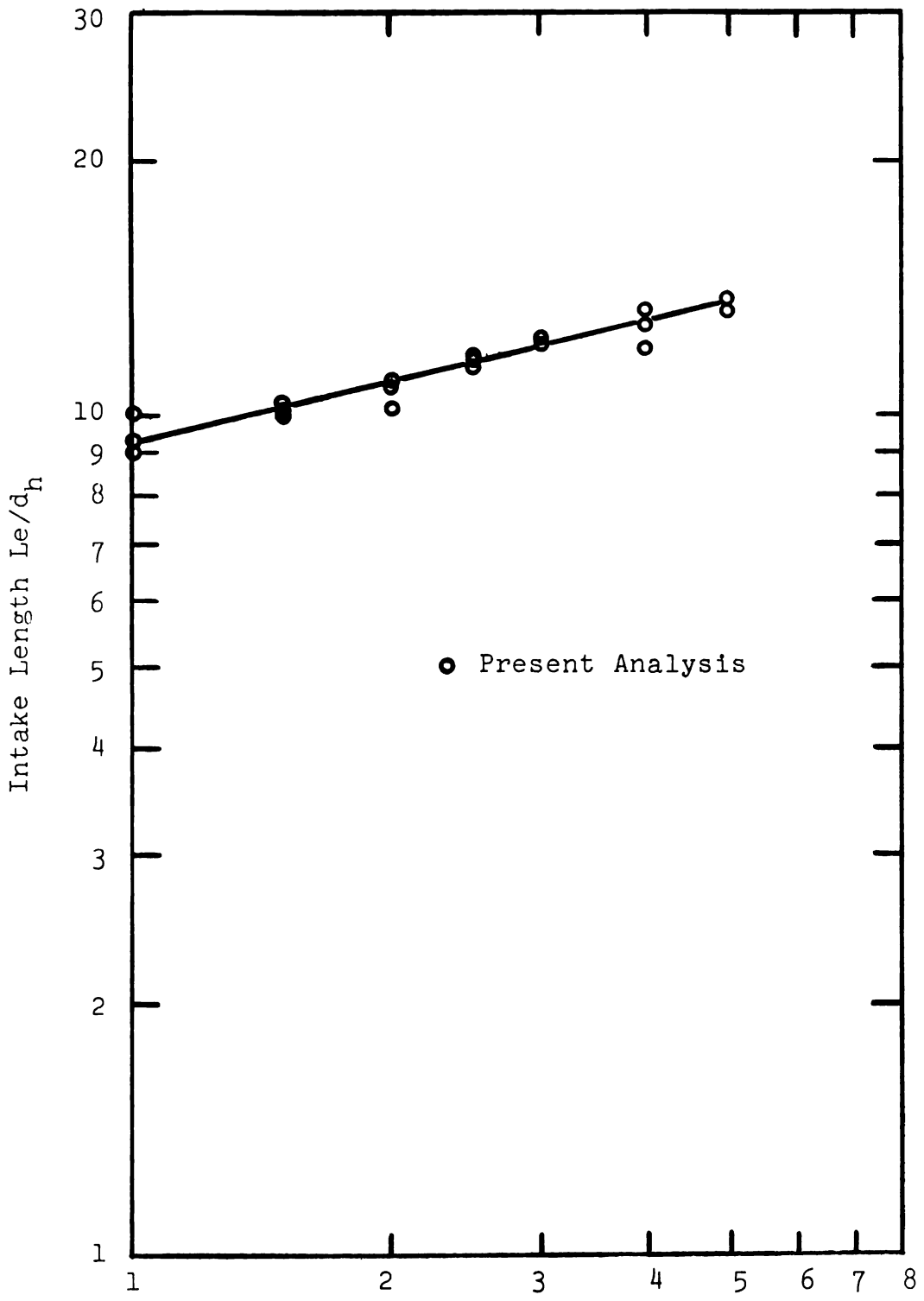

Fig. 17.--The intake length of Duct B.

For both ducts A and B, the hydraulic diameter is given by:

$$\frac{2ab}{a+b} = 1.6"$$

Pressure gradients for various Reynolds numbers are determined from the graphs of pressure against duct length.

The resulting values of f as calculated from Equation (45) are given in Table 6. These 8 sets of values are graphically presented in Figure 18. Friction factors for a smooth tube as given by Blasius Law are also plotted.

The coefficient of friction for the duct A is seen to depend on both Reynolds number and the relative roughness of the duct. Comparison with Nikuradse's (24) and Moody's (26) charts shows that the duct A very closely follows the pattern of rough pipes in the transition regime

$$5 \leq \frac{k\sqrt{\frac{\tau_w}{\rho}}}{\nu} \leq 70$$

i.e., the protrusions extend partly outside the laminar sub-layer and additional resistance is introduced by the form drag experienced by the protrusions in the boundary layer. The type of roughness which is experienced by the duct by having a galvanized steel roof, two pieces of lumber as the vertical sides and plywood as the bottom, may be (as mentioned in Chapter II) classified as being of the second

TABLE 6.--Coefficient of Friction for Duct A.

Re	f							
	Set I	Set II	Set III	Set IV	Set V	Set VI	Set VII	Set VIII
10,000	0.04410	0.04425	0.04385	0.04417	0.0455	0.04370	0.04409	0.04433
15,000	0.04240	0.04212	0.04110	0.04123	0.04317	0.04201	0.04170	0.04197
20,000	0.04120	0.04135	0.04101	0.04141	0.04139	0.04128	0.04057	0.04215
25,000	0.04150	0.04122	0.04113	0.04095	0.04125	0.04380	0.04109	0.04127
30,000	0.04165	0.04132	0.04137	0.04093	0.04117	0.04100	0.04088	0.04113
40,000	0.04060	0.04110	0.04080	0.04102	0.04121	0.04090	0.04118	0.04087
50,000	0.04109	0.04116	0.04025	0.04075	0.04130	0.04090	0.04120	0.04180

TABLE 7.--Coefficient of Friction f for Duct B.

	f							
	Set I	Set II	Set III	Set IV	Set V	Set VI	Set VII	Set VIII
10,000	0.0650	0.0691	0.0604	0.0654	0.0652	0.0658	0.0648	0.0657
15,000	0.0583	0.0577	0.0580	0.0602	0.0591	0.0562	0.0587	0.0574
20,000	0.0580	0.0570	0.0583	0.0579	0.0568	0.0579	0.0574	0.0575
25,000	0.0574	0.0568	0.0582	0.0577	0.0579	0.0544	0.0564	0.0572
30,000	0.0546	0.0572	0.0564	0.0570	0.0574	0.0581	0.0577	0.0585
40,000	0.0580	0.0571	0.0561	0.0564	0.0576	0.0577	0.0584	0.0574
50,000	0.0573	0.0562	0.0575	0.0566	0.0580	0.0578	0.0570	0.0565

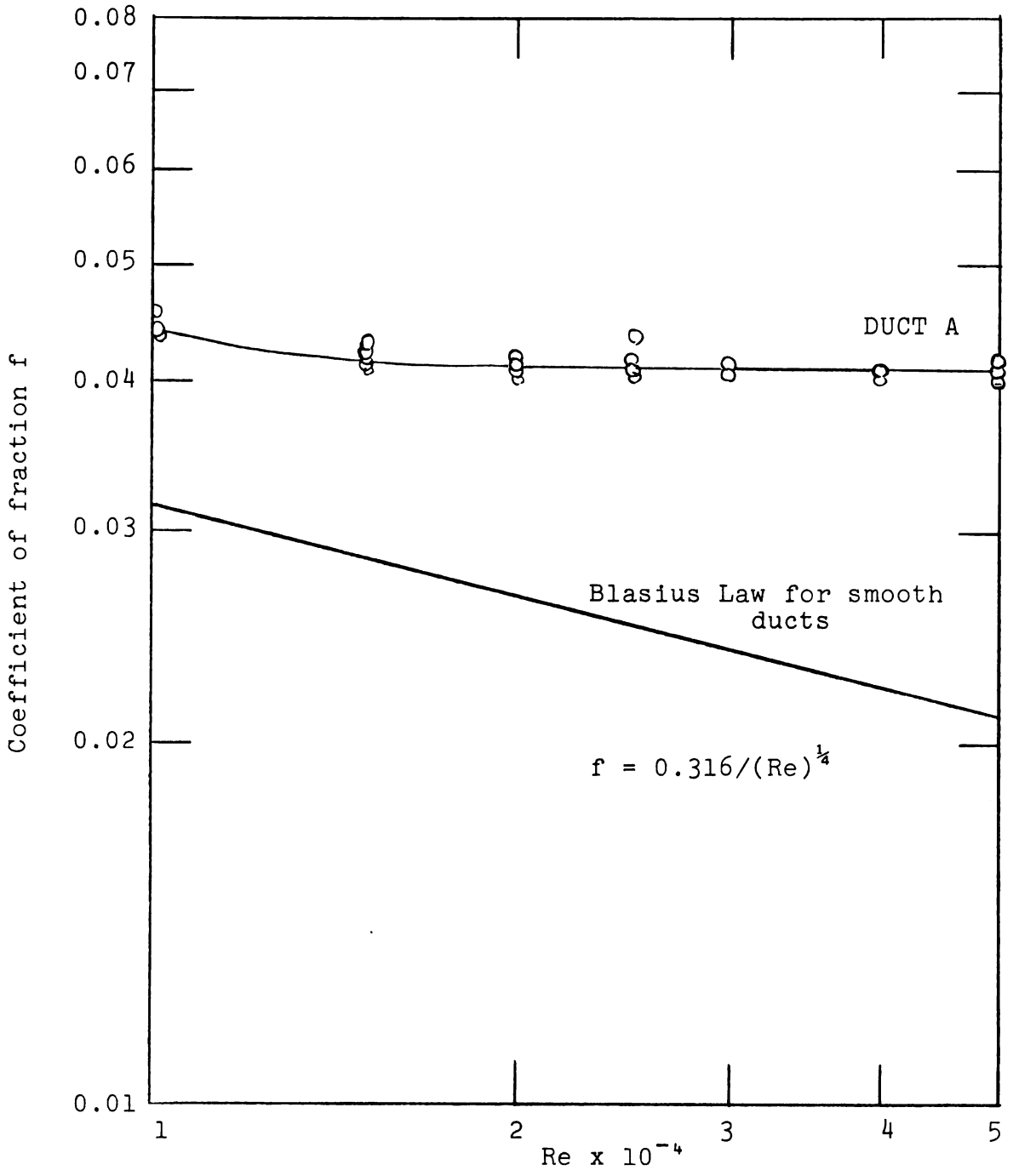

Fig. 18.--Coefficient of friction for Duct A.

type. In this kind of roughness, the friction coefficient depends on both the Reynolds number and the relative roughness.

The corresponding values of f for duct B are given in Table 7. The results are graphically presented in Figure 19. Friction coefficient for hydraulically smooth pipe based on Blasius Law are also given in the Figure for comparison.

The coefficient of friction for duct B, too, is seen to be dependent on both the Reynolds number and the relative roughness in the range of Reynolds number: 10,000 to 50,000. Duct B also lies in the transition regime of roughness. The roughness of a rectangular duct with a corrugated top, a plywood bottom and vertical walls made of lumber, may be (as mentioned in Chapter II) classified as being of the second type.

The friction coefficients for the two ducts are compared in Table 8. The values of f are taken from Figures 18 and 19.

Entrance and Intake Region Losses

As explained earlier, frictional pressure drop in a duct is calculated as if fully developed flow existed over the entire length L, and a second term is added which accounts for the increase in pressure drop due to entrance and intake region. The resulting equation for pressure drop is:

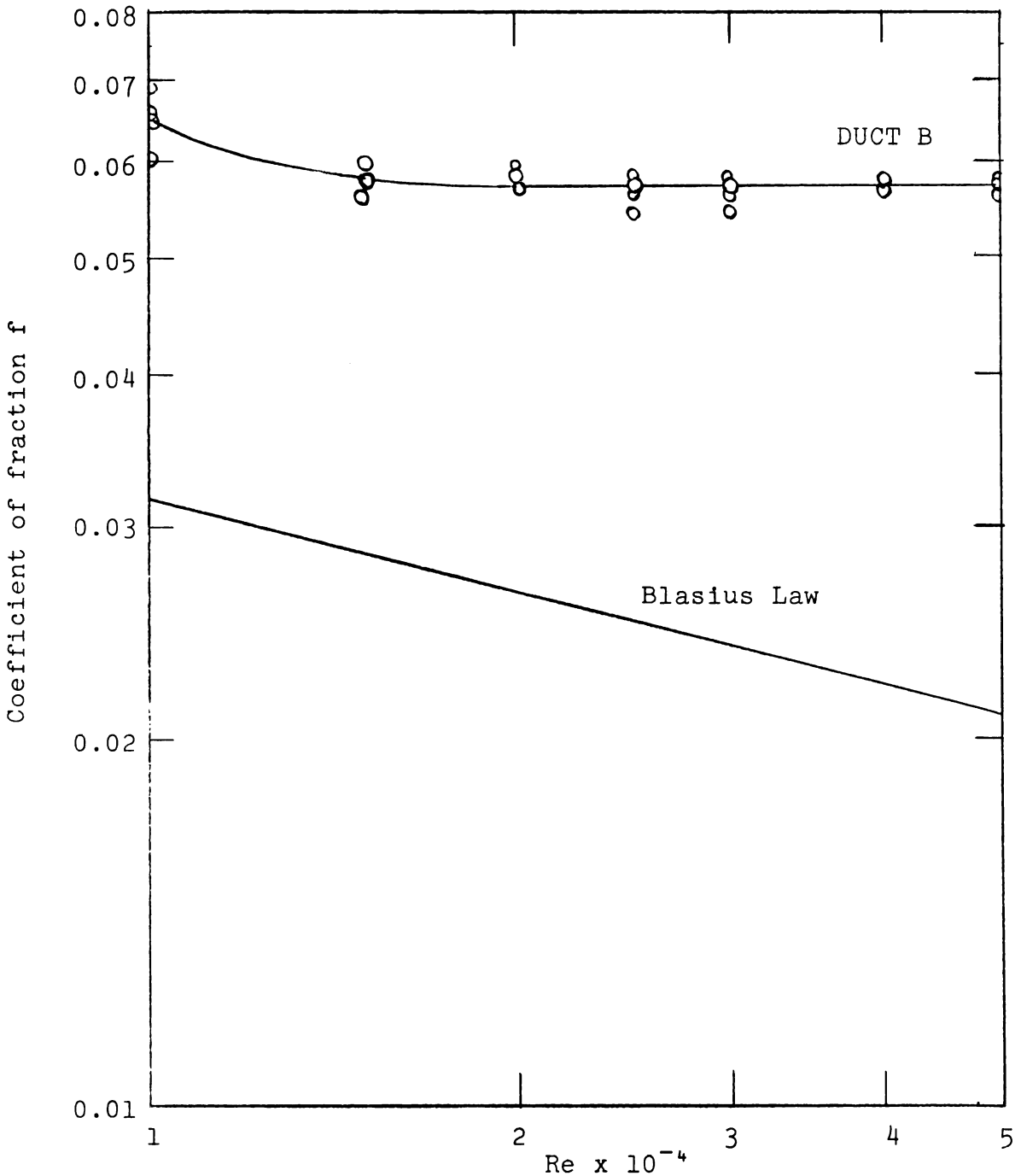

Fig. 19.--Coefficient of friction of Duct B.

TABLE 8.--Comparison of Values of f for Ducts A and B.

Reynolds number	Smooth duct Blasius Law	Duct A	Duct B	Per cent increase in f of duct a over smooth duct	Per cent increase in f of duct B over smooth duct	Per cent increase in f of duct B over duct A
10,000	0.0316	0.0440	0.0650	39.23	105.69	47.72
15,000	0.0285	0.0420	0.0585	47.36	105.36	39.28
20,000	0.0265	0.0414	0.0573	56.22	116.22	38.40
25,000	0.0250	0.0412	0.0573	64.80	129.20	39.07
30,000	0.0240	0.0410	0.0573	70.83	138.75	39.75
40,000	0.0223	0.0410	0.0573	83.85	156.95	39.75
50,000	0.0211	0.0410	0.0573	94.31	171.56	39.75

TABLE 9.--Entrance Loss Factor ($K_1 + K_2$).

Reynolds number	Factor $(K_1 + K_2)^a$
10,000	0.924
15,000	0.887
20,000	0.885
25,000	0.874
30,000	0.898
40,000	0.885
50,000	0.850

[a]Weighted average of all 8 sets of readings.

Average value of $K_1 + K_2 = 0.8861$.

$$P_o - P = f \frac{L}{d_h} \rho \frac{U_m^2}{2} + \overset{*}{K} \rho \frac{U_m^2}{2} \qquad (46)$$

where P_o is the pressure of stationary fluid ahead of the duct and P is the pressure at distance x from the entrance. Also $\overset{*}{K} = K_1 + K_2 + K_3 + K_4$.

The four components of K account for the following losses:

K_1 Loss due to acceleration of fluid from rest to the constant velocity u_m just before it reaches the inlet.

K_2 Loss due to abrupt contraction at the inlet.

K_3 Loss due to an increase of friction in the intake region.

K_4 Loss due to an increase in the momentum flux in the intake region; which is connected with the transformation of the velocity field.

In this thesis, factors $(K_1 + K_2)$ and $(K_3 + K_4)$ are found from the experiments.

The factor $(K_1 + K_2)$ is found from the pressure drop between the atmospheric pressure and the pressure indicated by the pressure tube a_1 (for duct A), and tube b_1 (for duct B). The factor $(K_3 + K_4)$ is found by subtracting $(K_1 + K_2)$ from K^* where K is found from Equation (46). The values of $(P_o - P)$ are, of course, found experimentally.

The results for duct A for the intake loss factors are given in Tables 9 and 10. The values of $\overset{*}{K} = K_1 + K_2 + K_3 + K_4$ are tabulated in Table 11. The corresponding values of entrance loss factors $(K_1 + K_2)$ and $(K_3 + K_4)$ and overall entrance loss factor $\overset{*}{K}$ for duct B are given in Tables 12, 13, and 14.

Relative Roughness

The following equation, based on Colebrook Function, is used to determine relative and absolute roughness of the duct under consideration:

$$\frac{K}{d_h} = \log^{-1}\left(0.57 - \frac{1}{2\sqrt{f}}\right) - \frac{9.3}{Re\sqrt{f}}$$

For duct A, the values of f are taken from Figure 18. The resulting values of K/d_h are given in Table 15.

Since $d_h = 1.6$ in., the resulting mean value of absolute roughness K for duct A equals 0.017664 in.

The values of relative roughness (K/d_h) and absolute roughness (K) for duct B are similarly based on values of f in Figure 19. The resulting values of relative roughness are given in Table 16.

With $d_h = 1.6$ in., the absolute roughness (K) for duct B equals 0.0464 in.

TABLE 10.--Entrance Loss Factor ($K_3 + K_4$) for Duct B.

Reynolds number	Factor ($K_3 + K_4$)[a]
10,000	0.235
15,000	0.293
20,000	0.266
25,000	0.271
30,000	0.267
40,000	0.208
50,000	0.290

[a]Weighted average of all 8 sets of readings.

Average value of $K_3 + K_4 = 0.2614$.

TABLE 11.--Factor $\overset{*}{K}$ for Duct A.

Reynolds number	$\overset{*}{K}$[a]
10,000	1.159
15,000	1.180
20,000	1.151
25,000	1.145
30,000	1.165
40,000	1.093
50,000	1.140

[a]Weighted average of all 8 sets of readings.

Average value of $\overset{*}{K} = 1.147$.

TABLE 12.--Entrance Loss Factor ($K_1 + K_2$) for Duct B.

Reynolds number	Factor ($K_1 + K_4$)[a]
10,000	0.770
15,000	0.685
20,000	0.759
25,000	0.690
30,000	0.718
40,000	0.741
50,000	0.744

[a]Weighted mean of 8 sets of readings.

Average = 0.729

TABLE 13.--Entrance Loss Factor ($K_3 + K_4$) for Duct B.

Reynolds number	Factor ($K_1 + K_4$)[a]
10,000	0.235
15,000	0.227
20,000	0.251
25,000	0.297
30,000	0.214
40,000	0.213
50,000	0.228

[a]Weighted mean of 8 sets of readings.

Average = 0.237.

TABLE 14.--Overall Entrance Loss Factor K^* for Duct B.

Reynolds number	K^*[a]
10,000	1.005
15,000	0.912
20,000	1.010
25,000	0.987
30,000	0.932
40,000	0.954
50,000	0.972

[a]Weighted mean of 8 sets of readings.

Average = 0.967.

TABLE 15.--Relative Roughness of Duct A.

Reynolds number	f	K/d_h
10,000	0.0440	0.01099
15,000	0.0420	0.01093
20,000	0.0415	0.01071
25,000	0.0412	0.01101
30,000	0.0410	0.01130
40,000	0.0410	0.01135
50,000		

Average = 0.01104.

TABLE 16.--Relative Roughness of Duct B.

Reynolds number	K/d_h *
10,000	0.03034
15,000	0.02904
20,000	0.02890
25,000	0.02925
30,000	0.02951

*Average = 0.02900.

TABLE 17.--Nusselt Numbers for Duct A.

Reynolds number	Nu
Set I	
9,890	34.12
14,800	48.45
20,000	60.33
24,785	71.31
29,780	89.10
39,780	104.80
Set II	
10,400	32.82
15,510	46.00
20,680	61.93
25,900	65.65
31,210	84.62
41,600	110.44

Heat Transfer Characteristics of the Ducts A and B

Two sets of readings were taken for each duct covering an approximate range of the Reynolds numbers 10,000 to 40,000. All the property values were inserted at average bulk temperature and corrected by using a multiplication factor:

$$\left(\frac{\mu_B}{\mu_w}\right)^{0.14}$$

Nusselt number as defined earlier was computed as:

$$Nu = \frac{m_a . \Delta h'}{t_{w_1} - t_B} \cdot \frac{d_h}{k}$$

The results are tabulated in Table 17.

Kolár (75) gives the following expression for heat transfer in tubes with symmetric boundary conditions:

$$h = 0.04\ k\ u_m \sqrt{\frac{f}{8}} \cdot \frac{1}{\nu} \cdot (Pr)^{0.5}$$

This expression holds for both smooth and rough tubes.

For hydraulically smooth tube, it may then be written as:

$$h = 0.04\ k\ u_m \sqrt{\frac{f_o}{8}} \cdot \frac{1}{\nu} \cdot (Pr)^{0.5}$$

The following expression results for the ratio of the film heat transfer coefficients:

$$\frac{(h)_{rough}}{(h)_{smooth}} = \sqrt{\frac{f}{f_o}}$$

An attempt was made in this thesis to see if this relation could successfully correlate the results for asymmetrically heated rough ducts.

The values of $\sqrt{\frac{f}{f_o}}$ for different Reynolds nubmers, for duct A, are given in Table 18. Values of f are taken from Figure 18. f_o, the friction coefficient for smooth duct, is given by Blasius equation.

The values of Nusselt numbers were determined from different expressions for an unsymmetrically heated smooth channel. These values are multiplied by $\sqrt{\frac{f}{f_o}}$ and plotted in Figure 20; experimentally-found values of Nusselt numbers are then compared.

Reference numbers and equation numbers in Figure 20 refer to the sources from which the values of the Nusselt numbers are taken for smooth ducts and channels.

The corresponding values for Nusselt number for duct B are given in Table 19. The values of factor $\sqrt{\frac{f}{f_o}}$

TABLE 18.--Factor $\sqrt{\frac{f}{f_o}}$ for Duct A.

Reynolds number	Factor $\sqrt{\frac{f}{f_o}}$
10,000	1.18
15,000	1.218
20,000	1.245
25,000	1.280
30,000	1.305
40,000	1.355
50,000	1.390

TABLE 19.--Nusselt Number for Duct B.

Reynolds number	Nu
Set I	
9,740	38.65
14,580	55.80
19.600	63.30
24,580	88.02
29,390	88.93
39,220	121.81
Set II	
10,310	40.50
15,600	54.22
20,610	67.63
25,900	89.25
31,180	93.62
41,900	127.35

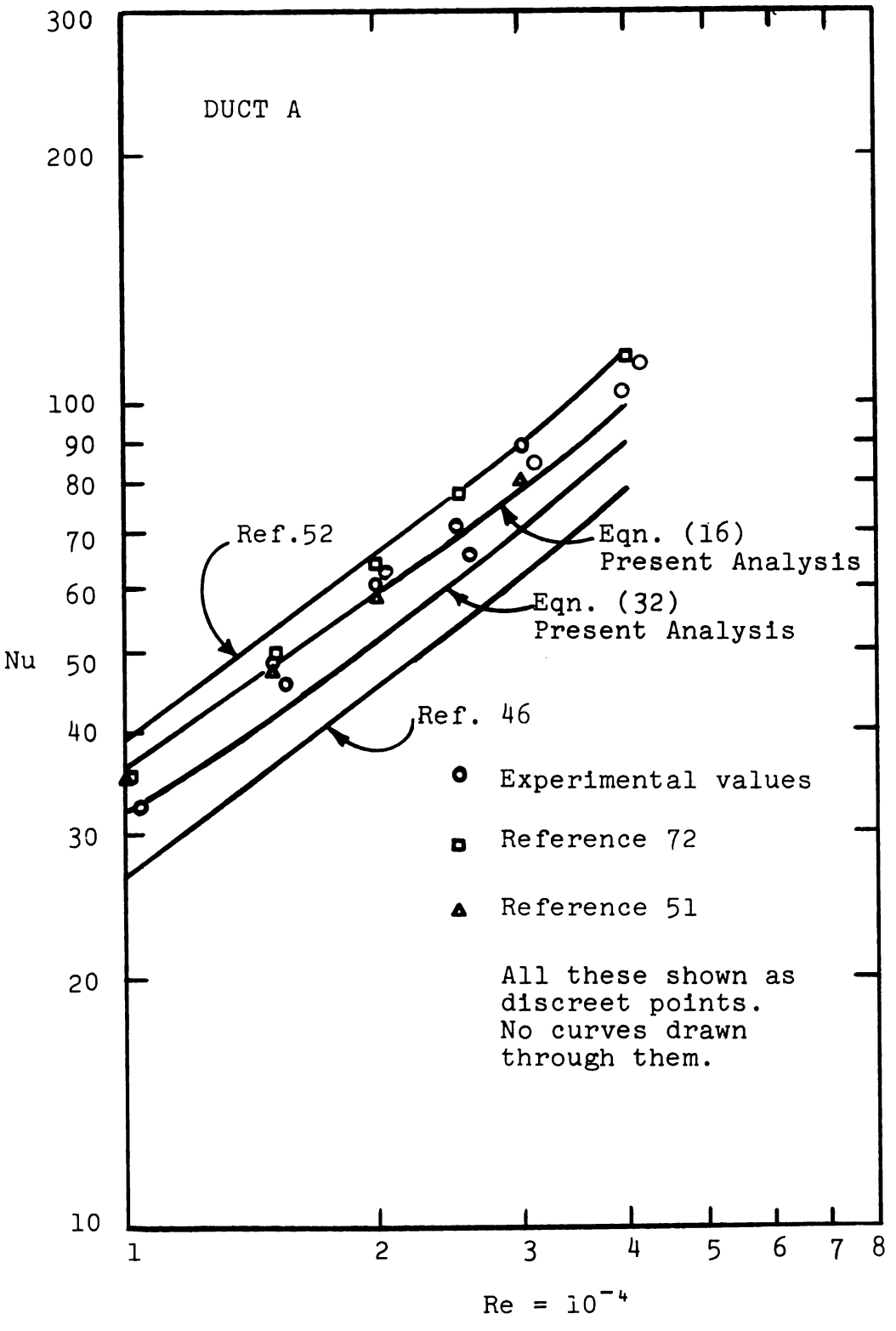

Fig. 20.--Comparison between theoretically and experimentally determined values of Nusselt numbers for Duct A.

for duct B are given in Table 20. Values of f are taken from Figure 19 and those of f_o from Blasius Law.

TABLE 20.--Factor $\sqrt{\frac{f}{f_o}}$ for Duct B.

Reynolds number	Factor $\sqrt{\frac{f}{f_o}}$
10,000	1.435
15,000	1.438
20,000	1.461
25,000	1.509
30,000	1.542
40,000	1.601
50,000	1.656

As before, the values of Nusselt number from different analyses for unsymmetrically heated smooth channel are multiplied by the factor $\sqrt{\frac{f}{f_o}}$ and plotted as a funciton of Reynolds number (Figure 21). The experimentally-found values of Nusslet numbers are plotted for comparison.

The Nusselt numbers for ducts A and B are presented together in Figure 22.

Madsen (54) has recommended a characteristic heat transfer coefficient for parallel plates with axially uniform but unsymmetrical heat fluxes. This heat transfer coefficient is independent of heat flux symmetry and is defined as follows:

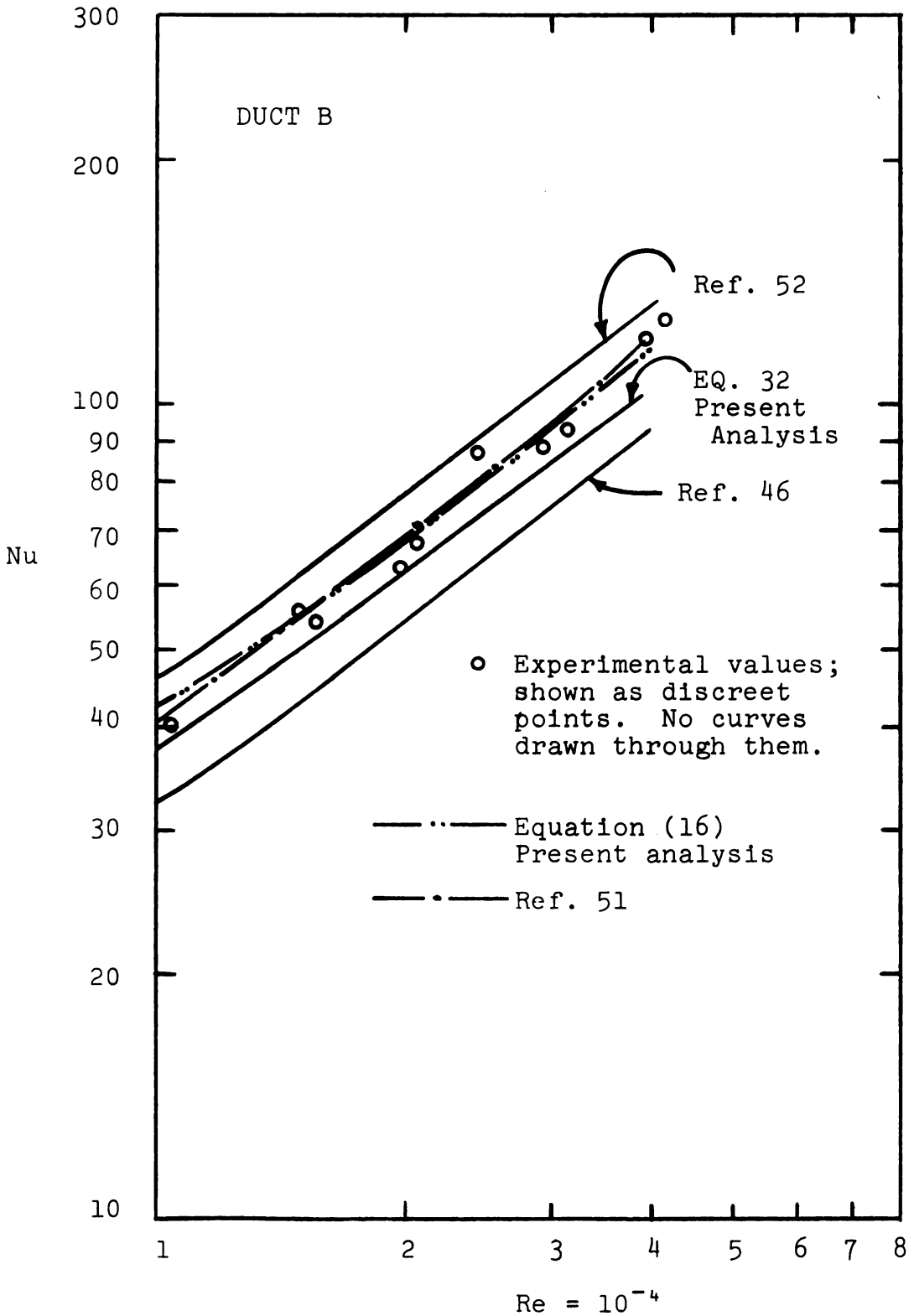

Fig. 21.--Comparison between theoretical and experimental values of Nusselt numbers for Duct B.

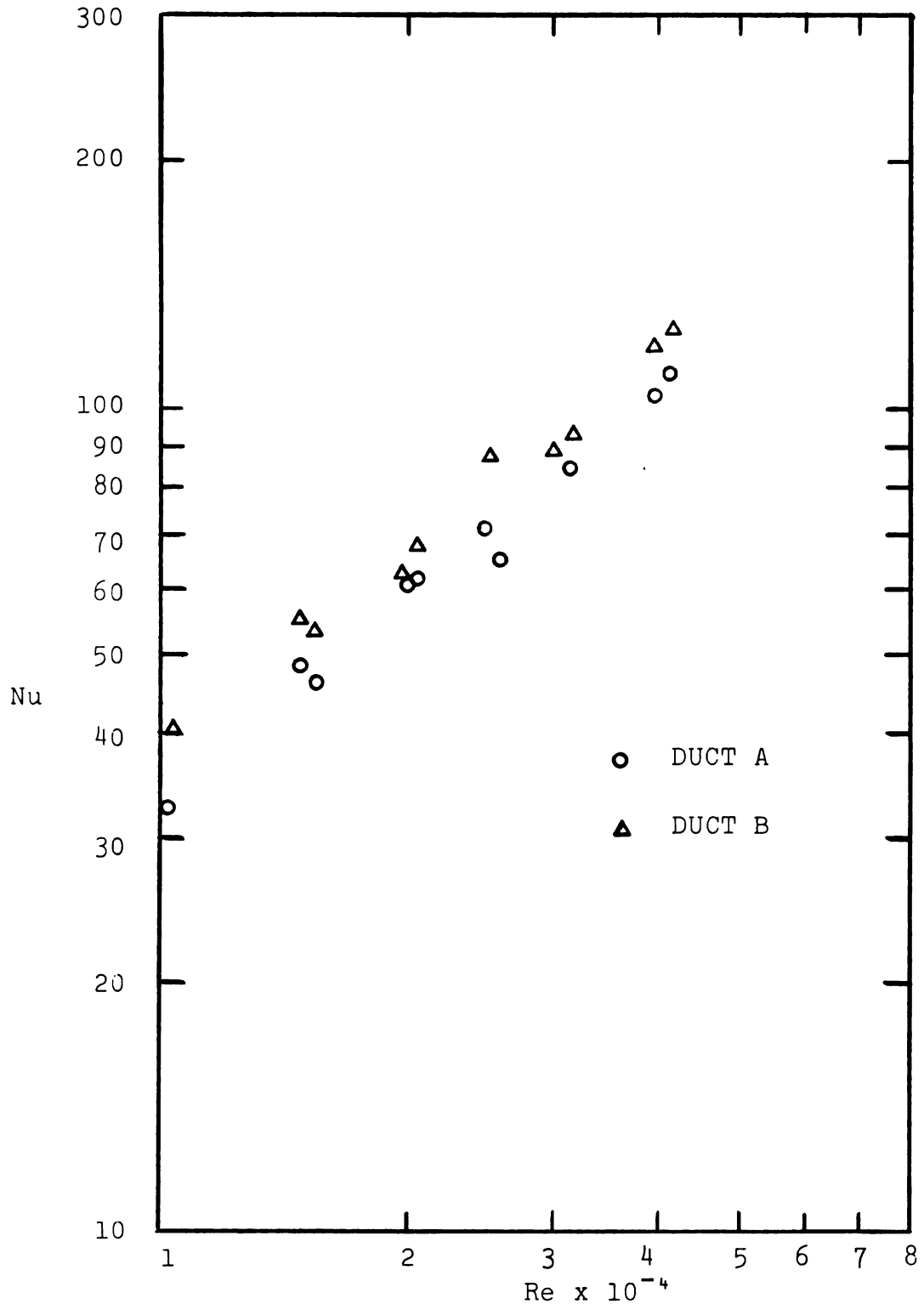

Fig. 22.--Nusselt numbers for Ducts A and B.

$$h_{general} = \frac{q_{w_1} - q_{w_2}}{(\overline{t_{w_1} - t_B}) + (\overline{t_{w_2} - t_B})}$$

For an asymmetrically heated channel, with one wall essentially adiabatic, the relationship reduces to:

$$h_{general} = \frac{q_w}{(\overline{t_{w_1} - t_B}) + (\overline{t_{w_2} - t_B})}$$

where the bar refers to the mean values of the temperature difference.

The general heat transfer coefficient suggested by Madsen (54) is for smooth ducts.

An attempt was made in this thesis to see if Madsen's Rule will carry over to the rough ducts. A certain modification is obviously necessary and the following procedure was used.

The heat transfer coefficients for symmetrically heated smooth channels obtained from different analyses were multiplied by the factor $\sqrt{\frac{f}{f_o}}$.

This gives a <u>modified</u> $h_{general}$ for rough ducts. Let it be denoted as $h^*_{general}$.

The value of $h^*_{general}$ as found from experiments for the rough ducts can be defined as:

$$h^{*}_{general} = \frac{m_a . \Delta h'}{(\overline{t_{w_1}} - t_B) + (\overline{t_{w_2}} - t_B)}$$

The experimental and theoretical values of $h^{*}_{general}$ (after changing them to corresponding Nusselt numbers) are plotted in Figures 23 and 24 for ducts A and B respectively.

The numbers in Figures 23 and 24 refer to the references from which analyses for smooth symmetrically heated channels are taken.

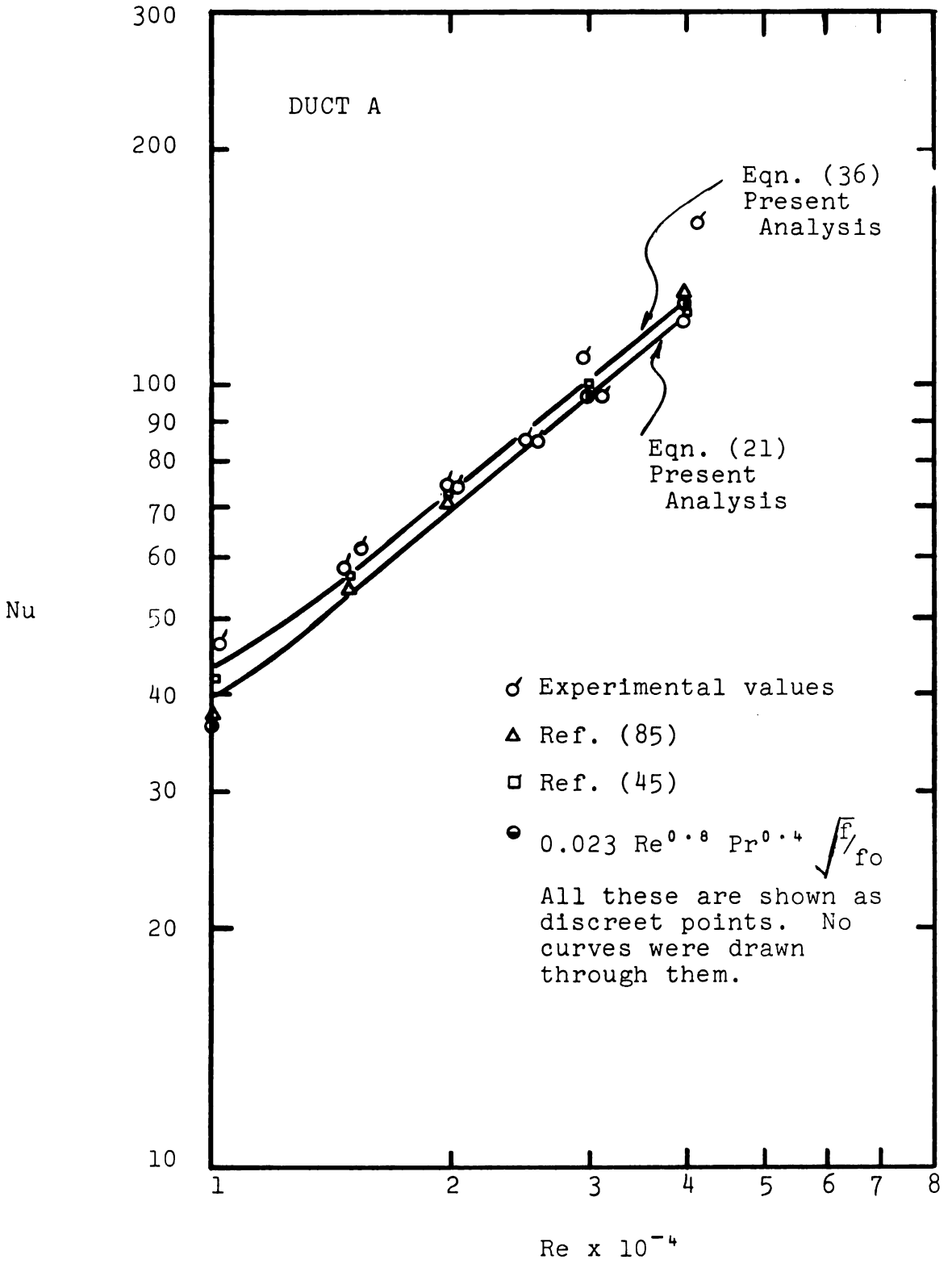

Fig. 23.--Verification of "modified" Madsen's Rule for Duct A.

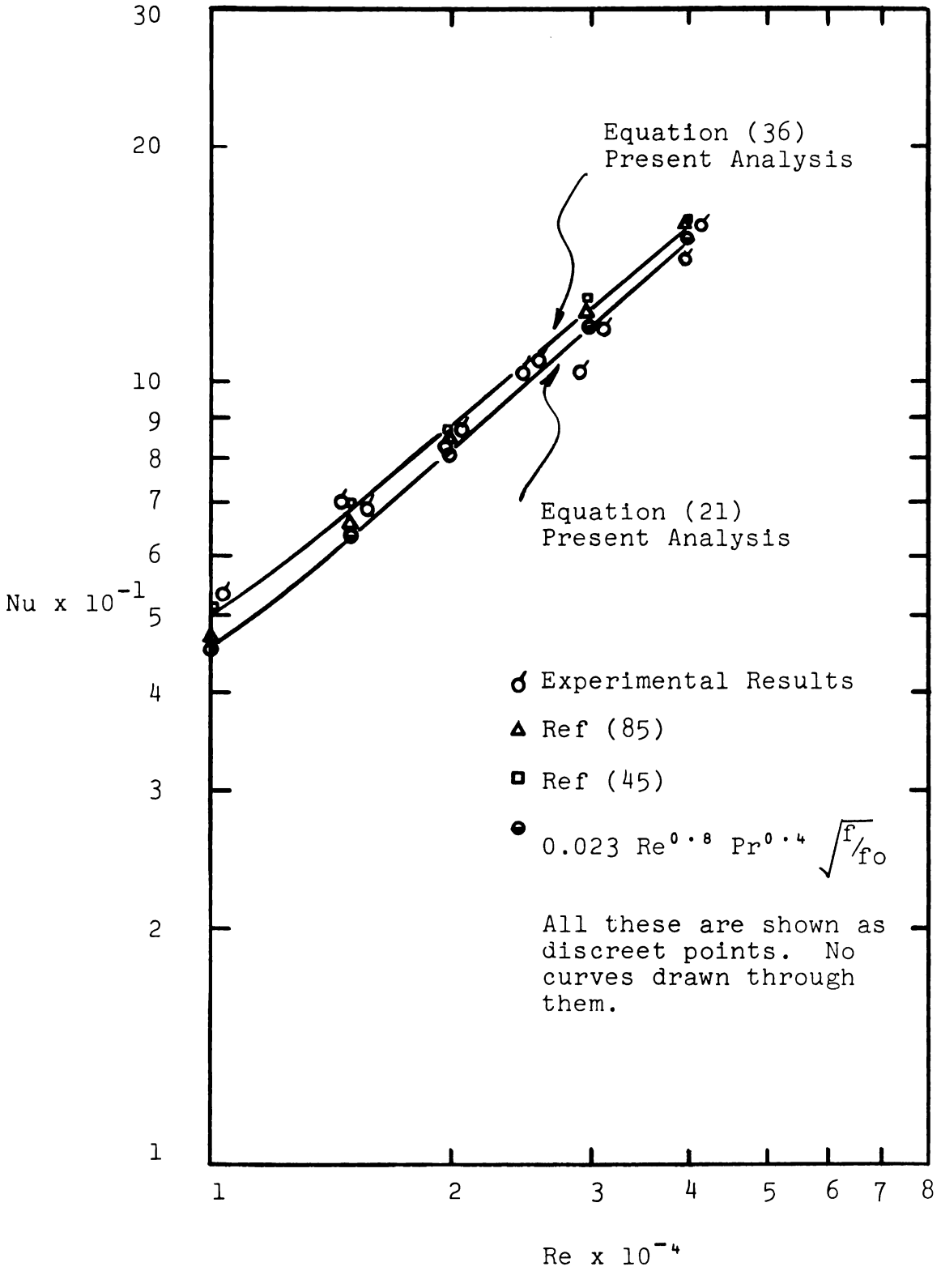

Fig. 24.--Verification of "modified" Madsen's Rule for Duct B.

CHAPTER VI

CONCLUSIONS

Two dimensional forced convection for a constant property, incompressible fluid in an unsymmetrically heated rough duct was studied in this thesis. The effects of conduction and radiation were neglected. For the range of the Reynolds numbers studied, the findings may be summarized as follows:

1. In fully developed turbulent flow, the friction coefficient for duct B is about 40 per cent higher than that for duct A.

2. The friction coefficient for both ducts is a function of the Reynolds number and relative roughness.

3. Duct B has a longer intake length, the boundary layer developing on one side only. The flow was fully developed in less than 15 hydraulic diameters.

4. The value of the factor K^* used in determining the inlet losses roughly equals unity for both the ducts.

5. The absolute roughness of duct A is about 0.011 and that of duct B equals 0.029.

6. The convection heat transfer coefficient for an unsymmetrically heated duct is less than that of the symmetrically heated duct. The analytical expressions developed in this thesis for unsymmetrically heated smooth channel apply satisfactorily to the case of an unsymmetrically heated rough duct when heat transfer coefficient is multiplied by $\sqrt{\frac{f}{f_o}}$.

7. Hydraulic diameter and Reynolds number based on inlet cross section of the corrugated-top-duct give satisfactory correlation.

8. The generalized heat transfer coefficient suggested by Madsen for smooth tubes, carried over to the rough ducts studied in this thesis. The heat ransfer coefficient, however, had to be corrected according to item 6 given above.

9. An obvious increase in heat transfer coefficient results when rough duct replaces a hydraulically smooth one. However, this increase has to be paid for by an increase in pressure drop; whereas the heat transfer coefficient is proportional to $\sqrt{\frac{f}{f_o}}$, the pressure varies as the ratio $\frac{f}{f_o}$.

10. The thermal entrance length appears to be less than 22 hydraulic diameters. Because of the asymptotic nature of the thermal development and insufficient points in the entrance region, it was not possible to assign a more precise value to the thermal entrance length.

11. In the analytic expressions developed in this thesis, equality of ε_m and ε_q for all y and Re was assumed. A marked difference, however, has been observed in several experimental studies.* A survey of experiments and theoretical work, however, reveals no consistent picture.

---

*For instance, see Ref. 79.

BIBLIOGRAPHY

1. Buelow, F. H. Drying grain with solar energy. Quarterly Bulletin, Michigan Agricultural Experiment Station 41:421. 1958.

2. Nikuradse, J. Investigation of Turbulent Flow in Tubes of Non-Circular Cross Section. Ingen.-Arch. 1:306-332. 1930.

3. Washington L., and Marks, W. M. Heat Transfer and Pressure Drop in Rectangular Air Passage. Ind. Eng. Chem., p. 337. 1937.

4. Schiller, L. Über den Strömungswiderstand von Rohren verschiedenen Querschitts und Rauhigkeitsgrades. Zeit. Ang. Math. und Mech., p. 2. 1923.

5. Davies, S. J., and White, C. M. An experimental study of the flow of water in pipes of rectangular section. Proc. Roy. Soc. (A), 119:92. 1928.

6. Eckert, E. R. G., and Irvine, T. F., Jr. Incompressible friction factor, transition and hydrodynamic entrance length studies of ducts with triangular and rectangular cross sections. Proceedings of the Fifth Midwestern Conference on Fluid Mechnics, University of Michigan. 1957.

7. Cornish, R. J. Flow in a pipe of rectangular cross section. Proc. Roy. Soc. (A), p. 691. 1928.

8. Eskinazi, S. Principles of Fluid Mechanics. Allyn and Bacon, Inc., Boston. P. 367. 1962.

9. Eckert and Drake. Heat and Mass Transfer. 2nd edition, p. 131. McGraw-Hill Book Co., Inc., New York.

10. Deissler, R. G. NACA Technical Notes No. 3016, pp. 1-87. October, 1953.

11. Prandtl, L. Ergeb. aerodynamischen, Versuchsanstalt Göttingen 3:4. 1927.

12. Deissler, R. G. Turbulent heat transfer and friction in the entrance region of smooth passages. Trans. ASME 77:1221-1233. 1955.

13. Pascucci. Sul Moto di Fluidi in Regime Turbolenta nel tratto Iniziale dei con Distribuzione Logaritmica di Velocita. atti Guidonia 4. 1953.

14. Latzko, H. Der Wärmeübergang an einen turbulenten Flüssigkeits-oder Gasstrom. Zeit. für angewandte Mathematik und Mechanik, 1 (4):268-290. 1921.

15. Schiller, L. and Kirsten, H. Die Entwicklung der Greschwindig Keitsverteilung bei der turbulenten rohrstromung. Ziet. für technische Physik 10:268-274. 1929.

16. Deissler, R. G. Analytical and experimental investigation of adiabatic turbulent flow in smooth tubes. NACA TN 2138. 1950.

17. Harnett, J. P., Kohn, J. and McComas, A. A comparison of measured and predicted friction factors for turbulent flow through rectangular ducts. Trans. ASME 82. 1962.

18. Clairborn, H. C. A critical survey of the literature on pressure drop in noncircular ducts and annuli. Oak Ridge National Laboratory, ORNL 1248. 1952.

19. Chemical Engineers Handbook. First edition, pp. 379-381.

20. Schiller, L. Investigations on laminar and turbulent flow. (German) Zeit. Agnew. Math. Mech. 2:96. 1922.

21. Goldstein S. Modern Developments in Fluid Mechanics. Vol. 1, pp. 299-310. 1938.

22. Fromm, K. Stromungswiderstand in rauhen rohren. Zamm 3:339. 1923.

23. Fritsch, W. Einflub der Wandrauhigkeit auf die turbulente Tesch windigkeitsverteilung in Rinnen. Zamm 8:199. 1928.

24. Nikuradse, J. Stromungsgesetze in rauhen Rohren. Forschungsheft, p. 361. 1933.

25. Colebrook, C. F. Turbulent flow in pipes with particular reference to the transition between the smooth and rough pipe laws. Journal, Institution of Civil Engineers. 1939.

26. Moody, L. F. Friction factors for pipe flow. Trans. ASME 66:671. 1944.

27. Pigott, R. J. S. The flow of fluids in closed conducts. Mech. Eng., p. 497. August, 1933.

28. Prandtl, L. Ziet. Physik 11:1072. 1929; 29:487. 1928.

29. Taylor, G. I. Rept. Mem. Brit. Aeronaut. Comm. 272:423. 1916.

30. Prandtl, L. Führer durch die Strömungslehre. Vieweg-Verlag, Brunswick, Germany. 1942.

31. Siegel, R. and Sparrow, E. M. Comparison of turbulent heat transfer results for uniform wall heat flux and uniform wall temperature. Journal of Heat Transfer 82:152. 1960.

32. Sparrow, E. M. and Siegel, R. Unsteady turbulent heat transfer in tubes. ASME Paper No. 59-HT-16.

33. Sparrow, E. M., Hallman, T. H. and Siegel, R. Turbulent heat transfer in the thermal entrance region of a pipe with uniform heat flux. Applied Sci. Res. 7 (A):37-52. 1957.

34. Siegel, R. and Sparrow, E. M. Turbulentflow in a circular tube with arbitrary internal heat sources and wall heat transfer. Journal of Heat Transfer, Trans. ASME, Series E, 81:280-290. 1959.

35. Dittus, F. W. and Boelter, L. M. K. Univ. of California Publs. Eng. 2:443. 1930.

36. McAdams, W. H. Heat Transmission, 3rd edition, p. 219. McGraw-Hill Book Co., New York. 1954.

37. Martinelli, R. C. Heat transfer to molten metals. Trans. ASME 69:947-959. 1947.

38. Lyon, R. N. Liquid metal heat transfer coefficients. Chem. Eng. Prog. 47:75-79. 1951.

39. Sieder, E. N. and Tate, G. E. Ind. Eng. Chem. 28:1429. 1936.

40. Trans. Am. Inst. Chem. Engrs. 29:174-210. 1933.

41. McAdams, Nicolai and Keenan. Nat. Adv. Comm. Aeronauti., Tn. 985, Washington, D. C. June, 1945.

42. Eckert, E. R. G. and Irvine, T. F., Jr. Pressure drop and heat transfer in a triangular duct. J. Ht. Tr. 82:125. 1960.

43. Carlson, L. W. and Irvine, T. F., Jr. Fully developed pressure drop in triangular ducts. Journal of Heat Transfer 83:441. 1961.

44. Deissler, R. G. and Taylor, M. F. Analysis of turbulent flow and heat transfer in noncircular passages. NACA Tech. Note 4384. 1958.

45. Sparrow, E. M. and Lin, S. H. Turbulent heat transfer in a parallel plate channel. Int. J. Heat and Mass Transfer 6:248. 1963.

46. Barrow, H. Convection heat transfer coefficients for turbulent flow between parallel plates with unequal heat fluxes. Int. Journal of Heat and Mass Transfer 1:469-487.

47. Barrow, H. An analytical and experimental study of turbulent gas flow between two smooth parallel walls with unequal heat fluxes. Int. J. of Heat and Mass Transfer 5:469-487.

48. Corccran, W. H., Opfell, J. B. and Sage, B. H. Momemtum transfer in fluids. Academic Press, New York. 1956.

49. ten Bosch, M. Die Wärmeübertragung, 3rd edition. Springer-Verlag, Berlin. 1936.

50. Hatton, A. P. Heat transfer in the thermal entrance region with turbulent flow between parallel plates at unequal temperatures. Appl. Sci. Res, Section A, 12.

51. Hatton, A. P. and Quarmby, A. The effect of axially varying and unsymmetrical boundary conditions on heat transfer with turbulent flow between parallel plates. Int. J. of Heat and Mass Transfer 6:903-915. 1963.

52. Hatton, A. P., Quarmby, A. and Grundy, I. Further calculations on heat transfer with turbulent flow between parallel plates. Int. J. of Heat and Mass Transfer 7:817-823.

53. Sparrow, E. M., Lloyd, J., and Hixon, C. Experiments on turbulent heat transfer in an asymmetrically heated rectangular duct. ASME Trans. J. of Heat Transfer, May 1966, pp. 170-174 .

54. Madsen, N. Comments on the effect of axially varying and unsymmetrical boundary conditions on heat transfer with turbulent flow between parallel plates. Int. J. of Heat and Mass Transfer 7:1143-1144.

55. Novotny, McComas, Sparrow and Eckert. Heat transfer for turbulent flow in rectangular ducts with two heated and two nonheated walls. A. I. Ch. E. Journal, July 1966, pp. 466-470.

56. Nusselt, W. See The calculation of heat transmission, by M. Fishenden and O. Saunders, H. M. S. O., p. 151. 1932.

57. Hausen, H. Zeit. Ver. Deut., Beih. Verfahrenstech., No. 4, 81-98. 1943.

58. Latzko, H. Zeit. für Agnew Math. Mech. 1:268. Translated into English in NACA Technical Memoranda No. 1068. 1944.

59. Eagle, A. and Ferguson, R. M. Proc. Instit. Mech. Engrs. 2:985. 1935.

60. Davies, V. C. and Al-Arabi, M. Proc. Instit. Mech. Engrs. 169:993. 1955.

61 Hartnett, J. P. Trans. Amer. Soc. Mech. Engrs. 77: 1211. 1955.

62. Al-Arabi, M. Effect of length on heat transfer for turbulent flow inside tubes. App. Sci. Res., Section A, 14:321.

63. Boelter, L., Young, G. and Iversen, H. Distribution of heat transfer rate in the entrance region of a circular tube. NACA Tech. Note 1451, July 1948.

64. Romanenko, P. and Krylova, N. A study of the effects of inlet conditions on heat transfer in the entry region of a tube. Int. Chem. Engrs., p. 587. 1964.

65. Linke, W. and Kunze, H. Allgem. Wärmetech 4:73-79. 1953.

66. Barrow, H. and Lee, Y. Thermal entry region in turbulent gas flow. Engineer, London, 215:169. 1963.

67. _____. Heat transfer within unsymmetrical thermal boundary conditions. Int. J. of Heat and Mass Transfer 6:580. 1963.

68. Soennecken, A. Der Wärmeübergang von Rohrwänden an Strömendes Wasser. Forsch-Arb. Ing. Wes. No. 109, Berlin. 1911.

69. Stanton, T. E. Friction. Longmans-Green, London. 1923.

70. Pohl, W. Einflus der Wandrauhigkeit auf den Wärmeügergang und Wasser. Forsch. Ing. Wes. 4:230-237. 1933.

71. Cope, W. F. The friction and heat transmission coefficient of rough pipes. Proc. Instit. Mech. Engr. 145:99. 1941.

72. Nunner, W. Heat transfer and pressure drop in rough tubes. V. D. I. Forsch. Series B. 22:5-39. 1956.

73. Brouillette, E. C., Mifflin, T. R. and Meyers, J. E. Heat transfer and pressure drop characteristics of internally finned tubes. ASME Paper No. 57-A-47, pp. 1-9. 1947.

74. Hobler, T. and Koziol, K. Heat transfer inside tubes with alternate bilateral contractions. Int. Chem. Eng., p. 672. October, 1965.

75. Kolář, V. Heat transfer in turbulent flow of fluids through smooth and rough tubes. Int. J. of Heat and Mass Transfer 8:639-683.

76. Der Wärmeübergang von Rohrwänden an Strömendes Wasser. Forsch-Arb. Ing. Wes. No. 109, Berlin. 1911.

77. Mizushina, T. Analogy between fluid friction and heat transfer in annuli. Int. Mech. Eng., p. 191. 1951.

78. Hatton, A. P. Heat transfer in the thermal entrance region with turbulent flow between parallel plates at unequal temperatures. App. Sci. Res., Seciton A, 12: 255.

79. Page, F., Jr., Schlinger, W. G., Breux, I. K. and Sage, B. H. Temperature gradients in turbulent gas streams--point values of eddy conductivity and viscosity in uniform flow between parallel plates. Ind. Eng. Chem. 44:424. 1952.

80. Azer, N. Z. and Chao, B. T. A mechanism of turbulent heat transfer in liquid metals. Int. J. of Heat and Mass Transfer 1:121. 1960.

81. Goff, J. A. Thermodynamic properties of moist air. Trans. ASHVE 55:474.

82. Heating, Ventilating, Air Conditioning Guide. American Society of Heating and Air Conditioning Engineers 37: 22-25. 1959.

83. McAdams, W. H. Heat Transmission. McGraw-Hill Company, Inc., p. 260. 1954.

84. Threlkeld, J. L. Thermal Environmental Engineering, 1st edition. Englewood Cliffs, New Jersey.

85. Colburn, A. P., Schoenborn, E. M. and Sietton, C. S. Nat. Advisory Comm. Aeronaut. Report No. U.D.-N.I. 1945, TN-1488. 1948.